NATIONAL ADVISORY COMMITTEE FOR AERONAUTICS

TECHNICAL NOTE 3514

RESPONSE OF HOMOGENEOUS AND TWO-MATERIAL LAMINATED CYLINDERS TO SINUSOIDAL ENVIRONMENTAL TEMPERATURE CHANGE, WITH APPLICATIONS TO HOT-WIRE ANEMOMETRY AND THERMOCOUPLE PYROMETRY

By Herman H. Lowell and Norman Patton

Lewis Flight Propulsion Laboratory
Cleveland, Ohio

Washington
September 1955

ERRATA

NACA TN 3514

RESPONSE OF HOMOGENEOUS AND TWO-MATERIAL LAMINATED CYLINDERS TO SINUSOIDAL ENVIRONMENTAL TEMPERATURE CHANGE, WITH APPLICATIONS TO HOT-WIRE ANEMOMETRY AND THERMOCOUPLE PYROMETRY

By Herman H. Lowell and Norman Patton

September 1955

Page 13, equation (15): The expression in parentheses following $\tan^{-1}$ should read

$$\left(\frac{\Phi_{R,b}\ \mathrm{ber}'_{0,b} + \Phi_{I,b}\ \mathrm{bei}'_{0,b}}{\Phi_{R,b}\ \mathrm{bei}'_{0,b} - \Phi_{I,b}\ \mathrm{ber}'_{0,b}}\right)$$

Page 49: Line 6 should read "equation (15) as modified for the cosinusoidal drive of the main text):"

Page 49, equation (B17): The expression following $\tan^{-1}$ should read

$$\left(\frac{\Phi_R\ \mathrm{ber}'_0(l_b) + \Phi_I\ \mathrm{bei}'_0(l_b)}{\Phi_R\ \mathrm{bei}'_0(l_b) - \Phi_I\ \mathrm{ber}'_0(l_b)}\right)$$

Page 88, table II(b), column 1, line 13: The expression $2^{1/4}$ should be $2^{-1/4}$.

NACA - Langley Field, Va.

TABLE OF CONTENTS

TABLE OF CONTENTS - Concluded

NATIONAL ADVISORY COMMITTEE FOR AERONAUTICS

TECHNICAL NOTE 3514

RESPONSE OF HOMOGENEOUS AND TWO-MATERIAL LAMINATED CYLINDERS TO SINUSOIDAL ENVIRONMENTAL TEMPERATURE CHANGE, WITH APPLICATIONS TO HOT-WIRE ANEMOMETRY AND THERMOCOUPLE PYROMETRY

By Herman H. Lowell and Norman Patton

SUMMARY

In current aeronautical research, rapidly responding thermocouples and hot-wire anemometers are required. A laminated cylinder consisting of an oxide core and thin metallic coating is known to provide a larger output signal than a conventional metallic wire at high rates of change of environmental conditions when all other variables of the physical situation are fixed. A generalized attack on the problem of the responses of homogeneous and two-material laminated cylinders to sinusoidal environmental temperature changes has accordingly been made. The results are applicable to situations in which small heat-transfer coefficient changes occur in the absence or presence of environmental temperature changes.

The response of homogeneous and two-material laminated cylinders are given quantitatively in a series of tables and graphs and are discussed qualitatively in detail. In the case of the laminated cylinder, results are given for all combinations of the indicated numeral values of the following parameters: ratio of shell thermal conductivity to core thermal conductivity (5, 10, 20, 40, and 80); ratio of core radius to over-all radius (0.75 and 0.90); and nondimensional heat-transfer coefficient, designated the Jakob number (a number of different values forming a geometrical progression covering a large range of physically possible operating conditions).

A parameter designated the "internal" time constant is introduced which uniquely characterizes the internal distribution of temperature within a homogeneous cylinder and thus facilitates meaningful presentation of both generalized and specific results for particular physical situations. Two parameters suffice to characterize the internal distribution of temperature within a two-material laminated cylinder. For a cylinder having n layers, n such parameters are required.

The responses of 0.0004-, 0.002-, and 0.010-inch-diameter homogeneous and laminated wires of platinum and/or fused quartz exposed to a representative air stream are considered in detail. Such laminated wires can achieve signal gains (relative to outputs of conventional wires) sufficient to increase the frequency limit of usable response by an order of magnitude greater than that associated with conventional wires. Realization of such gains, which are not manifested until the relative response of the laminated structure drops below 0.01, would require fabrication of structures such that the ratio of shell thickness to over-all radius is at most 0.1 but is preferably no greater than 0.05.

The theoretical material presented includes simplified, approximate treatments of the two-material structure which are not exact but which should yield results accurate enough for design use. In particular, they enable computation of the response characteristics correct to at least three figures over overlapping frequency ranges which, collectively, cover all of the meaningful frequency spectrum.

INTRODUCTION

In connection with investigations of the behavior of turbomachines or of proposed improved components, it is often necessary to obtain a detailed picture of the instantaneous thermal and mass-flow-rate structures of the air flows occurring throughout interblade channels, between stator and rotor cascades, within blade (or shroud) boundary layers, behind trailing edges, or within engine ducts. Fast thermocouples and hot-wire anemometers are often used in such research, but their faithfulness of response is inadequate for many purposes.

The response of such instruments may be improved (within obvious mechanical limitations) by reducing the element cross section and, to a lesser extent, by properly shaping the element so as to expose a maximum of surface to the stream. In many situations involving locally irregular flows, however, circularly cylindrical (or spherical) elements are the only stream-inserted instrument bodies that are acceptable aerodynamically.

The techniques of electrical compensation for thermal lags have been extensively discussed in the literature (e.g., refs. 1, 2, and 3). In general, these techniques require amplifying systems with the rising gain characteristics of "constant-current" systems or the so-called "constant-temperature" feedback systems having amplifiers with essentially flat frequency responses.

Irrespective of the successes of such techniques, as upper limits of required useful-response frequency bands are raised, it is clear that maximization of both absolute and relative voltages delivered to such compensation devices is desirable so as to maintain high inherent signal-to-noise ratios.

Conventional cylindrical elements, which have high strength when effective length-to-diameter ratios are kept within reasonable bounds, are comparatively simple to fabricate. Their performance, however, is affected adversely by several obvious circumstances, namely:

(1) The entire cross section of the element is electrically "active". The effective total heat capacity is, moreover, that of the entire element.

(2) Any change in environmental conditions is, necessarily, communicated first to exterior laminae and, subsequently, to the more central regions. As a consequence, differential phase lags occur.

(3) Attenuation of a thermal wave occurs as the wave progresses from exterior to axis.

The behavior of the homogeneous cylinder may accordingly be qualitatively described as follows: At comparatively low frequencies, the entire element responds as an integral unit. The response is then that of a first-order system; the time constant is proportional to the product of the boundary-layer thermal resistance and the total heat capacity of the element. At higher frequencies, however, attenuation and differential phase shifting of thermal waves begin to occur. The situation becomes far more complex. There is a decrease in over-all response not merely because of attenuation in the vicinity of the axis but also because the contributions to the electrical output (whatever the nature of that output may be) are not in phase. This phenomenon in turn causes a further decrease in output.

It was suggested at the Lewis laboratory in 1946 (unpublished work) that one technique whereby the situation could be ameliorated was to substitute for the homogeneous cylinder a two-material laminated cylinder (fig. 1). Some electrically nonconducting and thermally poor-conducting material such as an oxide was suggested for the core and an electrically active material of some kind such as a metal for the shell.

Such a structure would have certain advantages, and these advantages would be present whether the instruments in question were thermocouples, hot-wire anemometers, or resistance thermometers:

First, the electrically active material is now concentrated in a region that is the first to sense environmental changes. This effect tends to increase instrument response. In addition, however, the thermally poor-conducting material of the core tends to become thermally isolated from the surface region as the rapidity of an environmental change increases. Both of these effects combine to ensure, generally, a much greater amplitude of electrically active material response than

would normally occur for an ordinary metallic wire of the same size. At the same time, the lag of the response behind the external change becomes much smaller.

Second, for the same cross section of material and same wire length, errors associated with paraxial heat conduction are reduced because of the smaller thermal conductivity of the core material.

Third, the higher electrical resistance of such a structure results in a more efficient transfer of electrical energy to high impedance devices such as amplifier input circuits.

Finally, because of the smaller length-to-diameter ratios made possible by the lower thermal conductance, the laminated structure would have higher strength than ordinary wires when the proper materials are used. (It is of interest in this connection that synthethic sapphire - monocrystalline alumina - has been stressed to 155,000 pounds per square inch tensile stress at the National Bureau of Standards. Fused-quartz fibers are known to have breaking strengths ranging up to 10^6 psi.)

It will be impossible, however, to achieve substantial gains in all of the mentioned ways simultaneously; the unit will have to be designed for the application.

While use of such a structure is analogous to the use of film bolometers in infra-red radiation detectors, there are certain ways in which the responses of simple and compound cylinders differ materially from those of plane elements. It was therefore necessary to develop a quantitative treatment of the behavior of laminated-cylinder instrument elements. While the results probably parallel certain of the results obtained in the bolometer field, no effort has been made to correlate quantitatively the behavior of film bolometers and laminated cylinders. It is, however, clear that differences in the two sets of behavior characteristics will be small for moderately high rates of variation of environmental temperature, moderately high heat-transfer coefficients, and relatively very thin metallic films.

It is the purpose of this report to present a reasonably complete quantitative description of the thermal behavior of both simple (homogeneous, solid) circular cylinders and of two-material laminated cylinders exposed to circumferentially uniform environments. In the case of the laminated cylinder, the scope of the numerical results was necessarily limited. Specifically, the shell material was assumed to have higher conductivity than the core. Paraxial conduction was assumed to be of negligible magnitude.

Initially, a discussion is presented of the behavior of a simple circular cylinder; derivations of formulas taken from the literature are in appendix B.

A discussion is then presented of the behavior of the two-material laminated cylinder that places strong emphasis on the case in which the shell material is high in thermal conductivity. The appropriate time constants and nondimensional parameters are discussed. An exact analytical treatment of the general case is given in appendix C; that solution was used to confirm a few of the numerical results obtained by the numerical integration technique discussed in this report. An approximate analysis leading to formulas of sufficient simplicity to enable desk-computer calculations within reasonable time periods is presented in appendix D. (The exact theory of the hollow-cylindrical shell, useful under certain circumstances, is given in appendix F.)

The results of the extensive laminated-cylinder numerical computations made in connection with the present study are then presented and discussed. The numerical integration technique used is explained in appendix E, in which also is stated the procedure used in the calculation of the Kelvin-Bessel functions required in the calculations. Comparisons of the laminated-cylinder results with simple cylinder responses and with first-order calculations are made. Illustrative examples of applications to physical situations are included.

The important symbols used in the report are defined in appendix A.

THERMAL RESPONSES OF HOMOGENEOUS CYLINDERS AND OF CYLINDERS RESPONDING AS THOUGH HOMOGENEOUS

Assumptions and General Remarks

Steady-state thermal responses of circular cylinders to simple harmonic environmental temperature changes are considered in this section. It is assumed throughout that neither axial nor circumferential variations of heat-transfer coefficient, amplitude, or frequency of the temperature oscillation exist.

Only the assumption on circumferential variation requires discussion; in actuality, rather large circumferential irregularities often exist. A mean heat-transfer coefficient would be used in such a situation and its value obtained by an appropriate integration procedure. The question then arises as to the difference between the actual behavior of the cylinder and the behavior calculated under the assumption that the heat-transfer coefficient was uniform circumferentially and was (of course) equal to the mean value of the real situation. At the high

frequencies and low core (oxide) thermal diffusivities, at which the important phenomena discussed in this report will occur, both radial and circumferential spreading of local thermal events will occur to only a small degree. At the same time, circumferential gradients of heat-transfer coefficient will be small in comparison with radial temperature gradients. Accordingly, the assumption of constancy of a heat-transfer coefficient at an appropriate mean value will necessarily lead to results in accord with real cylinder behavior.

Through appropriate syntheses, thermal responses to nonsinusoidal periodic temperature drives may, of course, be obtained once the responses to simple harmonic drives of all relevant frequencies are elucidated. If generalized frequency response results are available, aperiodic solutions are obtainable.

Simple Cylinder

Time constant and Biot number. - It is convenient to speak of time constants of the system boundary-layer cylinder despite the fact that no exact simple relation exists between the behavior of first-order or second-order systems, on the one hand, and boundary-layer cylinder systems on the other.

"External" and "internal" time constants: The external time constant is that which characterizes the system when the cylinder responds as a unit. In the case of a wire through which little or no electrical current is flowing, the external time constant is given by

$$\tau_{ext} = \frac{r_b^2 \rho c_p}{k_f Nu_f} = \frac{r_b^2 k}{a^* k_f Nu_f} = \frac{r_b^2}{2a^* Bi} \tag{1}$$

in which Bi, a Biot modulus, is defined by

$$Bi \equiv \frac{h_f r_b}{k} \tag{2}$$

This is the conventional time constant used in first-order analyses of thermocouple responses.

When electrical heating occurs, the external time constant of a hot-wire anemometer, under constant-current conditions, is given by

$$\left(\frac{1 + c_r T_w}{1 + c_r T_{e,av}}\right)\left(\frac{r_b^2}{2a^* Bi}\right) = \left(\frac{1 + c_r T_w}{1 + c_r T_{e,av}}\right) \tau_{ext} \tag{3}$$

where c_r is the mean thermal coefficient of resistivity of the wire material over the temperature range 0° C to T_w and $T_{e,av}$ is the time-average value of the effective environment temperature. The effective environment temperature is defined as the temperature attained by the wire when not heated electrically in the absence of longitudinal conduction.

The internal time constant τ_{int} is arbitrarily defined as that period of time during which the area-averaged cylinder temperature change, in the case of a sudden surface temperature change, attains a magnitude of $1 - e^{-1}$ of the final (asymptotic) change. The numerical magnitude of the internal time constant may be obtained as follows:

The theory of the response of a (very long) homogeneous cylinder the surface temperature of which is suddenly changed from some initial value $t_{0,b}$ to zero is given in reference 4, pages 170 to 171. Carslaw and Jaeger give

$$\frac{t}{t_{0,b}} = \sum_{j=1}^{\infty} \frac{B_j}{t_{0,b}} J_0\left(m_j \frac{r}{r_b}\right) e^{-\frac{a^* m_j^2 \theta}{r_b^2}} \tag{4}$$

in which B_j is defined as follows:

$$\sum_{j=1}^{\infty} B_j J_0\left(m_j \frac{r}{r_b}\right) = t_0$$

where in the general case t_0, the initial temperature, is a function of the radial coordinate, and where m_j is one of the successive roots of $J_0(m_j) = 0$. The validity of this expansion is demonstrated in reference 5 (p. 576) wherein it is also shown that

$$B_j = \frac{2}{J_1^2(m_j)} \int_0^1 \frac{r}{r_b} t_0 J_0\left(m_j \frac{r}{r_b}\right) d\left(\frac{r}{r_b}\right)$$

For the case in which $\frac{\partial t_0}{\partial r} = 0$, t_0 is constant at some value, say t_0^*, and B_j becomes

$$\frac{2t_0^*}{m_j J_1(m_j)}$$

Equation (4) then becomes

$$\frac{t}{t_0^*} = 2\sum_{j=1}^{\infty} \frac{J_0\left(m_j \frac{r}{r_b}\right)}{m_j J_1\left(m_j \frac{r}{r_b}\right)} e^{-\frac{a^* m_j^2 \theta}{r_b^2}}$$

which is identical with equation (5), page 174 of reference 4. Carslaw and Jaeger give the average temperature (on an area-weighted basis) for this case finally as

$$\frac{\bar{t}}{t_0^*} = \frac{1}{\pi r_b^2} \int_0^{r_b} 2\pi r \frac{t}{t_0^*} dr = 4\sum_{j=1}^{\infty} \frac{e^{-m_j^2 \frac{a^* \theta}{r_b^2}}}{m_j^2} \tag{5}$$

Since τ_{int} was defined as the time at which $\frac{\bar{t}}{t_0^*} = e^{-1}$, it follows that

$$4\sum_{j=1}^{\infty} \frac{e^{-m_j^2 \frac{a^* \tau_{int}}{r_b^2}}}{m_j^2} = e^{-1}$$

If, now, the symbol λ is used to denote the value of the Fourier modulus $\frac{a^* \tau_{int}}{r_b^2}$ at which the above equality holds, the defining equation for λ becomes

$$\sum_{j=1}^{\infty} \frac{e^{-m_j^2 \lambda}}{m_j^2} = (4e)^{-1} \tag{6}$$

The roots of $J_0(m_j) = 0$ may be found in the sources cited on pages 261 to 262 of reference 6. It is possible to compute λ precisely by

calculating the value of the function represented by the left side of equation (6) for a succession of values in the immediate vicinity of an approximate value of the constant. It did not seem worthwhile to do this, however, since the usefulness of the concept would not be increased by the availability of an exact value. The approximate value of λ (0.111) was obtained in two ways: First, the values of $4\sum_{j=1}^{\infty}\frac{e^{-m_j^2\lambda^*}}{m_j^2}$ for values of the dummy parameter λ^* ranging from 0 to 1.00, as given in references 7 (p. 143) and 8 (p. 357), were plotted. The value $\lambda \cong 0.111$ is immediately obtained from such a plot. This value has been adopted as an exact one throughout this work.

An alternative method of determining the value of λ is the examination of curve III of figure 9 (p. 84) of reference 4, which presents both nondimensional temperature distributions and average temperatures for slabs, circular cylinders, and spheres as functions of the Fourier number $a^*\theta/r_b^2$. (It should be borne in mind, however, that u/V of the graph in question equals $(t_0^* - \bar{t})/t_0^*$ in the present notation.) Again, one arrives at the same value of λ to three significant figures using this second procedure.

The relation

$$\tau_{int} \cong \frac{\lambda r_b^2}{a^*} = \frac{0.111\ r_b^2}{a^*} \tag{7}$$

then yields τ_{int}. It is emphasized that equation (7) is adopted as the definition of τ_{int}.

The significance of the two time constants in connection with the present problem is the following: If $\tau_{ext} >> \tau_{int}$, then, regardless of the magnitude of the product $\omega\tau_{ext}$, the cylinder will respond as a unit.

In fact, a parameter of the highest importance is the Biot modulus previously defined (eq. (2)), for

$$\frac{\tau_{int}}{\tau_{ext}} = \frac{\lambda r_b^2}{a^*} \cdot \frac{2a^*Bi}{r_b^2} = 2\lambda Bi$$

that is,

$$Bi = \frac{h_f r_b}{k} = \frac{\tau_{int}}{2\lambda\tau_{ext}} \tag{8}$$

On the other hand, as the Biot number, initially small under the above hypothesis, tends toward and ultimately exceeds unity, the interior temperature ceases to be uniform and the phenomena occur which were discussed qualitatively in the INTRODUCTION.

Solutions in literature: Surface and interior response. - The ratio of local instantaneous temperature of a homogeneous cylinder to the maximum amplitude of harmonic environment temperature change $t_{e,M} \cos \omega\theta$ is given by the following:

$$\frac{t}{t_{e,M}} = \eta = \left[\frac{\text{ber}_0^2(\alpha r) + \text{bei}_0^2(\alpha r)}{\Phi_{R,b}^2 + \Phi_{I,b}^2}\right]^{1/2} \times$$

$$\cos\left\{\omega\theta - \tan^{-1}\left[\frac{\Phi_{I,b}\,\text{ber}_0(\alpha r) - \Phi_{R,b}\,\text{bei}_0(\alpha r)}{\Phi_{R,b}\,\text{ber}_0(\alpha r) + \Phi_{I,b}\,\text{bei}_0(\alpha r)}\right]\right\} \tag{9}$$

A result equivalent to this is derived in appendix B. It is there assumed, however, that the temperature drive is $t_{e,M} \sin(\omega\theta + \varepsilon)$. Equation (B15) there derived differs appropriately from equation (9). In equation (9), ber_0 and bei_0 (both real) are defined by

$$J_0(i^{3/2} x) \equiv \text{ber}_0 x + i\,\text{bei}_0 x$$

and

$$\left.\begin{aligned}\Phi_{R,b} &\equiv Ja^{-1}\,\text{ber}_0'(\alpha r_b) + \text{ber}_0(\alpha r_b)\\ \Phi_{I,b} &\equiv Ja^{-1}\,\text{bei}_0'(\alpha r_b) + \text{bei}_0(\alpha r_b)\end{aligned}\right\} \tag{10}$$

where

$$\alpha \equiv \sqrt{\frac{\omega}{a^*}}$$

and

$$Ja \equiv \frac{h_f}{k}\sqrt{\frac{a^*}{\omega}} \tag{11}$$

(A solution is given in reference 9 for the case of a step change of environment temperature; charts are presented on pages 278, 286, 289, 291, 413, 417, and 418 of that reference.)

Equation (9) seems to have been first derived by H. Gröber (ref. 10). In that reference, a very complete exposition is presented both for the temperature regimes and the instantaneous heat-flow rates in homogeneous slabs and cylinders upon subjection of such objects to periodic environmental temperature changes. (Much of this material may also be found in refs. 9 and 11.) It should be noted, however, that Gröbers' numerical results, while substantially correct, are not free from error. The numerical errors contained in the Gröber article are perpetuated in a somewhat truncated version of the original paper appearing in the more accessible reference 11 (pp. VI-30 to VI-37). Table I presents a comparison of the values of Gröber with the correct values as obtained directly or computed from the listings in reference 12 (pp. 182 to 201). Table I presents certain additional useful data.

In table II, equivalent numerical values of certain of the nondimensional moduli or parameters used by Gröber and in the present study are listed. This listing facilitates the comparison among his results and those more recently obtained by others.

At this point, it is desirable to bring together the various parameters already mentioned. Appendix A exhibits the interrelations among those parameters. The moduli Fo^* and Ja^* are included because of their use by Gröber.

The relative surface temperature values are given by

$$\eta_b = \left[\frac{\mathrm{ber}_0^2(\alpha r_b) + \mathrm{bei}_0^2(\alpha r_b)}{\Phi_R^2 + \Phi_I^2}\right]^{1/2} \times \cos\left\{\omega\theta - \tan^{-1}\left[\frac{\Phi_I\,\mathrm{ber}_0(\alpha r_b) - \Phi_R\,\mathrm{bei}_0(\alpha r_b)}{\Phi_R\,\mathrm{ber}_0(\alpha r_b) + \Phi_I\,\mathrm{bei}_0(\alpha r_b)}\right]\right\} \tag{12}$$

This relation is easily obtained from equation (9) by substituting r_b for r wherever it appears in that equation. The axis temperature η_{ax} is given by

$$\eta_{ax} = \left(\Phi_R^2 + \Phi_I^2\right)^{-1/2} \cos\left(\omega\theta - \tan^{-1}\frac{\Phi_I}{\Phi_R}\right) \tag{13}$$

inasmuch as $\mathrm{ber}_0(0) = 1$ while $\mathrm{bei}_0(0) = 0$.

It is clear that the ratio of the maximum values or of any pair of values occurring at the same epoch angles relative to the maximums at the two locations (axis and surface) will be given by

$$\frac{\eta_{ax,M}}{\eta_{b,M}} = \left[\mathrm{ber}_0^2(\alpha r_b) + \mathrm{bei}_0^2(\alpha r_b)\right]^{-1/2} \tag{14}$$

Gröber (ref. 10) gives numerical values in both tabular and graphic form of η_b, η_{ax}, and $\eta_{ax,M}/\eta_{b,M}$. Examination of table I will indicate that his values of ber_0 and bei_0 are correct or virtually so except at the highest values of the argument αr. Accordingly, it was desirable to reproduce his germane tables and figures without change, although values corresponding to his large arguments must not be considered exact.

The surface temperature attenuation factors and phase shifts listed in Gröber's table 1 for the case of the semiinfinite slab are reproduced here as table III. The sole parameter in this case is $Ja^{*2} = \frac{2\pi h_f^2}{k\rho c_p \omega}$. Tables IV and V (Gröber's numbers 4 and 5) apply to the case of the cylinder; the parameters are Ja^{*2} and $Fo^* = \frac{2\pi k}{\rho c_p r_b^2 \omega}$. Figures 2 and 3 (from Gröber) exhibit the data of tables IV and V in graphic form.

The limiting situations were summarized by Gröber (ref. 10) as follows:

"(a) If the heat-transfer coefficient is infinitely large [external time constant zero, internal arbitrary] so that $h^2 a t_0 = \infty$ [$Ja^* = \infty$] then the surface temperature will be forced to follow the oscillations of environmental temperature immediately and with undiminished amplitude; therefore, $\eta_0 = 1$ [$\eta_b = 1$] and $\varepsilon = 0^\circ$ [the phase shift at the surface is zero].

"(b) This same consideration is valid when the cylinder is infinitely thin, that is, $(at_0)/R^2 = \infty$ [$\alpha r = 0$ and both time constants are zero].

"(c) If the heat-transfer coefficient is infinitely small [external time constant infinitely great], so that $h^2 a t_0 = 0$ [$Ja^* = 0$], then the calculation yields a phase shift which increases from 45° to 90°, that is, from 1/8 to 1/4 of a period. This phase shift is not too meaningful because the oscillations of surface temperature are throttled down to zero by the adverse heat-transfer conditions.

"(d) When the cylinder is infinitely thick [ratio of internal to external time constant very high], then, simply, the laws [of heat transfer] for infinitely thick bodies [slabs] apply, and for this reason the first vertical numerical series in tables 4 and 5 agrees with table 1."

Gröber continues his discussion of a homogeneous cylinder as follows:

"Now we can determine more accurately the domain of the 'infinitely thin' and of the 'infinitely thick' cylinders.

"(a) If the calculation shows that $(at_0)/R^2$ [Fo*] is greater than about 5 [Fo > 0.7958; $\alpha r < 1.121$; $\omega\tau_{int} < 0.139$] then the cylinder (according to table 6) responds as a unit over its entire thickness. This does not mean however that the cylinder [temperature] oscillation entirely follows that of the ambient temperature; only when η_0 [η_b] (according to table 4) is approaching unity does this occur and only then are we permitted to treat the cylinder as infinitely thin.

"(b) We will in the following consider the temperature waves as cut off when they have decreased to 2 percent of their surface values. It can now be read off from table 6 that the temperature waves no longer reach the axis when $(at_0)/R^2$ [Fo*] is less than about 0.07 [Fo < 0.0114; $\alpha r > 9.474$; $\omega\tau_{int} > 9.96$]. But this failure indicates that the cylinder is infinitely thick and the equations . . . [for the semiinfinite slab] are applicable. These imply that the surface is plane. Approximately, therefore, the depth of penetration . . . is only about a third to a fifth of the cylinder radius."

Mean response of simple cylinder. - The instantaneous mean temperature with respect to radius of a homogeneous cylinder, taking into account the variation in relative phase over the cross section, is of considerable interest. This relation, derived in appendix B, results from an elementary area-weighting averaging process:

$$\bar{\eta} = \frac{2}{\alpha r_b}\left[\frac{\mathrm{ber}'_{0,b} + \mathrm{bei}'_{0,b}}{\Phi^2_{R,b} + \Phi^2_{I,b}}\right]^{1/2} \cos\left[\omega\theta - \tan^{-1}\left(\frac{\Phi_{R,b}\,\mathrm{bei}'_{0,b} + \Phi_{I,b}\,\mathrm{bei}'_{0,b}}{\Phi_{R,b}\,\mathrm{bei}'_{0,b} - \Phi_{I,b}\,\mathrm{ber}'_{0,b}}\right)\right] \tag{15}$$

(The notation $\mathrm{ber}'_{0,b} \equiv \mathrm{ber}'_0(\alpha r_b)$ has been introduced here. Note also that $\mathrm{ber}'_0(\alpha r_b) = \left\{d\left[\mathrm{ber}_0(\alpha r)\right]/d(\alpha r)\right\}_{r_b}$.)

The maximum amplitude of $\bar{\eta}_M$ has been plotted in figure 4(a) as a function of the variable $\omega\tau_{ext} = \omega r_b \rho c_p / 2h_f$ and of the parameter $\omega\tau_{ext}/\omega\tau_{int} = \tau_{ext}/\tau_{int} = (2\lambda Bi)^{-1} = k/2\lambda h_f r_b$. It will be noted that, for a homogeneous cylinder, large deviations from the first-order response occur only at values of $\tau_{ext}/\tau_{int} < 10$, and even then only for $\omega\tau_{ext} < 20$. The physical reason for this remarkable fact appears to be that the increase in surface temperature amplitude with decrease in τ_{ext}/τ_{int} tends to compensate for the decrease in deep-interior amplitude. This point is brought out quantitatively in the following list of homogeneous-cylinder amplitude values:

$\omega\tau_{ext} = 31.62$		
$\omega\tau_{int}$	Approximate surface amplitude (Gröber)	Exact mean amplitude
0	0.03161 (first-order)	0.03161
.1	.031	.03150
.3162	.035	.03126
1.0	.043	.03067
3.162	.075	.02981
10	.140	.02845

In this list, for a virtually constant relative mean amplitude, the surface temperature amplitude increases by a factor of 4.5 in going from a τ_{ext}/τ_{int} ratio of infinity to a ratio of 3.162; this behavior is typical.

Simple-cylinder surface temperature analog. - This phenomenon can be understood when a simple surface temperature analog is considered, namely, a circuit (fig. 5) consisting of a "black box," a source of (alternating) potential, and a high resistance in series representing the thermal resistance of the boundary layer around the cylinder. The "black box" may then be considered to be an analog of the cylinder itself. The potential is then equivalent to the environmental temperature oscillation while the current of the analog is equivalent to the heat-flow sinusoid. Provided the impedance of the black box remains at most about a third of the impedance of the external resistor, no change of distribution of impedance within the box or of over-all box impedance will substantially affect the current (heat) flow level. If, however, the cylinder as a whole is to receive about the same amount of heat per unit time irrespective of the deep-interior changes of temperature, it must follow that the near-surface variations must increase correspondingly.

The black box contents may be represented, very roughly, by two resistors and an inductance (fig. 5) and, in that case, will behave approximately as the actual cylinder will at high $\omega\tau_{ext}$ values; as the frequency increases, the current in resistor A will increase at the expense of that in B.

Relative responses at surface and over entire cylinder. - The ratio of surface amplitude to mean amplitude (disregarding the phase difference, of course) follows from equations (12) and (15):

$$\frac{\eta_{b,M}}{\overline{\eta}_M} = \frac{\alpha r_b}{2}\left(\frac{\mathrm{ber}_{0,b}^2 + \mathrm{bei}_{0,b}^2}{\mathrm{ber}_{1,b}^2 + \mathrm{bei}_{1,b}^2}\right)^{1/2} \tag{16}$$

(Note that $\mathrm{ber}_1^2 + \mathrm{bei}_1^2 = \mathrm{ber}_0'^2 + \mathrm{bei}_0'^2$.)

As in the case of equation (14), this ratio is, of course, independent of the heat-transfer coefficient, that is, of the Jakob number; a few values of $\overline{\eta}_M/\eta_{b,M}$ are listed in table VI and plotted on figure 6.

The corresponding decrease of phase shift is given by the relation

$$\overline{\varphi} - \varphi_b = \frac{\dfrac{\mathrm{ber}_{0,b}' \, \mathrm{ber}_{0,b}}{\mathrm{bei}_{0,b}' \, \mathrm{bei}_{0,b}} + 1}{\dfrac{\mathrm{ber}_{0,b}}{\mathrm{bei}_{0,b}} - \dfrac{\mathrm{ber}_{0,b}'}{\mathrm{bei}_{0,b}'}} \tag{17}$$

It should be noted again that relations (12), (16), and (17) apply to the homogeneous cylinder. They imply, however, that some means has been found whereby temperature conditions at the surface can be determined by suitable instrumentation. Apart from optical means or the use of very high frequencies, no physical mechanism is actually available whereby this wholly theoretical improvement may be realized in the case of an electrically conductive cylinder. Moreover, the (metallic) interior of the homogeneous cylinder is strongly coupled (thermally) to the surface so that the realizable improvement would be small in any case.

Quasi-Homogeneous-Cylinder Configurations

General considerations. - In figure 7(a) a homogeneous metallic cylinder has been replaced by a laminated structure. An insulating layer (possibly of some oxide) is placed between the metallic core and

the outer shell of metal. The purposes might be provision of a necessary electrical separation and retention of an auxiliary source of heat.

The volumetric specific heats of most nonporous materials are very nearly equal, so that the substitution of the oxide shell has little if any affect on the thermal capacity of the device. This fact aids in the analysis of the situation. On the other hand, the radial thermal resistance will be markedly increased if the oxide stratum has significant thickness.

Assuming, however, that both shells - particularly the oxide - are of negligible thickness, it is clear that the improvement factor is given approximately by equation (16) as a function of αr_b (or of $\omega\tau_{int,2}$).

In figure 7(b), the original homogeneous wire has been replaced by an oxide core, a thin concentric electrically conducting shell, and a cover shell of the same oxide. This arrangement would be desirable, for example, if corrosion protection of the metal were required, particularly for high-temperature applications. This configuration is desirable from the performance standpoint only when the oxide cover layer is very thin.

The equations of the homogeneous cylinder are again valid approximately provided the metallic layer is very thin, so that the sum of the thermal resistances of the oxide core, metallic shell, and oxide cover shell is not significantly less than that of an oxide cylinder of the same over-all radius. In this instance, the response will of course fall off rapidly with increase in cover shell thickness, although there is no thickness limitation on the cover shell from the analytical standpoint.

Relative improvement for very thin shells. - If, in figure 7(b), the radius of the very thin metallic shell is equal to the outside radius r_b (outside oxide layer of zero thickness), the approximate improvement factor and decrease in phase lag in comparison with the homogeneous metallic wire (the frequency and heat-transfer coefficient remaining fixed) are given by the following:

$$\frac{\eta_{b,1,M}}{\eta_{2,M}} = \left[\frac{\mathrm{ber}_0^2(\alpha_1 r_b) + \mathrm{bei}_0^2(\alpha_1 r_b)}{\Phi_{R,1}^2 + \Phi_{I,1}^2}\right]^{1/2} \frac{\alpha_2 r_b}{2} \left[\frac{\Phi_{R,2}^2 + \Phi_{I,2}^2}{\mathrm{ber}_0'^2(\alpha_2 r_b) + \mathrm{bei}_0^2(\alpha_2 r_b)}\right]^{1/2} \tag{18}$$

and

$$\bar{\varphi}_2 - \varphi_{b,1} = \tan^{-1} \frac{\left[\frac{\Phi_{R,2}\ \mathrm{ber}_0'(\alpha_2 r_b)}{\Phi_{I,2}\ \mathrm{bei}_0'(\alpha_2 r_b)} + 1\right]}{\left[\frac{\Phi_{R,2}}{\Phi_{I,2}} - \frac{\mathrm{ber}_0'(\alpha_2 r_b)}{\mathrm{bei}_0'(\alpha_2 r_b)}\right]} -$$

$$\tan^{-1} \frac{\left[\frac{\mathrm{ber}_0(\alpha_1 r_b)}{\mathrm{ber}_0(\alpha_1 r_b)} - \frac{\Phi_{R,1}}{\Phi_{I,1}}\right]}{\left[\frac{\Phi_{R,1}\ \mathrm{ber}_0(\alpha_1 r_b)}{\Phi_{I,1}\ \mathrm{ber}_0(\alpha_1 r_b)} + 1\right]} \tag{19}$$

These were obtained in an obvious manner from equations (9) and (15); note that in this situation $r_a = r_b$. In equations (18) and (19),

$$\left.\begin{aligned}
\Phi_{R,2} &\equiv \mathrm{Ja}_2^{-1}\ \mathrm{ber}_0'(\alpha_2 r_b) + \mathrm{ber}_0(\alpha_2 r_b) \\
\Phi_{I,2} &\equiv \mathrm{Ja}_2^{-1}\ \mathrm{bei}_0'(\alpha_2 r_b) + \mathrm{bei}_0(\alpha_2 r_b) \\
\Phi_{R,1} &\equiv \mathrm{Ja}_1^{-1}\ \mathrm{ber}_0'(\alpha_1 r_b) + \mathrm{ber}_0(\alpha_1 r_b) \\
\Phi_{I,1} &\equiv \mathrm{Ja}_1^{-1}\ \mathrm{bei}_0'(\alpha_1 r_b) + \mathrm{bei}_0(\alpha_1 r_b)
\end{aligned}\right\} \tag{20}$$

The improvement factor and decrease in phase lag are functions of any of a number of dependent sets of four parameters, for example, k_2/k_1, a_1^*/a_2^*, $\alpha_2 r_b$, and Ja_2. It happens, however, that $k_2/k_1 \cong (a_2^*/a_1^*)$, so that one of these variables is in practice supernumerary. Since the number of calculations required for a generalized solution would be prohibitively large, numerical results are best obtained for specific cases.

In figure 7(b), it is apparent that the thin shelled case is much more accurately described by the homogeneous-cylinder equations (with appropriate arguments) than is the situation of figure 7(a). The reason is that the oxide layer of figure 7(a) must be extremely thin if it is not to act as a thermal barrier, whereas in the case of figure 7(b) the metallic layer may have an appreciable thickness without seriously jeopardizing the accuracy of the simple analysis. On the other hand, it is

highly desirable from the viewpoint of attainment of high response speed to have the oxide layer of figure 7(a) as thick as practicable. Ultimately, the two-material configuration of figure 1 is again reached.

The situation of figure 7(a), for the case of a very thin surface (metallic) layer, may be more accurately analyzed as a thick-shell problem that is the reverse of the situation of figure 1; the techniques are discussed in the following section of the report. When the thick-shell approach is used, there is, of course, no limitation as to the oxide shell relative thickness. No actual computations have been carried out for this case, however.

THE TWO-MATERIAL LAMINATED CYLINDER (FINITE SHELL THICKNESS)

Moduli

The parameters required for the description of the behavior of a laminated cylinder (when the shell thickness is not small) are discussed in the present section. In addition, a qualitative description of that behavior is presented in terms of those parameters.

It should be noted that when the thermal conductivity of the core of such a structure is small as compared with conductivity levels of metals, the decoupling of surface from interior is greatly magnified. This effect, together with the limitation of the sensory portion of the instrument to the thermally active surface section, constitutes the chief advantages of the structure under consideration. The resulting performance is best explained in terms of certain nondimensional moduli derived from an appropriate set of time constants based on the preceding homogeneous-cylinder treatment.

$\tau_{ext,2}$ is the time required for the uniform temperature of a solid, homogeneous cylinder of radius r_b and made of hypothetical material of infinite thermal conductivity but having the same volumetric specific heat $\rho_2 c_{p,2}$ as the laminated-cylinder shell to change by $1 - e^{-1}$ of the total change when the environment temperature is suddenly altered to a new fixed value. The heat-transfer coefficient h_f is assumed fixed.

$\tau_{int,2}$ is the time required for the mean temperature of a solid, homogeneous cylinder of radius r_b and made of the same (real) material (of finite thermal conductivity) as the laminated-cylinder shell to change by $1 - e^{-1}$ of the total change when the surface temperature is suddenly altered. In this case, the value of h_f is not germane.

Finally, $\tau_{int,1}$ is the time required for the mean temperature of a solid, homogeneous cylinder of radius r_a and made of the same real material as the laminated-cylinder core to change by $1 - e^{-1}$ of the total change when the temperature at radius r_a is suddenly altered; here, again, external conditions are not relevant.

Three of the moduli of interest are then, explicitly, the following:

$$\left.\begin{aligned} \omega\tau_{ext,2} &= \frac{\omega r_b \rho_2 c_{p,2}}{2h_f} \\ \omega\tau_{int,2} &= \frac{\omega\lambda r_b^2 \rho_2 c_{p,2}}{k_2} \\ \omega\tau_{int,1} &= \frac{\omega\lambda r_a^2 \rho_1 c_{p,1}}{k_1} \end{aligned}\right\} \tag{21}$$

It is a straightforward matter to show, by means of the Buckingham Π theorem or otherwise, that any physical situation describable in terms of the eight variables r_a, r_b, h_f, k_1, k_2, a_1^*, a_2^*, and ω can be described in terms of $\omega\tau_{ext,2}$, $\omega\tau_{int,2}$, $\omega\tau_{int,1}$, and two additional nondimensional moduli not as yet selected. The resulting five nondimensional moduli must constitute an independent set. The additional moduli $\beta = r_a/r_b$ and $\Gamma = (k_2/k_1)\,(a_1^*/a_2^*)^{1/2}$ occur naturally in the exact theory of this configuration as presented in appendix C and are therefore adopted as the final two moduli. (Note that Γ and Γ^* in the calculations of the present treatment are equal; see appendix A.)

The relation

$$\omega\tau_{int,1} = \omega\tau_{int,2}\,\beta^2 \left(\frac{\rho_1 c_{p,1}}{\rho_2 c_{p,2}}\right)\left(\frac{k_2}{k_1}\right) \tag{22}$$

or

$$\omega\tau_{int,1} = \omega\tau_{int,2}\,\beta^2 \left(\frac{k_2}{k_1}\right) \tag{23}$$

when

$$\rho_1 c_{p,1} = \rho_2 c_{p,2}$$

should now be noted. It is to be recalled that the ultimate purpose is that of restricting temperature changes to the shell by decoupling the core from the shell; this expression states that the internal time constant of the core (with an increase of which the decoupling effect, of course, increases) exceeds that of the original wholly metallic wire by a factor which is proportional both to the square of the radius ratio r_a/r_b and to the thermal conductivity ratio k_2/k_1. The importance of maximization of β is thus emphasized.

Qualitative Response Description

In terms of the moduli mentioned, the behavior of the laminated structure may now be qualitatively discussed as follows: At frequencies so low that $\omega\tau_{int,1}$ is less than about 0.5, the entire cylinder responds as a unit and the laminated structure is indistinguishable from a homogeneous wire. Normally, $\omega\tau_{ext,2}$ under these circumstances is very small, so that the cylinder follows the external changes precisely; an exception would occur only for a vanishingly small heat-transfer coefficient, which would mean an exceptionally small Biot number $\tau_{int,2}/2\lambda\tau_{ext,2}$.

As the frequency increases, the thermal response of the core deteriorates much more rapidly than would that of a high-thermal conductivity core under the same conditions. In consequence, the shell gradually becomes isolated from the core; this process may be considered virtually complete at some $\omega\tau_{int,1}$ value between 15 and 20, depending on the ratio of core surface to mean core response that is accepted as representing "isolation". At the intermediate $\omega\tau_{int,1}$ value of 10, for example, the ratio of oxide surface amplitude to mean oxide amplitude is about 4.9, whereas at the $\omega\tau_{int,1}$ value of 17.5 it is 13.2.

Whereas the cylinder response as a whole deteriorates more rapidly with increase of frequency than does that of a homogeneous metallic cylinder, the response of the metallic shell falls off less rapidly, since exchange of heat with the relatively unresponsive core decreases with increasing frequency. At $\omega\tau_{int,1}$ values greater than about 20, the response of the shell is essentially identical with that of a shell lined on the inside by a layer of zero thermal conductivity, that is, the response is virtually the same as that of a hollow, evacuated shell. It follows that the shell response, ignoring the existence of thermal gradients within the metal, is then approximately that of a first-order system having a time constant given by

$$\tau_{ext,2,a-b} = \tau_{ext,2}\,(1 - \beta^2) \qquad (24)$$

The response associated with this single time constant $\tau_{ext,2,a-b}$ is never quite realized because the core is never perfectly decoupled from the shell and because the shell temperature (amplitude) is never quite constant.

At still higher frequencies - frequencies such that $\omega\tau_{int,2}$ is greater than about 4 to 5 - the nonuniformity of shell temperature becomes marked, and it is no longer proper to consider that the shell responds as a unit.

An approximate analysis valid under all sets of conditions such that the thermal amplitude gradient in the shell is small ($\omega\tau_{int,2}$ less than about 4) is presented in appendix D. Explicitly, it is there assumed that the shell responds as a unit, but no such assumption is made concerning the core. The relations established by that analysis are accurate for low and moderate frequencies unless k_2/k_1 is less than about 5.

Calculations and Results: Finite Shell Thicknesses

General considerations. - The mathematical techniques used in these calculations are described in detail in appendix E. In this section, selection of modulus values, organization of the calculations, and the nature and utilization of the results are discussed.

Moduli and organization of calculations. - As was mentioned previously, the relevant moduli in the laminated-cylinder situation are the following: $\omega\tau_{ext,2}$, $\omega\tau_{int,2}$, $\omega\tau_{int,1}$, β, and Γ. It was desirable that wide ranges of those variables be covered; that the ranges of greatest physical interest be emphasized; that regular sets of results be available in each of which only one variable among k_2, k_1, ω, h_f, r_b, and r_a is considered as varying; and that interpolation among calculated results be reasonably easy. For materials of present interest $\rho_1 c_{p,1}$ is always nearly equal to $\rho_2 c_{p,2}$, hence the calculations were restricted to cases in which the equality holds precisely. Instead of Γ, the ratio k_2/k_1 was taken as a primary modulus.

Calculations were made for the two relative shell thicknesses corresponding to β values of 0.75 and 0.90. It was felt that the results for these thicknesses, together with appropriate homogeneous-cylinder calculations for the cases $\beta = 0$ and $\beta =$ unity, corresponding to homogeneous metallic and oxide cylinders, respectively, would serve to establish the mean shell amplitudes and phase shifts of chief interest from the instrumentation standpoint.

Further, calculations were made for five k_2/k_1 ratios and five $\omega\tau_{int,2}$ values according to table VII, in which arbitrary case numbers and group letter designations are indicated together with the corresponding modulus magnitudes.

It is clear that the effects of variation of any single modulus among $\omega\tau_{int,2}$, k_2/k_1 and β may be observed by comparing results within an appropriate set of cases. In the case of β variations, it is necessary to consider also results for corresponding homogeneous-cylinder calculations ($\beta = 0$ and 1). In the case of k_2/k_1 variations, it may occasionally be helpful to consider results for corresponding homogeneous-cylinder calculations ($k_2/k_1 = 1$). 2922

Each $\omega\tau_{int,2}$ value corresponds to a definite $\alpha_2 r_b$ value according to the relation given in appendix A. The nondimensional variable of the heat-flow equations was $l_1 \equiv \alpha_1 r$ in these calculations (although $\alpha_2 r$ could have been used as well). The parameter αr can be considered a kind of nondimensional radius; it is, at any rate, convenient to speak of an outer "radius" $\alpha_2 r_b$ (or alternatively $\alpha_1 r_b$) and an inner "radius" $\alpha_2 r_a$ (or $\alpha_1 r_a$).

The assumed relation between $\alpha_1 r$ and $\alpha_2 r$ is the following:

$$\alpha_1 r = \alpha_2 r \, (k_2/k_1)^{1/2} \tag{26}$$

If $\rho_1 c_{p,1} \neq \rho_2 c_{p,2}$, this relation becomes

$$\alpha_1 r = \alpha_2 r \, (k_2/k_1)^{1/2} \, (\rho_1 c_{p,1}/\rho_2 c_{p,2})^{1/2}$$

For each of the 50 case numbers of table VIII, the combination of β, k_2/k_1 and $\omega\tau_{ext,2}$ leads to a core "radius" according to the relation

$$\alpha_1 r_a = \beta \alpha_2 r_b (k_2/k_1)^{1/2} \tag{27}$$

Relations (26) and (27) are valid only in the case of equality of the volumetric specific heats. An alternative point of view is that of considering that an $\omega\tau_{int,1}$ value is arrived at according to the relation

$$\omega\tau_{int,1} = \lambda\beta^2 \, (\alpha_2 r_b)^2 \, (k_2/k_1)$$

Outline of calculation procedures. - The initial mathematical procedure then consisted of performing a numerical integration of the appropriate Bessel's equation over the range $\alpha_1 r_a$ to $\alpha_1 r_b = \alpha_1 r_a \beta^{-1}$, that is, the equation is integrated outward through the shell to the surface. The starting values at the shell inner surface are the values of the ber_0 and bei_0 functions for the argument $\alpha_1 r_a$. The boundary conditions (including the change of properties) at the core-shell interface are taken into account; the details are given in appendix E. Table VIII exhibits the values of $\alpha_1 r_a$, $\alpha_1 r_b$, $\alpha_2 r_a$ and $\alpha_2 r_b$ for the 50 cases.

The results of such an integration is a pair of numbers - the values of the real and imaginary parts of the solution of the Bessel's equation at $\alpha_1 r_b$. In effect, the variation with radius of amplitude and phase of the temperature oscillation relative to conditions at the surface are obtained in this manner. The principal remaining task was that of ascertaining the actual surface amplitude and relative phase angle which, together with a given nondimensional heat-transfer coefficient $Ja_2 = h_f/(\omega k_2 \rho_2 c_{p,2})^{1/2}$, comprise a triad of values consistent with environment amplitude and phase angle. The details of this procedure are also given in appendix E together with the relations required for the calculation of local and mean shell amplitudes and phase angles.

It is sufficient here to remark that a total of 19 Ja_2 values was used with each of the 50 cases so as to cover adequately the physical realm of interest. The values of Ja_2 were arrived at by calculation according to the relation

$$Ja_2 = (\omega\tau_{int,2})^{1/2} \Big/ 2\lambda^{1/2}\, \omega\tau_{ext,2} \tag{28}$$

in which $(2\lambda^{1/2})^{-1} = 1.50075\ldots$ for $\lambda = 0.111$. The values of $\omega\tau_{int,2}$ previously mentioned were used with the set of $\omega\tau_{ext,2}$ values comprising the geometrical progression $0.1\times10^{n/4}$, where n goes from 0 to 22. It is to be noted that while pairs of successive values of $\omega\tau_{int,2}$ differ by the constant factor $10^{1/2}$, the successive values of $\omega\tau_{ext,2}$ and of Ja_2 differ by $10^{1/4}$.

The interrelations among Ja_2, Ja_2^{-1}, Bi_2, $\omega\tau_{int,2}$, $\omega\tau_{ext,2}$, Fo_2, Fo_2^*, and $\alpha_2 r_b$ are exhibited in table IX. This table will be discussed at greater length in the following section.

Results of Laminated-Cylinder Calculations and Discussion

Identity of results. - Mean relative amplitude and phase shift as well as the local (internal) variations of relative amplitude and phase shift for a wide variety of conditions are presented in table X and figures 8 to 11. The mean values are discussed first, since they are of primary importance.

The results of the laminated-cylinder and of certain additional related calculations are presented in table X. As indicated previously, the mean amplitude and phase shift were obtained for each of the listed values of the dimensionless heat-transfer coefficient Ja_2. The original calculations, discussed in appendix E, were carried out to seven or eight figures but the final results are correct only to within one unit at the fifth figure and to four units at the sixth figure. In table X, the values reproduced were rounded off to five significant figures in the case of the relative amplitudes and five significant figures in the case of the tangents of the phase angles. The laminated-cylinder phase shifts $\overline{\varphi}_2$ are given only to three decimal places because these were rounded off in that manner preparatory to curve plotting. The remaining phase shifts are given either to five significant figures or four decimal places. While $\overline{\varphi}_2$ is given only to three decimal places, greater accuracy can be recovered, if desired, by using the corresponding $\tan \overline{\varphi}_2$ values; the latter are included here because many of the formulas of the present work involve the tangent of the angle rather than the angle itself.

The arrangement of the laminated-cylinder ($\beta = 0.90$ and 0.75) results in table X corresponds to the case number order of table VII. Comparisons among different sets of results may therefore easily be made, as indicated previously in connection with the discussion of table VII.

In addition, results are included of calculations for corresponding oxide-cylinder surface cases and exact and "first order" (uniform temperature assumption) homogeneous-cylinder cases. The value of Ja_1 used in each oxide-cylinder calculation was, of course, equal to $Ja_2\sqrt{k_2/k_1}$. It follows that the homogeneous-oxide-cylinder surface $\eta_{b,M}$ and φ_b values represents limiting values which may be approached in real situations but never attained, since they correspond to $\beta = 1$ ($r_a = r_b$).

Qualitative examination of results. - A number of interesting comparisons can be made. At the smaller $\omega\tau_{ext}$ values (less than about 3), the homogeneous-cylinder amplitude at a given Ja_2 is actually slightly greater than the laminated-shell value but as the $\omega\tau_{ext}$ value continues to increase (say, to 10), the shell values at the various k_2/k_1 ratios

become greater, particularly at the high k_2/k_1 values. A related, and rather remarkable, variation of $\bar{\eta}_2$ among the shell values at the lowest $\omega\tau_{ext,2}$ values may be noted, namely, an initial decrease of $\bar{\eta}_2$ with increasing k_2/k_1, followed by a reversal of this trend. At successively higher $\omega\tau_{ext,2}$ values, this reversal is gradually eliminated until the homogeneous-cylinder amplitudes fall invariably below all the others. No satisfactory explanation of all of these effects is available.

A detailed comparison of the results at the several β values indicates that at moderate $\omega\tau_{int,2}$ values, the improvement factor decreases markedly as the shell thickness increases moderately. For example, at an $\omega\tau_{int,2}$ value of 1.0 and an $\omega\tau_{ext,2}$ value of 100, the amplitude values for $k_2/k_1 = 40$ are as follows: $\beta = 1$ (oxide surface), 0.090430; $\beta = 0.90$, 0.037681; $\beta = 0.75$, 0.020378; and $\beta = 0$ (homogeneous cylinder - exact solution), 0.0099049. The successive ratios of mean shell response to oxide-cylinder surface response for the 0.90 shell, 0.75 shell, and 0.0 shell (i.e., homogeneous metallic cylinder) are 0.417, 0.225, and 0.1095, respectively. Therefore, the decrease in amplitude, in going from the β = unity (oxide cylinder) case to the 0.75 shell case, is much greater than the change between the 0.75 shell case and the $\beta = 0$ (homogeneous cylinder) case.

Variable-frequency plots. - Certain additional comparisons are best made in connection with the discussion of the variable-frequency plots. Mean relative amplitude and phase angle are plotted in figures 8 and 9, respectively, as functions of the parameter $\omega\tau_{int,2}$; in the meantime $\omega\tau_{ext,2}$ is permitted to vary in the manner in which it would if ω alone were varying in the case of each modulus.

Amplitude curves for each lettered group (β and k_2/k_1 constant) constitute a single part of figure 8, while the phase results constitute a single part of figure 9. The parameter held constant in the case of each phase shift curve and in the case of each of the principal amplitude curves (running from upper left to lower right) is the Biot number Bi_2, the value of which is indicated on each curve. The independent variable has been taken as $\omega\tau_{int,2}$ to conserve space. In effect, the sole variable of these principal curves is the frequency (although other possibilities, not all particularly useful, will be mentioned). In addition, secondary curves are drawn on the amplitude sheets (fig. 8); their meaning and use are explained elsewhere.

The amplitude and phase shift values for these plots were selected with the help of table IX and the expression

$$Ja_2 = \frac{1.50075 \cdot \cdot \cdot (\omega\tau_{int,2})^{1/2}}{\omega\tau_{ext,2}} \tag{29}$$

It is clear that upon increasing or decreasing the frequency by some factor, Ja_2 will decrease or increase, respectively, by the square root of that factor while $\omega\tau_{int,2}$ and $\omega\tau_{ext,2}$ will vary directly with the factor.

In table IX, it will be noticed that the successive combinations of $\omega\tau_{ext,2}$, $\omega\tau_{int,2}$, and Ja_2 required for a given amplitude curve lie along a diagonal line inclined upward from left to right and along which the Biot number is constant. The fact that a succession of columns of table IX must be traversed indicates that the successive mean amplitudes and phase shifts must be found, not in the results for any one case, but rather in a properly chosen set. For example, if cylinder responses are desired for a β of 0.75 and k_2/k_1 of 5, the successive pairs of values would be chosen from among the F group of cases, namely, 1, 5, 12, 22, and 32 (see table VII); the amplitude and phase shift for the Ja_2 value 0.084394 would be selected from the case 1 results (see table X), the amplitude and phase shift for the Ja_2 value 0.047458 from the case 5 results, etc.

All of the calculated results were grouped in this manner to facilitate plotting. Although the sole variable of the principal curves is frequency, it is possible to select other variables or combinations of variables in such a way that the curves may be interpreted as representing the effects of variations of such single variables or combinations. Explicitly, either ω, ρ, c_p, $\omega\rho$, ωc_p, or $\omega\rho c_p$ may be considered to be the sole variable of these presentations.

When the different amplitude curves of a single part of figure 8 are compared, it should be noted that $\omega\tau_{ext,2}$ is not constant along a vertical (constant $\omega\tau_{int,2}$) line crossing successive curves. The $\omega\tau_{ext,2}$ scale values increase by a factor of $10^{1/4}$ as each successive curve is reached (proceeding from top to bottom). The secondary curves of figure 8 bring out these $\omega\tau_{ext,2}$ changes more clearly and enable easy intercomparison of amplitudes for different primary curves. Their significance will be discussed subsequently.

In these plots, the curves were drawn for values of $\omega\tau_{int,2} < 0.1$ and > 10 by extrapolation; curve values lying outside of the range $\sim 0.07 < \omega\tau_{int,2} < \sim 15$ should not be considered to be quantitatively correct even though considerable care was exercised in the fairing process. Curve values within the $\omega\tau_{int,2}$ range mentioned are generally correct to within ± 1 percent. On the other hand, values for $\omega\tau_{int,2}$ lying outside of the range in question may be as much as 10 percent in error in isolated cases, though these large errors are improbable and will be reached (if at all) only at $\omega\tau_{int,2}$ values of about 0.025 at one end of the scale and of 40 at the other end. In general, values within the ranges $0.025 \leq \omega\tau_{int,2} \leq 0.07$ and $15 \leq \omega\tau_{int,2} \leq 40$ are probably correct to within 4 percent.

2262

At high $\omega\tau_{ext,2}$ values (fig. 10), $\bar{\eta}_2$ values for various k_2/k_1 ratios tend to coincide or even "cross over." For example, the Bi = 0.450 amplitudes exhibit this behavior; at smaller Bi numbers the tendency is less marked, although still present (for example, the Bi = 0.00450 amplitude curves).

CE-4 back

The improvement in response exhibited in figure 10 in going from a 0.25 relative thickness shell ($\beta = 0.75$) to a 0.1 shell ($\beta = 0.90$) is very marked at all Biot numbers at $\omega\tau_{ext,2}$ values that are in each case high enough to ensure substantial improvement of response for the change from the conventional wire to the laminated structure. The $\beta = 0.90$, Bi = 0.450 curves depart markedly from the first-order curve at an $\omega\tau_{ext,2}$ value of about 7, and the $\beta = 0.75$, Bi = 450 amplitudes are significantly lower at that point. Similarly, while the $\beta = 0.90$ and $\beta = 0.75$ curves for Bi = 0.00450 overlap extensively at an $\omega\tau_{ext,2}$ value of 100 (where, at k_2/k_1 less than 80, little gain is available), the $\beta = 0.90$ curves are all substantially above the $\beta = 0.75$ curves at $\omega\tau_{ext,2}$ values of 700 and beyond.

The significance of the secondary curves (running from lower left to upper right) of figure 8 is now discussed. Consider, for example, in figure 8(a), the third curve from the bottom. This curve intersects the principal curves at points such that $\omega\tau_{int,2}$ changes by successive factors of $10^{1/4}$, as does Bi_2. At the same time, $\omega\tau_{ext,2}$ remains fixed and Ja_2^{-1} (or Ja_2) changes by successive factors of $10^{1/8}$. The only physical variable contained in $\omega\tau_{int,2}$ that is not a factor of $\omega\tau_{ext,2}$ is k_2. Accordingly, these secondary curves display the change of $\bar{\eta}_2$ with the thermal conductivity level of the entire laminated cylinder and it is clear that k_1 must change proportionally so as to maintain constancy of the ratio k_2/k_1.

In particular, the curves, rising toward the right, display the increase of $\bar{\eta}_2$ with decreasing k_1 and k_2 at high and moderate values of $\omega\tau_{ext,2}$ (for example, the curves at low and intermediate $\bar{\eta}_2$ values of the D group, figure 8(d)) as well as the tendency for $\bar{\eta}_2$ to reach a maximum at moderate $\omega\tau_{int,2}$ values and low $\omega\tau_{ext,2}$ values, the maximum being followed by a falling off of $\bar{\eta}_2$ at higher $\omega\tau_{int,2}$ values. For example, the $\omega\tau_{ext,2} = 1.78$ secondary curve of the D group reaches a maximum of 0.82 at about an $\omega\tau_{int,2}$ value of 3 while $\bar{\eta}_2$ values at higher and lower $\omega\tau_{int,2}$ values are lower. This characteristic of the secondary curves (attainment of a maximum) is more pronounced in the case of the $\beta = 0.75$ groups, as is evident upon comparison of the figure 8(d) and figure 8(a) secondary curves. No satisfactory explanation of this phenomenon is available. 2922

Finally, it should be noted that the successive combinations of Ja_2, Bi_2, $\omega\tau_{int,2}$, and (fixed) $\omega\tau_{ext,2}$ for the secondary amplitude curves lie along a diagonal of table IX running from the lower right to upper left, the case numbers changing appropriately.

Other ways in which these results may be used are now considered. The successive table IX modulus combinations that are encountered during excursions parallel to the two principal diagonal directions and in a vertical (columnar) direction have been previously discussed. Such excursions - with appropriate case number changes - were found to yield increasing frequency (or ρ, c_p, $\omega\rho$, ωc_p, or $\omega\rho c_p$) data, thermal conductivity data, and heat-transfer data for ascending-to-the-upper-right diagonal excursions, descending-to-the-lower-right diagonal excursions, and top-to-bottom columnar excursions, respectively. These are exemplified within table IX by the sets of entries identified in the footnotes. It should now be noted that Ja_2 is independent of r_b, and a consideration of the changes of $\omega\tau_{int,2}$ and $\omega\tau_{ext,2}$ along a row of table IX leads to the conclusion that, at a fixed Ja_2 value in the correct sequence of case numbers, successive increases of r_b by factors of $10^{1/4}$ cause changes of those moduli and of Bi_2 corresponding to successive entries in any row (proceeding toward the right). At each step, $\omega\tau_{int,2}$ increases by $10^{1/2}$, $\omega\tau_{ext,2}$ increases by $10^{1/4}$, and Bi_2 increases by $10^{1/4}$. As an example (table XI), $\bar{\eta}_2$ for $\beta = 0.90$, $k_2/k_1 = 40$, $\omega\tau_{int,2} = 0.1$, $\omega\tau_{ext,2} = 100$, and $Ja_2 = 0.004746$ is 0.022456, while $\bar{\eta}_2$ for the same β, k_2/k_1, and Ja_2 but for $\omega\tau_{int,2} = 0.3162$ and $\omega\tau_{ext,2} = 178$ is 0.017124. The respective Biot numbers are 0.0045045 and 0.0080103.

Extension of Calculations to Lower and Higher Frequencies

If desired, the approximate treatment presented in appendix D may be used to extend the plots of figures 8 and 9 to low values of $\omega\tau_{int}$. The calculations of this kind made to date are considered insufficient to warrant inclusion in the present report.

At very high $\omega\tau_{int}$ values, the core is virtually decoupled, so that the so-called "exact" hollow-shell theory of appendix F is applicable. While that theory is not actually exact in this case, the errors would be small.

NUMERICAL EXAMPLES AND DISCUSSION

General Considerations

Two kinds of "numerical examples" will be presented in this section. First, numerical values of amplitude and phase shift at isolated pairs of $\omega\tau_{int,2}$ and $\omega\tau_{ext,2}$ values are given in table XI for certain sets of cylinders having a common outer radius. The cylinders considered are: A homogeneous metallic wire ($\beta = 0$), laminated cylinders ($\beta = 0.90$) for $k_2/k_1 = 5$, and 40, and an oxide cylinder ($\beta = 1.00$). In the case of the oxide cylinder, the thermal conductivity is also assumed to be either one-fifth or one-fortieth of the conductivity of the metallic homogeneous cylinders. The same metal is assumed to be used in both the homogeneous and laminated cylinders. Second, numerical results for large ranges of $\omega\tau_{ext,2}$ are given for three hypothetical laminated wires of a specified size and exposed to a specified air flow.

Selected Sets of Generalized Results

The first set of results, already published in large part in reference 15, is exhibited as table XI which, for ease of reproduction, has been split into two parts (with some overlapping). It is emphasized that these excerpted sets constitute merely a small portion of the results presented in table X. In the first part, the values of the parameters k_2/k_1, $\omega\tau_{int,2}$, Ja_2, $\alpha_1 r_a$, $\alpha_1 r_b$, $\alpha_2 r_a$, and $\alpha_2 r_b$ are given. The latter four parameters apply, as a group, only in the laminated-cylinder situation, and then only for $\beta = 0.90$. In the homogeneous-metallic-cylinder situation, no second material is present, so that α_1 has no meaning (since $r_a = 0$); in that case, only $\alpha_2 r_b$ has significance. In the zero-thickness shell case, that is, the situation involving the surface temperature amplitude and phase when a surface-coated oxide cylinder

replaces the metallic cylinder, the applicable parameter is $\alpha_1 r_b$. In effect, the $\omega\tau_{int}$ product for the (entire) metallic cylinder has been replaced by the $\omega\tau_{int}$ product of the oxide cylinder.

In any given row of the table, the following may be considered to be fixed: r_b, ω, h_f, and the ratio of metal to oxide (if any) thermal conductivity. From row to row r_b, ω, and h_f are of course free to change in any manner as long as the resulting nondimensional parameters have the values listed.

The significant facts brought out in table XI are the following:

(1) For small and moderately large values of $\omega\tau_{int}$ at large $\omega\tau_{ext}$ values, the exact and "first-order" solutions for the homogeneous-cylinder situation are nearly identical, so that, for such $\omega\tau_{int}$ - $\omega\tau_{ext}$ combinations, it is sufficiently accurate to compare the laminated-cylinder or thin-layer coated oxide-cylinder solutions with first-order solutions.

(2) $\beta = 0.90$ amplitudes and phase shifts are distinctly inferior to those of the $\beta = 1$ (thin-layer) oxide cylinders. Whereas all-oxide cylinders are capable of indefinitely large gains, $\beta = 0.90$ cylinders are inherently incapable of gains greater than about 5. For example, in the last line of table XI the amplitude gain in going from a metallic cylinder to a $\beta = 0.90$ cylinder of $k_2/k_1 = 40$ is 3.8+, whereas the gain for the $\beta = 1$ case is 9.6+.

That this limitation must be present follows from the consideration that the ratio of metallic cross section to total cross section (in the case of the $\beta = 0.90$ laminated structure) is just $\frac{r_b^2 - r_a^2}{r_b^2} = 1 - \beta^2 = 0.19$. The first-order response of a hypothetical hollow metallic shell of the same dimensions would thus be 5.23 times as great as the first-order response of the original metallic cylinder (or, for that matter, of the laminated cylinder when $\rho_1 c_{p,1} = \rho_2 c_{p,2}$). Since the response of the laminated cylinder is never quite as good as that of such a hollow shell, a $\beta = 0.90$ structure cannot have a gain greater than about 5.

The exact expression for the amplitude at very large $\omega\tau_{ext}$ values may easily be deduced from the definitions of $\Phi_{R,b}$ and $\Phi_{I,b}$:

$$\lim_{Ja_2 \to 0} (\Phi_{R,b}^2 + \Phi_{I,b}^2)^{-1/2} = Ja_2 (R_b'^2 + Im_b'^2)^{-1/2} (a_1^*/a_2^*)^{1/2} \tag{30}$$

Using, for example, equation (E15), it follows then that as Ja_2 approaches zero,

$$\bar{\eta}_{2,M} = \frac{2Ja_2\left[(R_b' - \beta R_a')^2 + (Im_b' - \beta Im_a')^2\right]^{1/2}}{l_b^*(1 - \beta^2)(R_b'^2 + Im_b'^2)^{1/2}} \tag{31}$$

A group of the factors on the right may be expressed as follows:

$$\frac{2Ja_2}{l_b^*(1 - \beta^2)} = \frac{2h_f a_2^*}{l_b(1 - \beta^2)\,\omega k_2}$$

$$= \left[(\omega\tau_{ext,2})(1 - \beta^2)\right]^{-1}$$

$$= (\omega\tau_{ext,2,a-b})^{-1} \tag{32}$$

(This should be compared with equation (24).)

In equation (32), $\tau_{ext,2}$ equals $(r_b\rho_2 c_{p,2})/2h_f$; this is, of course, the external time constant of a homogeneous cylinder consisting entirely of material 2 (or material 1 if $\rho_1 c_{p,1} = \rho_2 c_{p,2}$). The time constant of a homogeneous cylinder consisting entirely of material 2 but of radius r_a would be $(r_a\rho_2 c_{p,2})/2h_f$. The external time constant of the shell would be obtained by using the thermal capacity of the shell alone, and this time constant is

$$\tau_{ext,2,a-b} = \left[\rho_2 c_{p,2}(r_b^2 - r_a^2)\right]/2r_b h_f = \left[\rho_2 c_{p,2} r_b(1 - \beta^2)\right]/2h_f$$

It follows that

$$\bar{\eta}_{2,M} = \frac{1}{\omega\tau_{ext,2,a-b}} \frac{\left[(R_b' - \beta R_a')^2 + (Im_b' - \beta Im_a')^2\right]^{1/2}}{(R_b'^2 + Im_b'^2)^{1/2}} \tag{33}$$

It will be noted that $\beta R_a'/R_b'$ and $\beta Im_a'/Im_b'$ will be rather small when there is little heat exchange between core and shell - which will be particularly true at high k_2/k_1 ratios. Indeed, if $(R_b' - \beta R_a') \to R_b'$ and $Im_b' - \beta Im_a' \to Im_b'$, then the above relation reduces simply to

$$\lim_{Ja_2 \to 0,\ \frac{k_2}{k_1} \to \infty} \bar{\eta}_{2,M} = (\omega\tau_{ext,2,a\text{-}b})^{-1} \qquad (34)$$

which is what would be expected at high $\omega\tau_{ext}$ values

Values of the factor $\left\{\left[(R_b' - \beta R_a')^2 + (Im_b' - \beta Im_a')^2\right]/(R_b'^2 + Im_b'^2)\right\}^{1/2} \equiv \zeta^{-1}$ are given in table XII and represent the extent to which core-shell coupling persists in each case. Note, however, that the asymptotic condition always represents an improvement over the simple-cylinder situation.

2922

Results for Actual Situations and Discussion

The second "numerical example" concerns three platinum - fused-quartz wires of different size - specifically, 0.0004 (wire A), 0.002 (wire B), and 0.010 (wire C) inch in diameter. The 0.0004-inch-diameter wire is typical of hot-wire anemometry; no significantly smaller drawn wire is commercially available. A somewhat smaller etched tungsten or Wollaston-process noble-metal wire is, however, available. The numerical example given here may be used to determine the advantage (if any) of a larger laminated wire over homogeneous wires of this (0.0004 in.) diameter or smaller. The largest wire (0.010 in. diam) is representative of most thermocouples used, for example, in jet engine studies. Wire B (intermediate size, 0.002 in.) was selected as a compromise wire for comparison purposes.

The thermal conductivities of platinum and fused quartz vary in such a manner with temperature that a temperature can be found (in the vicinity of 350° C) at which the ratio k_2/k_1 is precisely 40. It is not, however, necessary that this exact temperature be known, since the response of a hypothetical laminated structure of these materials does not vary radically with slight departures of the ratio from an assumed nominal number (such as 40). Accordingly, it is assumed that each of the laminated wires A, B, and C consists of a core of fused quartz covered by a concentric shell of platinum, the value of β being 0.90 (thickness 0.1 r_b). At the operating temperature, the volumetric specific heat ρc_p of each material will be about 0.60 cal cm^{-3} $^{\circ}C^{-1}$, and the thermal diffusivity of platinum may be taken as 0.29 cm^2 sec^{-1} at the operating temperature with little error (0.293 was actually used in the original calculations).

Air-flow conditions are assumed to be the following: Mach number, 0.5; static pressure, 1 atmosphere; total temperature, 500° R.

Orthogonal incidence is assumed. Calculation of τ_{ext} is facilitated by the use of a nomograph (fig. 17 of ref. 16) for the calculation of such time constants. The nomograph is most easily used in this instance by obtaining the time constant of a wire of a particular diameter and then using the fact that the time constant varies as the 1.5 power of the diameter when all other variables remain fixed. From the nomograph, a constant of 0.040 second is obtained for a 0.006-inch-diameter wire. It follows that τ_{ext} for wire A is 688 microseconds, for wire B is 7.70 milliseconds, and for wire C is 86.1 milliseconds. (The external time constant of a platinum 0.0002-inch wire, used later in comparisons, is 243 microseconds under the assumed conditions.)

The several time constants and Biot numbers are exhibited in the following list:

Wire	Size, in.	External time constant, $\tau_{ext,2}$, sec	External cut-off frequency where $\omega\tau_{ext,2}=1$, cps	Internal time constant, $\tau_{int,2}$, sec	External cut-off frequency where $\omega\tau_{int,2}=1$, cps	Biot number, Bi_2	External-internal time constant ratio, $\tau_{ext,2}/\tau_{int,2}$ (a)
-	0.0002	243×10^{-6}	655	----------	---------	--------	----
A	.0004	688×10^{-6}	231.3	0.0978×10^{-6}	1,627,000	0.000640	7030
B	.0020	7.70×10^{-3}	20.67	2.444×10^{-6}	65,100	.00143	3150
C	.010	86.1×10^{-3}	1.848	61.1×10^{-6}	2,605	.00320	1409

[a] $\tau_{ext}/\tau_{int} = 1/0.222\ Bi$.

The frequencies corresponding to the $\omega\tau_{int,2}$ values 0.01, 0.0316228, 0.1, etc., are then easily calculated. The frequencies are given in the following table:

$\omega\tau_{int,2}$ (approx.)	Wire A, 0.0004 in.		Wire B, 0.0020 in.		Wire C, 0.010 in.	
	External time constant, $\omega\tau_{ext}$	Frequency, cps	$\omega\tau_{ext}$	Frequency, cps	$\omega\tau_{ext}$	Frequency, cps
0.01	70.4	16,270	31.49	651	14.09	26.05
.0316	222.6	51,460	99.7	2,059	44.6	82.4
.1	704	162,700	314.9	6,510	140.9	260.5
.316	2226	514,600	997	20,590	446	824
1	7040	1,627,000	3149	65,100	1,409	2,605
3.16	----	---------	9970	205,900	4,460	8,240
10	----	---------	----	-------	14,090	26,050

Frequencies at which wire response is less than about 0.0003 are not given, since these lack practical significance.

The curves of figure 11 exhibit the variation with frequency of the response of the three kinds of wires, namely, laminated cylinders of diameters A, B, and C; homogeneous metallic (platinum) cylinders of the same respective diameters; and fused-quartz cylinders of the same respective diameters having infinitesimal surface metallic layers.

The homogeneous-cylinder results are not exact, but are "first order"; these are not seriously in error at any $\omega\tau_{int} - \omega\tau_{ext}$ value combination for which these results have been computed.

The oxide-surface results are taken from unpublished computations made at the Lewis laboratory which are known to be correct to five significant figures.

The construction of these curves is of some interest: The Biot number of wire B corresponds closely with one of the values of the original computations. Therefore, in the case of the laminated wire B, it was necessary merely to slide the (translucent) sheet of graph paper (fig. 11) over the proper original set of amplitude curves (fig. 8) and so to line up the two sheets that the vertical lines representing frequencies of the abscissa scale of the figure 11 sheet fell on top of the corresponding $\omega\tau_{int}$ values of the original curves and that the amplitude scales were alined.

In the case of the oxide-surface amplitudes of wire B, computed points were available which also correspond closely to the Biot number of that wire. The first-order points were of course obtained in an elementary fashion from the function $\left[1 + (\omega\tau_{ext})^2\right]^{-1/2}$.

In the case of wires A and C, interpolation procedures were required which are described in appendix G.

The several curves of figure 11 are of interest from a number of viewpoints. For example, it would not ordinarily be thought feasible to use a 0.01 wire at frequencies as high as 10,000 cps, yet the relative response of the 0.01-inch-laminated cylinder for the case $\beta = 1$ is about 0.0035 - small, but well within compensable limits (that is, the signal-to-noise ratio will in general be usably high). While a "surface" layer is very nearly realizable in the case of a 0.01 wire, the $\beta = 0.90$ and 0.75 curves clearly indicate the penalty involved if the layer relative thickness is for some reason permitted to be substantial.

A comparison of the response of the 0.0002-inch-conventional wire, the response of the 0.0004-inch-laminated cylinder for a β of 0.90, and the response of the 0.002-inch-surface-coated-oxide cylinder ($\beta = 1$) reveals that these responses are roughly the same in the vicinity of 700 kilocycles per second. The 700-kilocycle-per-second region is of special interest in the case of these particular response curves for two reasons: First, at frequencies greater than 700 kilocycles per second these responses drop below the level (0.001) at which the noise-to-signal ratio is often high enough to cause prohibitive difficulties in the evaluation of output waveforms; and second, it is currently considered desirable to extend hot-wire response to the 10^6 cps area in supersonic work. It therefore follows that the goal of 10^6 cps useful response can be approached by using an extremely thin coating on "wires" of sizes greater than 0.001 inch.

Ribbons of 0.00006-inch thickness have actually been rolled from platinum-rhodium and platinum-iridium wires of about 0.00044-inch diameter by a manufacturer specializing in fine-wire drawing. These ribbons, when wound in the form of an open helix on a 0.002-inch core (for example), yield a β value of about 0.94, so that the actual response realized by using such ribbons will be intermediate between those of the $\beta = 0.90$ and $\beta = 1$ situations. A ribbon thickness of 0.00006 inch does not represent the lower limit attainable by the use of known wire-flattening techniques, so that further improvement is still possible in that direction.

It is pertinent here to remark that as $h_f \to 0$ or $\omega \to \infty$, the surface response of a cylinder approaches (and, in fact, becomes for all practical purposes at moderate frequencies in the case of an oxide cylinder) the parameter Ja itself (which is, of course, independent of r_b). That this is true is easily shown: First, it is clear that as Ja approaches zero, the surface amplitude is given by the following:

$$\eta_{b,M} \underset{Ja \to 0}{\longrightarrow} \frac{(ber_{0,b}^2 + bei_{0,b}^2)^{1/2}\ Ja}{(ber_{0,b}'^2 + bei_{0,b}'^2)^{1/2}}$$

Second, it should be noted (ref. 17, pp. 333-335, e.g.) that both $(ber_{0,b}^2 + bei_{0,b}^2)^{1/2}$ and $(ber_{0,b}'^2 + bei_{0,b}'^2)^{1/2}$ approach the same function $e^{x/\sqrt{2}}/(2\pi x)^{1/2}$ as ω approaches ∞. The above expression for η_b, therefore, does approach Ja. The corresponding asymptotic phase angle is 45°, which is obtained in a similar manner by noting that as the argument increases

$$ber_0'(x) \to \frac{\sqrt{2}}{2}\,(ber_0(x) - bei_0(x))$$

and

$$bei_0'(x) \to \frac{\sqrt{2}}{2}\,(ber_0(x) + bei_0(x))_0$$

It is very interesting, in this connection, that the corresponding asymptotic relations for the slab are identical, as, of course, they must be of necessity. (They are not derived here, but may be easily obtained from, e.g., material in ref. 11 or eqs. (6a) or (6b) of ref. 10.) An inspection of the three surface curves will indicate that to the right of the point of departure of each surface curve from the corresponding first-order response curve each surface "curve" becomes a straight line. The ordinates of all points lying along each such straight line can be rather accurately established by using the simple relation given above ($\eta_{b,M} = Ja$) provided the Jakob number is computed for the oxide (that is, by using the thermal conductivity of the oxide: $Ja_1 = \sqrt{k_2/k_1}\ Ja_2$).

The ratio of surface ($\beta = 1$) response to first-order response increases indefinitely with frequency. Inasmuch as the surface response falls off at the rate of 3 decibels per octave (that is, by a factor of $\sqrt{2}/2$ for each doubling of frequency), whereas the first-order response falls off at 6 decibels per octave, the relative gain of the oxide surface hybrid "wire" increases at the rate of 3 decibels per octave. The actual ratio depends upon the numerical values of the parameters of a particular situation in the following manner:

$$\frac{\text{Asymptotic surface response}}{\text{Asymptotic first-order response}} = (Ja_1)(\omega\tau_{ext,2})$$

This response ratio may also be expressed as

$$(\omega\tau_{int,2})^{1/2}\left(\frac{k_2\rho_2 c_{p,2}}{k_1\rho_1 c_{p,1}}\right)^{1/2}(2\lambda^{1/2})^{-1} = \left(\frac{\omega\rho_2^2 c_{p,2}}{k_1\rho_1 c_{p,1}}\right)^{1/2}\frac{r_b}{2}$$

It should be noted that the asymptotic surface responses of these wires of different size are different because the respective heat-transfer coefficients are different. In particular, inasmuch as Ja_1 varies directly with h_f, and h_f varies with a power of wire diameter lying between -0.5 and -0.2 for the Reynolds number (based on wire diameter) regime in question (0 to about 5000), the surface response will increase with decreasing wire diameter. All other variables are assumed fixed. It is felt that comparisons of this kind, based as they are on some fixed air flow, are much more meaningful than comparisons which would involve an assumption of constancy of h_f. In general, then, even if a zero-thickness metallic layer is assumed approachable at all wire sizes, it still is desirable to minimize wire diameter from the frequency-response standpoint. This conclusion holds, of course, for coatings not approaching zero in relative thickness - for example, whenever an actual ribbon of fixed thickness is available. The same 0.00006-inch ribbon, when combined with a core of 0.00188-inch diameter, will yield a β ratio of 0.94 at an over-all diameter of 0.002 inch; when combined with a core of 0.00028-inch diameter, the 0.00006-inch ribbon will yield a β ratio of 0.70 at an over-all diameter of 0.0004 inch. (Incidentally, the ribbon will be much more difficult to wind at the 0.0004-in. size, but the winding can be effected if the ribbon is electrically heated during the winding process.)

Under such conditions, the response of the 0.002-inch-laminated wire (at a β of 0.94) will be markedly inferior to that of the 0.0004-inch-laminated wire (at a β of 0.70) up to frequencies of the order of 100 kilocycles per second. At this frequency, however, the response ratio has dropped to about two-to-one ($\sim$0.003 as compared with $\sim$0.0015). At still higher frequencies, there is little difference between their responses, so that for work involving frequencies above 100 kilocycles per second, the much stronger 0.002-inch (or possibly 0.0015 in.) wire might well be employed.

The homogeneous (metallic) cylinder points, although calculated, were not plotted because, in general, they are not significantly less than the corresponding first-order points on log-log plots covering the wire sizes and frequencies of present interest in thermocouple or hot-wire anemometer research. As a typical example, the first-order and "exact" (homogeneous-cylinder-of-finite-conductivity) amplitudes, at a frequency of 65,100 cps for the 0.002-inch wire, are 0.000317 and 0.000316, respectively.

CONCLUSIONS AND SUMMARY OF RESULTS

This report is chiefly concerned with the responses of infinitely long, circular cylinders to sinusoidal changes of environmental effective temperature. Both homogeneous cylinders and laminated structures are considered. Local and mean instantaneous relative temperature amplitudes and phases are determined and presented. The analytical and numerical results are applicable to situations in which the heat-transfer coefficient alone is changing provided the changes are small and to situations in which both temperature and small heat-transfer coefficient changes are occurring simultaneously.

Analytical and numerical results concerning homogeneous cylinders, as previously given in the literature, are extended and organized on the basis of two time constants. In particular, a relation yielding the space-mean value of the instantaneous temperature of a homogeneous cylinder has been obtained. The two time constants are the conventional time constant, herein designated the "external" time constant, of a hot-wire anemometer or thermocouple, and a so-called "internal" time constant. The latter is the time required for the mean cylinder temperature to change by $1 - e^{-1}$ of the total change after a sudden change of cylinder surface temperature to some new value.

Interrelations among these time constants, certain additional parameters now in use, and the parameters used in earlier work are given.

The conclusion is reached that the deviation of the behavior of ordinary (metallic) wires from that usually assumed in conventional ("first-order") analyses is negligible for most engineering purposes.

The behavior of a homogeneous cylinder of low-thermal conductivity covered by an electrically sensitive layer of negligible thickness is considered. It is concluded that the response, in the sense of ratio of temperature oscillation amplitude within the very thin surface layer to external temperature oscillation amplitude, is better than that of a homogeneous metallic cylinder by a factor which is of the order of ten under many conditions, but which may be substantially higher.

A treatment of the general case of the two-material laminated cylinder (finite shell thickness) is then given. The analytical solution is obtained and is used primarily to check extensive generalized numerical results obtained by the method of numerical integration.

The behavior of laminated cylinders consisting of a core of low-thermal conductivity and a surrounding concentric shell of electrically sensitive material in perfect thermal contact with the core is investigated numerically and presented graphically for all combinations of

the following variables: ratio of thermal conductivity of shell to that of core: 5, 10, 20, 40, and 80; ratio of shell thickness to over-all radius: 0.75 and 0.90; 19 different values of the nondimensional heat-transfer coefficient (designated the Jakob number); product of angular frequency and internal time constant: 0.10, 0.316228, 1.0, 3.16228, and 10.0.

Typical response gains for a relative shell thickness of 0.1 (of over-all radius) are of the order of 4.5; these gains are not generally manifested until the response of the laminated cylinder drops below the 0.01 level. Gains for the 0.25 shell thickness situation are markedly lower; response is critically dependent on shell thickness. In general, significant improvement in response is affected by a change from a shell relative thickness of 0.1 to 0.05.

Dependency of laminated-cylinder response upon the ratio of shell thermal conductivity to core thermal conductivity is strong but not critical. While the larger gains are not achieved until conductivity ratios of the order of 15 are reached, the improvement beyond that ratio is significant but not substantial. In general, a conductivity ratio of at least 20 will ensure gains of the order of those cited above.

The responses of 0.0004-, 0.002-, and 0.010-inch-diameter homogeneous and laminated wires of platinum and/or fused quartz exposed to a typical air stream are considered in some detail.

It is concluded that while conventional amplifying equipment by no means exhausts the intelligence-conveying capabilities of ordinary wires (particularly those of less than 0.0004-inch diameter), the use of laminated structures should make possible 670,000 cps response at wire sizes of the order of 0.002 inch and 10,000 cps response at wire sizes of the order of 0.01 inch. In particular, responses of these wires at the respective mentioned frequencies are about 0.001, which is, roughly, the limit of compensable response.

In general, it is concluded that development of laminated structures characterized by very thin relative shell thicknesses and moderately large ratios of shell thermal conductivity to core conductivity will improve the frequency-response capabilities of hot-wire anemometers and exposed-wire resistance thermometers and thermocouples by about an order of magnitude.

Finally, a simple, approximate theory of the laminated structure is given which assumes that the shell temperature is uniform, and the exact theory of the hollow shell which the laminated structure closely approaches at high frequencies is given.

Lewis Flight Propulsion Laboratory
National Advisory Committee for Aeronautics
Cleveland, Ohio, May 25, 1955

APPENDIX A

SYMBOLS

The following symbols are used in this report:

A	$\left(\frac{\alpha_2}{\alpha_1}\right)^2$; when assumption is made that $\rho_1 c_{p,1} = \rho_2 c_{p,2}$, $\left(\frac{\alpha_2}{\alpha_1}\right)^2 = \frac{k_1}{k_2}$
a^*	thermal diffusivity of cylinder material ($a^*_{1,2}$ has special meaning $k_1/\rho_2 c_{p,2}$)
B_j	j^{th} coefficient of series of eq. (4)
Bi	Biot number, $h_f r_b/k$ (note: k in this case must be conductivity of cylinder material)
ber_p, bei_p	Bessel-Kelvin functions of order p defined by relation $J_p(xi^{3/2}) \equiv ber_p(x) + i\, bei_p(x)$ (Note: The notation $ber_{p,a} \equiv ber_p(r_a)$, etc., is occasionally used)
C	initially undetermined complex constant, see appendix B
$C_2^*, D_2^*, E_2^*, G_2^*$	dimensionless constants, see eq. (C12)
c_p	specific heat at constant pressure
c_r	temperature coefficient of resistivity
F_I	imaginary part of Bessel function of second kind of zero order of argument $xi^{3/2}$
F_R	real part of Bessel function of second kind of zero order of argument $xi^{3/2}$
Fo	Fourier number, $a^*/\omega r_b^2$
Fo_1	$a_1^*/\omega r_b^2$ (note $Fo_{1,2}$ has special meaning $a^*_{1,2}/\omega r_b^2$)
Fo_2	$a_2^*/\omega r_b^2$

Fo^*	$2\pi Fo$; equivalent to at_0/R^2 of Gröber's notation
f_I	imaginary part of $J_0(xi^{3/2})$; equivalent to bei_0 in this report
f_R	real part of $J_0(xi^{3/2})$; equivalent to ber_0 in this report
h^*	ratio of heat-transfer coefficient h_f to thermal conductivity k_1 or k_2
h_f	heat-transfer coefficient
I_p	$J_p(xi)$
Im	real coefficient of i in imaginary part of particular complex function
i	$\sqrt{-1}$
J_p	Bessel function of order p of first kind
Ja	Jakob number, $h_f/(\omega k \rho c_p)^{1/2}$
Ja_1	$h_f/(\omega k_1 \rho_1 c_{p,1})^{1/2}$
Ja_2	$h_f/(\omega k_2 \rho_2 c_{p,2})^{1/2}$
Ja^*	$\sqrt{2\pi}$ Ja; equivalent to $h^2 at_0$ of Gröber's notation
k	thermal conductivity
ker_0, kei_0	$-(\pi/2)(yer_0 + bei_0)$ and $(\pi/2)(ber_0 - yei_0)$, respectively
l	$\alpha_1 r$
l_a	$\alpha_1 r_a$
l_b	$\alpha_1 r_a$
l^*	$\alpha_2 r$
l_a^*	$\alpha_2 r_a$
l_b^*	$\alpha_2 r_b$
m_j	j^{th} root of $J_0(m_j) = 0$

Nu_f	Nusselt number, $2r_b h_f/k_f$
p	number whose real part is positive and great enough to ensure convergence of a transform integral (see appendix B)
q	p/a^* where p is used in sense of appendix B
R	real part of particular complex function
r	radial coordinate
s	constant (in statement of Inversion Theorem of Laplace Transformation) which replaces p in appendix B
T	temperature
t	variable part of temperature
x, x^*	arbitrary variables
Y_p	Bessel function of order p of second kind; see appendix C
yer_p, yei_p	real and imaginary parts, respectively, of $Y_p(xi^{3/2})$
z	arbitrary complex independent variable; (see appendix G for special meaning)
α	$\sqrt{\omega/a^*}$
β	r_a/r_b
Γ	$(k_2/k_1)(a_1^*/a_2^*)^{1/2}$; identical with Γ^* when $\rho_1 c_{p,1} = \rho_2 c_{p,2}$
Γ^*	$(k_2/k_1)^{1/2}$
γ	Euler's constant, 0.5772 . . .
ε	phase angle
ζ	$\left[\dfrac{(R_b' + Im_b')^2}{(R_b' - \beta R_a')^2 + (Im_b' - \beta Im_a')^2}\right]^{1/2}$

η	varying part of local instantaneous temperature relative to half-amplitude of varying part of effective environmental instantaneous temperature, $t/t_{e,M}$
θ	time
λ	constant defined by eq. (6) but taken as 0.111 in this report
μ	attenuation, db
ξ	$(1-\beta^2)/2Fo_{1,2}^{1/2}$
ρ	density
τ	time constant
τ_{ext}	period required for cylinder to attain $1-e^{-1}$ of the final change of temperature when the environmental temperature is suddenly changed; identical with conventional time constant of thermocouple pyrometry; see eq. (3) for case of hot-wire anemometer
$\tau_{ext,1}$	$(\omega r_b \rho_1 c_{p,1})/2h_f$
$\tau_{ext,2}$	$(\omega r_b \rho_2 c_{p,2})/2h_f$
$\tau_{ext,2,a-b}$	$[\omega r_b \rho_2 c_{p,2}(1-\beta^2)]/2h_f$
τ_{int}	period for area-averaged cylinder temperature to change by $1-e^{-1}$ of the final change when surface temperature is suddenly altered
$\tau_{int,1}$	$\omega\lambda r_a^2/a_1^*$
$\tau_{int,2}$	$\omega\lambda r_b^2/a_2^*$
Φ_I	$bei_0 + Ja^{-1}\, bei_0'$
Φ_R	$ber_0 + Ja^{-1}\, ber_0'$
φ	phase shift (lag)
ψ	initially undetermined function of radial coordinate satisfying Bessel eq. for region indicated by subscript

ω angular frequency, 2π times frequency

Subscripts:

a interface

av temporal mean

ax axial

a-b region included between interface and outer surface

b outer surface

C in-phase component

e effective

ext external

f film; see, however, symbols h^* and h_f

I imaginary part or, with Φ, real function of bei_0 and bei_0'

i arbitrary integer

int internal

j one of a series

M maximum

p order of Bessel function

R real part or, with Φ, real function of ber_0 and ber_0'

S out-of-phase component

w wire

0 initial

1 oxide

2 metal

Superscripts:

$-$	mean with respect to radius
$*$	defined only as combined with symbol
$\sim$	Laplace transform
$'$	differentiation with respect to αr

CYLINDER HEAT-TRANSFER NONDIMENSIONAL MODULI

$$Bi = JaFo^{-0.5} = \frac{h_f r_b}{k} = \frac{k_f Nu_f}{2k} = \frac{\tau_{int}}{2\lambda\tau_{ext}} = \frac{\omega\tau_{int}}{2\lambda\omega\tau_{ext}} = (\alpha r_b)Ja$$

$$Fo = Ja^2 Bi^{-2} = \frac{a^*}{\omega r_b^2} = \frac{k}{\omega\rho c_p r_b^2} = (\alpha r_b)^{-2} = \frac{1}{2Bi\omega\tau_{ext}} = \frac{\lambda}{\omega\tau_{int}}$$

$$Ja = BiFo^{0.5} = \frac{h_f}{k}\sqrt{\frac{a^*}{\omega}} = \frac{h_f}{(\omega k\rho c_p)^{0.5}} = \sqrt{\frac{Bi}{2\omega\tau_{ext}}} = \frac{(\omega\tau_{int})^{0.5}}{2\lambda^{0.5}\omega\tau_{ext}}$$

$$\alpha r_b = Fo^{-0.5} = BiJa^{-1} = r_b\sqrt{\frac{\omega}{a^*}} = \sqrt{2Bi\omega\tau_{ext}} = \lambda^{-0.5}(\omega\tau_{int})^{0.5}$$

$$\omega\tau_{ext} = \frac{k}{k_f Nu_f Fo} = \frac{\omega r_b^2 k}{a^* k_f Nu_f} = \frac{\omega k r_b}{2a^* h_f} = \frac{\omega r_b \rho c_p}{2h_f} = \frac{\omega r_b^2 \rho c_p}{k_f Nu_f} = \frac{\omega\tau_{int}}{2\lambda Bi}$$

$$\omega\tau_{int} = \frac{\lambda}{Fo} = \lambda(\alpha r_b)^2 = \frac{\omega\lambda r_b^2 \rho c_p}{k} = \frac{\omega\lambda r_b^2}{a^*} = 2\lambda Bi\omega\tau_{ext}$$

$$\frac{\omega\tau_{ext}}{\omega\tau_{int}} = \frac{1}{2\lambda Bi} = \frac{4.50450^+}{Bi}$$

$$Fo^* = 2\pi\, Fo$$

$$Ja^* = \sqrt{2\pi}\, Ja$$

APPENDIX B

HOMOGENEOUS-CYLINDER RELATIONS

Although Gröber (ref. 10) obtained the correct relations for the local temperature in a homogeneous cylinder, the validity of his derivation is at least open to question. The derivation given in reference 4 (Carslaw and Jaeger, p. 276) is therefore presented; this solution is given herein in a more explicit form than in reference 4. The sinusoidal temperature "drive" with phase advance ε of that reference is retained.

The equation of heat flow may be written:

$$\frac{\partial^2 t}{\partial r^2} + \frac{1}{r}\frac{\partial t}{\partial r} - \frac{1}{a^*}\frac{\partial t}{\partial \theta} = 0 \tag{B1}$$

When the Laplace transformation is applied, the result of which will be indicated by a tilde ($\sim$) over a symbol, the equation becomes the following if the initial temperature is everywhere zero:

$$\frac{d^2\tilde{t}}{dr^2} + \frac{1}{r}\frac{d\tilde{t}}{dr} - q^2\tilde{t} = 0 \tag{B2}$$

where $q^2 \equiv p/a^*$, and it is understood that p is a number whose real part is positive and great enough to make the transform integrals convergent.

The boundary condition becomes

$$\left(\frac{d\tilde{t}}{dr} + h^*\tilde{t}\right)_{r=r_b} = h^*\tilde{t}_e \tag{B3}$$

Now, if $t_e = t_{e,M}\sin(\omega\theta + \varepsilon)$, as is assumed by Carslaw and Jaeger, then

$$\tilde{t}_e = t_{e,M}\left(\frac{\omega\cos\varepsilon + p\tan\varepsilon}{p^2 + \omega^2}\right) \tag{B4}$$

which is easily obtainable from the elementary transforms for sines and cosines, or from a table.

Since a solution of equation (B2) is

$$\tilde{t} = CI_0(qr) \tag{B5}$$

where C is an undetermined constant and I_0 is the solution of the zero order of the first kind of the modified Bessel equation, the following may be obtained from equations (B3), (B4), and (B5):

$$C = \frac{h^* t_{e,M}}{\left[qI_1(qr_b) + h^* I_0(qr_b)\right]} \left(\frac{\omega \cos \varepsilon + p \sin \varepsilon}{p^2 + \omega^2}\right) \tag{B6}$$

(Use was made of the fact that $d\tilde{t}/dr = CqI_1(qr)$.)

It follows that equations (B5) and (B6) that

$$\tilde{t} = \frac{h^* t_{e,M} I_0(qr)}{\left[qI_1(qr_b) + h^* I_0(qr_b)\right]} \left(\frac{\omega \cos \varepsilon + p \sin \varepsilon}{p^2 + \omega^2}\right) \tag{B7}$$

The Inversion Theorem of the Laplace Transformation states that

$$t = \frac{1}{2\pi i} \int_{\gamma - i\infty}^{\gamma + i\infty} e^{s\theta} \tilde{t}(s) ds$$

where s, in general complex, here replaces p in q and γ is an arbitrary constant; q (now) is equal to $\sqrt{s/a^*}$.

The evaluation of this integral in terms of the residues of $e^{s\theta}\tilde{t}(s)$, insofar as the nontransient terms of the solution are concerned, is very simple. The two zeros of the denominator at which the nontransient residues must be evaluated are $s_1 = i\omega$ and $s_2 = -i\omega$, so that $s^2 + \omega^2 = 0$. If the theorem is used that a residue K_j equals the quotient (at the pole j) of a nonzero numerator of a complex fraction and the value of the derivative (here, 2s) of the denominator (here, $s^2 + \omega^2$), then, if K_1 is the residue corresponding to s_1, the following is obtained:

$$K_1 = e^{i\omega\theta} \frac{h^* t_{e,M} I_0\left(r\sqrt{\frac{i\omega}{a^*}}\right) (\omega \cos \varepsilon + i\omega \sin \varepsilon)}{2i\omega\left[\sqrt{\frac{i\omega}{a^*}}\, I_1\left(r_b\sqrt{\frac{i\omega}{a^*}}\right) + h^* I_0\left(r_b\sqrt{\frac{i\omega}{a^*}}\right)\right]}$$

or

$$K_1 = \frac{e^{i(\omega\theta + \varepsilon)}\, h^* t_{e,M} I_0\left(r\sqrt{\frac{i\omega}{a^*}}\right)}{2i\left[\sqrt{\frac{i\omega}{a^*}}\, I\left(r_b\sqrt{\frac{i\omega}{a^*}}\right) + h^* I_0\left(r_b\sqrt{\frac{i\omega}{a^*}}\right)\right]} \tag{B8}$$

The steady-state portion of the solution is then given by

$$t = \frac{2\pi i}{2\pi i}(K_1 + K_2) = K_1 + K_2 \tag{B9}$$

where K_2 is the conjugate of K_1 and is the residue at the pole s_2.

The equivalents

$$\alpha = \sqrt{\frac{\omega}{a^*}} \tag{B10}$$

$$Ja^{-1} = \frac{k\alpha}{h} = \frac{\alpha}{h^*} \tag{B11}$$

$$I_0(\alpha r i^{1/2}) = \mathrm{ber}_0(\alpha r) + i\,\mathrm{bei}_0(\alpha r) = J_0(\alpha r i^{3/2}) \tag{B12}$$

$$\begin{aligned} I_1(\alpha r i^{1/2}) &= i^{-1} J_1(\alpha r i^{3/2}) \\ &= -i\left[\mathrm{ber}_1(\alpha r) + i\,\mathrm{bei}_1(\alpha r)\right] \\ &= \mathrm{bei}_1(\alpha r) - i\,\mathrm{ber}_1(\alpha r) \end{aligned} \tag{B13}$$

are noted in which I_j is the solution of j^{th} order of the first kind of the modified Bessel equation.

Equation (B9) then becomes, putting $\zeta \equiv \alpha r$ and $\zeta_b = \alpha r_b$,

$$\eta \equiv \frac{t}{t_{e,M}} = \left\{ \frac{\mathrm{ber}_0(\zeta) + i\,\mathrm{bei}_0(\zeta)\; e^{i(\omega\theta + \varepsilon)}}{2i\left[i^{1/2}\, Ja^{-1}\left(\mathrm{bei}_1(\zeta_b) + \mathrm{ber}_1(\zeta_b)\right) + \mathrm{ber}_0(\zeta_b) + i\,\mathrm{bei}_0(\zeta_b)\right]} \right\} + \text{conjugate of } \{\} \tag{B14}$$

In the conjugate of the expression $\{\}$, the expressions $\mathrm{ber}_0(\zeta) - i\,\mathrm{bei}_0(\zeta)$ and $\mathrm{bei}_1(\zeta) + i\,\mathrm{ber}_1(\zeta)$ appear. They are, respectively, equivalent to $I_0(\zeta i^{3/2})$ and $I_1(\zeta i^{3/2})$.

After a number of elementary operations, equation (B14) reduces to

$$\eta = \frac{\left[\mathrm{ber}_0^2(\zeta) + \mathrm{bei}_0^2(\zeta)\right]^{1/2}}{\left(\Phi_R + \Phi_I\right)^{1/2}} \sin\left[\omega\theta + \varepsilon - \tan^{-1}\frac{\Phi_I \mathrm{ber}_0(\zeta) - \Phi_R\,\mathrm{bei}_0(\zeta)}{\Phi_R\,\mathrm{ber}_0(\zeta) + \Phi_I\,\mathrm{bei}_0(\zeta)}\right] \tag{B15}$$

in which the subscript "b" in $\Phi_{R,b}$ and $\Phi_{I,b}$ is understood.

2922

This expression is equivalent to equation (9) of the main text; this will be apparent when it is recalled that the temperature drive assumed in the main text is $t_{e,M} \cos \omega\theta$ instead of $t_{e,M} \sin (\omega\theta + \varepsilon)$.

The mean value of η (i.e., $\overline{\eta}$) on an area-weighted basis is desired. This is obtained by evaluating the following expression (obtained from equation (B15):

$$\overline{\eta} = \frac{2}{r_b^2} \int_0^{r_b} \left(\Phi_R^2 + \Phi_I^2\right)^{-1} r \left\{ \left[\Phi_R \operatorname{ber}_0(\zeta) + \Phi_R \operatorname{bei}_0(\zeta)\right] \cos \omega\theta + \left[\Phi_I \operatorname{ber}_0(\zeta) - \Phi_R \operatorname{bei}_0(\zeta)\right] \sin \omega\theta \right\} dr \qquad \text{(B16)}$$

Use is made of the following:

$$\int_0^y x \operatorname{ber}_0 x \, dx = y \operatorname{bei}_0' y$$

and

$$\int_0^y x \operatorname{bei}_0 x \, dx = -y \operatorname{ber}_0' y$$

Equation (B16) and the latter lead to

$$\overline{\eta} = \frac{2}{\zeta_b^2(\Phi_R^2 + \Phi_I^2)} \left\{ \left[\Phi_R(\zeta_b)\operatorname{bei}_0'(\zeta_b) - \Phi_I(\zeta_b)\operatorname{ber}_0'(\zeta_b)\right] \cos \omega\theta + \left[\Phi_I(\zeta_b)\operatorname{bei}_0'(\zeta_b) + \Phi_R(\zeta_b)\operatorname{ber}_0'(\zeta_b)\right] \sin \omega\theta \right\}$$

Further manipulation of this expression leads to the desired relation

$$\overline{\eta} = \frac{2\left[\operatorname{ber}_1^2(\zeta_b) + \operatorname{bei}_1^2(\zeta_b)\right]^{1/2}}{\zeta_b(\Phi_R^2 + \Phi_I^2)^{1/2}} \cos\left[\omega\theta - \tan^{-1} \frac{\Phi_R \operatorname{ber}_0'(\zeta_b) + \Phi_R \operatorname{bei}_0'(\zeta_b)}{\Phi_R \operatorname{bei}_0'(\zeta_b) - \Phi_I \operatorname{ber}_0'(\zeta_b)}\right] \qquad \text{(B17)}$$

Note that $(\operatorname{ber}_1^2 x + \operatorname{bei}_1^2 x) = (\operatorname{ber}_0'^2 + \operatorname{bei}_0'^2)$.

This expression is identical with equation (15) in the text.

APPENDIX C

LAMINATED-CYLINDER THEORY

It is possible to use the Laplace Transform approach in this case, but since the transient terms were not desired, it was felt that any gain in conciseness would be more than offset by the loss in directness of the physical approach, that is, the inability of the user of the results to compare intermediate steps of the derivation with previously obtained results and derivations. Further, the derivation of the steady-state solution proves to be a relatively simple and straightforward matter even when the classical technique is employed.

The heat-flow equations

$$\frac{\partial t_1}{\partial \theta} = a_1^* \left(\frac{\partial^2 t_1}{\partial r^2} + \frac{1}{r} \frac{\partial t_1}{\partial r} \right) \tag{C1}$$

and

$$\frac{\partial t_2}{\partial \theta} = a_2^* \left(\frac{\partial^2 t_2}{2} + \frac{1}{r} \frac{\partial t_2}{\partial r} \right) \tag{C2}$$

apply in the core and shell regions, respectively.

The following are the boundary conditions:

$$-\left(\frac{\partial t_2}{\partial r} \right)_b = h^* (t_{2,b} - t_e) \tag{C3}$$

$$\left(\frac{\partial t_1}{\partial r} \right)_a = \frac{k_2}{k_1} \left(\frac{\partial t_2}{\partial r} \right)_a \tag{C4}$$

$$(t_1)_a = (t_2)_a \tag{C5}$$

If t_e is now assumed equal to $t_{e,M} \cos \omega\theta$, t_1 and t_2 will be represented by the real parts of the solutions (with undetermined complex coefficients)

$$t_1 = e^{i\omega\theta} (C_{1,1} \psi_{1,1} + C_{1,2} \psi_{1,2}) \tag{C6}$$

and

$$t_2 = e^{i\omega\theta} (C_{2,1} \psi_{2,1} + C_{2,2} \psi_{2,2}) \tag{C7}$$

where $\psi_{i,1}$ is the complex solution of the zero order of the first kind of the modified Bessel's equation

$$\frac{d^2\psi_i}{dr^2} + \frac{1}{r}\frac{d\psi_i}{dr} - i\alpha_i^2 \psi_i = 0 \tag{C8}$$

for the i^{th} region, and $\psi_{i,2}$ is the solution of zero order of the second kind of the same equation.

Only the reduction of t_2 to its final form will be followed in some detail, since the steps required for t_1 will then be obvious.

The real part of t_2 is given by the expression

$$t_2 = \frac{1}{2}\left(\left\{e^{i\omega\theta}\left[C_{2,1}\left(\text{ber}_0(\zeta^*) + i\,\text{bei}_0(\zeta^*)\right) + C_{2,2}\left(F_R(\zeta^*) + iF_I(\zeta^*)\right)\right]\right\} + \text{conjugate of } \{\}\right) \tag{C9}$$

in which

$$\zeta^* \equiv \alpha_2 r$$

$$\text{ber}_0(\zeta^*) + i\text{bei}(\zeta^*) = \psi_{2,1} = J_0\left(\zeta^* i^{3/2}\right)$$

and

$$F_R(\zeta^*) + iF_I(\zeta^*) = \psi_{2,2}$$

usually taken as $\text{ker}_0(\zeta^*) + i\text{kei}_0(\zeta^*)$ in this work. Note that if the definition given in reference 13 of the function of the second kind $(Y_p(z))$ is adopted, then if $z \equiv xi^{3/2}$, that is, $Y_0(xi^{3/2}) = \text{yer}_0(x) + i\text{yei}_0(x)$, the following are true:

$$\text{ker}_0 x = -\frac{\pi}{2}(\text{yer}_0 x + \text{bei}_0 x)$$

$$\text{kei}_0 x = \frac{\pi}{2}(\text{ber}_0 x - \text{yei}_0 x)$$

The reference 13 definition of $Y_p(z)$ is

$$Y_p(z) \equiv \frac{2}{\pi}\left\{\left(\gamma + \ln\frac{z}{2}\right)J_p(z) - \frac{1}{2}\sum_{j=0}^{p-1}\frac{(p-j-1)!}{j!}\left(\frac{z}{2}\right)^{2j-p} + \right.$$

$$\frac{1}{2}\sum_{j=0}^{\infty}\frac{(-1)^{j+1}\left(\frac{z}{2}\right)^{p+2j}}{j!(j+p)!}\left[1 + \frac{1}{2} + \ldots + \frac{1}{j-1} + \frac{1}{j} + \right.$$

$$\left.\left. 1 + \frac{1}{2} + \ldots + \frac{1}{p+j-1} + \frac{1}{p+j}\right]\right\} \qquad (C10)$$

2922

where γ (Euler's number) = 0.5772157 . . . .

The expression $C_{2,1,R} + iC_{2,1,I}$ is now substituted for the complex quantity $C_{2,1}$, $C_{2,2,R} + iC_{2,2,I}$ for $C_{2,2}$, and $\cos\omega\theta + i\sin\omega\theta$ for $e^{i\omega\theta}$ in equation (C9). The expression to which equation (C9) reduces when these substitutions are made and the terms of the "Conjugate" are explicitly introduced is

$$t_2 = \left[C_{2,1,R}\,\mathrm{ber}_0(z^*) - C_{2,1,I}\,\mathrm{bei}_0(z^*) + C_{2,2,R}F_R(z^*) - C_{2,2,I}F_I(z^*)\right]\cos\omega\theta -$$

$$\left[C_{2,1,I}\,\mathrm{ber}_0(z^*) + C_{2,1,R}\,\mathrm{bei}_0(z^*) + C_{2,2,I}F_R(z^*) + C_{2,2,R}F_I(z^*)\right]\sin\omega\theta \qquad (C11)$$

The new dimensionless constants

$$\begin{aligned} C_2^* &\equiv C_{2,1,R}/t_{e,M} \\ G_2^* &\equiv C_{2,2,R}/t_{e,M} \\ D_2^* &= -C_{2,1,I}/t_{e,M} \\ E_2^* &= -C_{2,2,I}/t_{e,M} \end{aligned} \qquad (C12)$$

are now introduced, as well as the equivalences $f_R = \mathrm{ber}_0$ and $f_I = \mathrm{bei}_0$. The local relative temperature $\eta_2 = t_2/t_{e,M}$ then becomes

$$\eta_2 = \left[C_2^* f_R(z^*) + G_2^* F_R(z^*) + D_2^* f_I(z^*) + E_2^* F_I(z^*)\right]\cos\omega\theta +$$

$$\left[D_2^* f_R(z^*) + E_2^* F_R(z^*) - C_2^* f_I(z^*) - G_2^* F_I(z^*)\right]\sin\omega\theta \qquad (C13)$$

This relation is formally identical to the relation obtained as the solution of an electrical problem in reference 18.

Similarly, the relative temperature within the core is found to be

$$\eta_1 = \left[C_1^* f_R(\zeta) + D_1^* f_I(\zeta)\right] \cos \omega\theta + \left[D_1^* f_R(\zeta) - C_1^* f_I(\zeta)\right] \sin \omega\theta \quad (C14)$$

in which C_1^* and D_1^* are additional real, undetermined, dimensionless constants and $\zeta = \alpha_1 r$.

The constants C_1^*, C_2^*, . . ., G_2^* are then determined by using equations (C3), (C4), (C5), (C13), and (C14) to obtain a set of six simultaneous linear algebraic equations. The set of equations is the following, noting that

$$\Gamma = \left(\frac{k_2}{k_1}\right)\left(\frac{a_1^*}{a_2^*}\right)^{1/2}$$

$$Ja_2 = \left(\frac{h_f^2}{\omega k_2 \rho_2 c_{p,2}}\right)^{1/2}$$

and, for example,

$$f_I'(\zeta_a) = \left[\frac{df_I}{d(\alpha_1 r)}\right]_{r=r_a}$$

or

$$f_I'(\zeta_a^*) = \left[\frac{df_I}{d(\alpha_2 r)}\right]_{r=r_a}$$

$$-f_I(\zeta_a)\ C_1^*+f_I(\zeta_a^*)\ C_2^*+f_R(\zeta_a)\ D_1^*-f_R(\zeta_a^*)\ D_2^*+F_I(\zeta_a^*)\ G_2^*-F_R(\zeta_a^*)\ E_2^* = 0$$

$$f_R(\zeta_a)\ C_1^*-f_R(\zeta_a^*)\ C_2^*+f_I(\zeta_a)\ D_1^*-f_I(\zeta_a^*)\ D_2^*-F_R(\zeta_a^*)\ G_2^*-F_I(\zeta_a^*)\ E_2^* = 0$$

$$f_I'(\zeta_a)\ C_1^*-\Gamma f_I'(\zeta_a^*)\ C_2^*-f_R'(\zeta_a)\ D_1^*+\Gamma f_R'(\zeta_a^*)\ D_2^*-\Gamma F_I'(\zeta_a^*)\ G_2^*+\Gamma F_R'(\zeta_a^*)\ E_2^* = 0$$

$$-f_R'(\zeta_a)\ C_1^*+\Gamma f_R'(\zeta_a^*)\ C_2^*-f_I'(\zeta_a)\ D_1^*+\Gamma f_I'(\zeta_a^*)\ D_2^*+\Gamma F_R'(\zeta_a^*)\ G_2^*+\Gamma F_I'(\zeta_a^*)\ E_2^* = 0$$

$$-\left[Ja_2 f_I(\zeta_b^*)+f_I'(\zeta_b^*)\right] C_2^*+\left[Ja_2 f_R(\zeta_b^*)+f_R'(\zeta_b^*)\right] D_2^*$$

$$-\left[Ja_2 F_I(\zeta_b^*)+F_I'(\zeta_b^*)\right] G_2^*+\left[Ja_2 F_R(\zeta_b^*)+F_R'(\zeta_b^*)\right] E_2^* = 0$$

$$\left[Ja_2 f_R(\zeta_b^*)+f_R'(\zeta_b^*)\right] C_2^*+\left[Ja_2 f_I(\zeta_b^*)+f_I'(\zeta_b^*)\right] D_2^*$$

$$+\left[Ja_2 F_R(\zeta_b^*)+F_R'(\zeta_b^*)\right] G_2^*+\left[Ja_2 F_I(\zeta_b^*)+F_I'(\zeta_b^*)\right] E_2^* = Ja_2 \qquad (C15)$$

2922

Formally, this set of equations represented the solution of the problem. In practice, the set was modified for computational purposes by the elimination of G_2^*; the fifth of equations (C5) was used for that purpose. The values of the functions f_j and F_j, etc., were obtained either from tabulated values (for arguments ≤ 10), by use of the normal series (for arguments ranging from 1 to 30), or by the use of the asymptotic series (for arguments ranging from 7 to 85).

The resulting set of five simultaneous equations was solved for $C_1^*, \ldots, E_2^*$ in each numerical case; a special program deck using the Crout reduction technique was used for this purpose with the Card-Programmed Calculator of the Lewis laboratory. The resulting values of the constants were found to satisfy the set of equations to better than seven significant figures in each case. Calculation of one set of constants required about three minutes.

In practical work, the instantaneous mean shell temperature and relative phase are much more useful than a knowledge of the variation of local relative temperature. An averaging process was accordingly carried out as follows in the same manner as for the homogeneous cylinder (appendix B): In equation (C13), $\eta_{2,C}$ and $\eta_{2,S}$ are defined as the bracketed expressions multiplying $\cos \omega\theta$ and $\sin \omega\theta$, respectively. Thus

$$\eta_{2,C} = C_2^* f_R(\tau^*) + G_2^* F_R(\tau^*) + D_2^* f_I(\tau^*) + E_2^* F_I(\tau^*) \tag{C16}$$

and

$$\eta_{2,S} = D_2^* f_R(\tau^*) + E_2^* F_R(\tau^*) - C_2^* f_I(\tau^*) - G_2^* F_I(\tau^*) \tag{C17}$$

Note that these relations are formally identical with certain of the relations of reference 18.

Then, averaging may be carried out as indicated in the following expression:

$$\bar{\eta}_2 = \frac{2}{\alpha_2^2(r_b^2 - r_a^2)} \int_{\alpha_2 r_a}^{\alpha_2 r_b} (\eta_{2,C} \cos \omega\theta + \eta_{2,S} \sin \omega\theta)(\alpha_2 r)\, d(\alpha_2 r) \tag{C18}$$

If, now, the in-phase and out-of-phase components of instantaneous mean relative shell temperature are designated $\bar{\eta}_{2,C}$ and $\bar{\eta}_{2,S}$, respectively, equation (C18) becomes

$$\bar{\eta}_2 = (\bar{\eta}_{2,C}^2 + \bar{\eta}_{2,S}^2)^{1/2} \cos\left(\omega\theta - \tan^{-1} \frac{\bar{\eta}_{2,S}}{\bar{\eta}_{2,C}}\right)^{1/2} \tag{C19}$$

in which, noting $\beta = r_a/r_b$,

$$\left.\begin{aligned} \bar{\eta}_{2,C} = \frac{2}{\tau_b^*(1-\beta^2)} \Big\{ & C_2^*\left[f_I'(\tau_b^*) - \beta f_I'(\tau_b^*)\right] + G_2^*\left[F_I'(\tau_b^*) - \beta F_I'(\tau_b^*)\right] - \\ & D_2^*\left[f_R'(\tau_b^*) - \beta f_R'(\tau_b^*)\right] - E_2^*\left[F_R'(\tau_b^*) - \beta F_R'(\tau_b^*)\right] \Big\} \end{aligned}\right\}$$

and

$$\left.\begin{aligned} \bar{\eta}_{2,S} = \frac{2}{\tau_b^*(1-\beta^2)} \Big\{ & D_2^*\left[f_I'(\tau_b^*) - \beta f_I'(\tau_b^*)\right] + E_2^*\left[F_I'(\tau_b^*) - \beta F_I'(\tau_b^*)\right] + \\ & C_2^*\left[f_R'(\tau_b^*) - \beta f_R'(\tau_b^*)\right] + G_2^*\left[F_R'(\tau_b^*) - \beta F_R'(\tau_b^*)\right] \Big\} \end{aligned}\right\} \tag{C20}$$

The mean relative temperature of the core is also given as a matter of completeness, although is has no relevance in the present work:

$$\bar{\eta}_1 = \frac{2}{\zeta_a}\left\{\left[C_1^* f_I'(\zeta_a) - D_1^* f_R'(\zeta_a)\right]^2 + \left[D_1^* f_I'(\zeta_a) + C_1^* f_R'(\zeta_a)\right]^2\right\}^{1/2} \cos\left\{\omega\theta - \tan^{-1}\frac{\left[D_1^* f_I'(\zeta_a) + C_1^* f_R'(\zeta_a)\right]}{\left[C_1^* f_I'(\zeta_a) - D_1^* f_R'(\zeta_a)\right]}\right\} \tag{C21}$$

APPENDIX D

THEORY OF THERMAL RESPONSE OF COMBINATION OF CORE OF FINITE CONDUCTIVITY AND OF THICK SHELL HAVING INFINITELY GREAT CONDUCTIVITY

The approximate relations derived in this appendix were checked by making a few calculations and comparing these results with those of the exact theory. The two sets of results agreed generally to two or three units at the third significant figure.

The following may be written immediately:

$$\pi(r_b^2 - r_a^2)\rho_2 c_{p,2} \frac{\partial t_2}{\partial \theta} = - 2\pi r_a k_1 \left(\frac{\partial t_1}{\partial r}\right)_{r_a} + 2\pi r_b h_f (t_e - t_2) \qquad (D1)$$

where t_2, the metal shell temperature, is assumed constant in amplitude and phase over the shell cross section.

The following may also be written:

$$t_e = t_{e,M} \cos \omega\theta \qquad (D2)$$

$$t_2 = t_{2,M} \cos(\omega\theta - \varphi_2) \qquad (D3)$$

$$t_1 = t_{1,M} \cos(\omega\theta - \varphi_1) \qquad (D4)$$

In equations (D3) and (D4), $t_{2,M}$ and φ_2 are independent of the radial coordinate, whereas $t_{1,M}$ and φ_1 are functions of the radial coordinate.

From equations (D2), (D3), and (D4) are obtained:

$$\eta_e \equiv \frac{t_e}{t_{e,M}} = \cos \omega\theta \qquad (D5)$$

$$\eta_2 \equiv \frac{t_2}{t_{e,M}} = \frac{t_{2,M}}{t_{e,M}} \cos(\omega\theta - \varphi_2) = \eta_{2,M} \cos(\omega\theta - \varphi_2) \qquad (D6)$$

where

$$\eta_{2,M} = \frac{t_{2,M}}{t_{e,M}}$$

$$\eta_1 \equiv \frac{t_1}{t_{e,M}} = \frac{t_{1,M}}{t_{e,M}} \cos(\omega\theta - \varphi_1) = \eta_{1,M} \cos(\omega\theta - \varphi_1) \tag{D7}$$

and

$$\eta_{1,M} \equiv \frac{t_{1,M}}{t_{2,M}} \cdot \frac{t_{2,M}}{t_{e,M}} = \eta_{2,M}\psi_{1,M}(\alpha_1 r) = \frac{t_{1,M}}{t_{e,M}} \tag{D8}$$

where

$$\psi_{1,M}(\alpha_1 r) \equiv \frac{t_{1,M}}{t_{2,M}}$$

Further, we can write

$$\varepsilon_1 \equiv \varphi_1 - \varphi_2 \tag{D9}$$

so that, finally,

$$\eta_1 = \eta_{2,M}\psi_{1,M} \cos(\omega\theta - \varphi_2 - \varepsilon_1) \tag{D10}$$

Note that $\psi_{1,M}$ and ε_1 are the amplitude and phase lag angles of η_1 with respect to η_2.

When $\beta \equiv r_a/r_b$ and equations (D5) to (D10) are used, equation (D1) may be transformed into a nondimensional relation:

$$\frac{r_b^2 - r_a^2}{2} \rho_2 c_{p,2} \frac{\partial t_2}{\partial\theta} = r_b h_f (t_e - t_2) - r_a k_1 \left(\frac{\partial t_1}{\partial r}\right)_{r_a} \tag{D1a}$$

$$\frac{(1 - \beta^2)}{2} \rho_2 c_{p,2} \frac{\partial \eta_2}{\partial\theta} = \frac{h_f}{r_b} (\eta_e - \eta_2) - \frac{\beta}{r_b^2} k_1 \left[\frac{\partial \eta_1}{\partial\left(\frac{r}{r_b}\right)}\right]_{r_a} \tag{D1b}$$

$$\frac{(1-\beta^2)}{2}\sqrt{\frac{\rho_2 c_{p,2}}{k_1}}\frac{\partial\eta_2}{\partial\theta} = \frac{h_f(\eta_e-\eta_2)}{r_b\sqrt{k_1\rho_2 c_{p,2}}} - \frac{\beta}{r_b^2}\sqrt{\frac{k_1}{\rho_2 c_{p,2}}}\left[\frac{\partial\eta_1}{\partial\left(\frac{r}{r_b}\right)}\right]_{r_a} \tag{D1c}$$

$$-\frac{\eta_{2,M}(1-\beta^2)}{2}\sqrt{\frac{\omega r_b^2}{a^*_{1,2}}}\sin(\omega\theta-\varphi_2) =$$

$$\frac{h_f\left[\cos(\omega\theta)-\eta_{2,M}\cos(\omega\theta-\varphi_2)\right]}{\sqrt{\omega k_1\rho_2 c_{p,2}}} - \beta\sqrt{\frac{a^*_{1,2}}{\omega r_b^2}}\left[\frac{\partial\eta_1}{\partial\left(\frac{r}{r_b}\right)}\right]_{r_a} \tag{D1d}$$

where

$$a^*_{1,2} \equiv k_1/\rho_2 c_{p,2}$$

We may now write

$$Fo_{1,2} \equiv \frac{a^*_{1,2}}{\omega r_b^2} \equiv (\alpha_{1,2} r_b)^{-2} \tag{D11}$$

where

$$\alpha_{1,2} \equiv \sqrt{\frac{\omega}{a^*_{1,2}}}$$

and

$$Ja_{1,2} \equiv \frac{h_f}{\sqrt{\omega k_1\rho_2 c_{p,2}}} \tag{D12}$$

and so obtain

$$\frac{\eta_{2,M}(1-\beta^2)}{2Fo_{1,2}^{1/2}}\sin(\omega\theta-\varphi_2) =$$

Continued on next page.

$$\beta Fo_{1,2}^{1/2}\left[\frac{\partial \eta_1}{\partial\left(\frac{r}{r_b}\right)}\right]_{r_a} - Ja_{1,2}\left[\cos(\omega\theta) - \eta_{2,M}\cos(\omega\theta - \varphi_2)\right] \qquad (D1e)$$

Now

$$\frac{\partial \eta_1}{\partial\left(\frac{r}{r_b}\right)} = \alpha_1 r_b \frac{\partial \eta_1}{\partial(\alpha_1 r)}$$

and since

$$Fo_{1,2}^{*}\alpha_1 r_b = \sqrt{\frac{\rho_1 c_{p,1}}{\rho_2 c_{p,2}}}$$

the following is finally obtained:

$$\frac{\eta_{2,M}(1 - \beta^2)\sin(\omega\theta - \varphi_2)}{2Fo_{1,2}^{1/2}} = \beta\sqrt{\frac{\rho_1 c_{p,1}}{\rho_2 c_{p,2}}}\left[\frac{\partial \eta_1}{\partial(\alpha_1 r)}\right]_{r_a} -$$

$$Ja_{1,2}\left[\cos(\omega\theta) - \eta_{2,M}\cos(\omega\theta - \varphi_2)\right] \qquad (D1f)$$

Now, it has been shown by Carslaw and Jaeger, pages 273 to 274, for example, that the steady-state response of a homogeneous cylinder (in this case, core) to a cosinusoidal surface temperature drive is given by

$$\eta_1 = \eta_{2,M}\left[\frac{ber_0^2(l) + bei_0^2(l)}{ber_0^2(l_a) + bei_0^2(l_a)}\right]^{1/2}$$

$$\cos\left[\omega\theta - \varphi_2 - \tan^{-1}\frac{(bei_0(l_a)\,ber_0(l) - ber_0(l_a)\,ber_0(l))}{(ber_0(l_a)\,ber_0(l) + bei_0(l_a)\,bei_0(l))}\right]$$

(D13)

in which $l \equiv \alpha_1 r$ and $l_a \equiv \alpha_1 r_a$; this equation should be compared with equation (D10) if explicit expressions for $\psi_{1,M}$ and ε_1 are sought. For convenience, we write hereinafter $ber_0 \equiv ber_0(l)$ and $ber_{0,a} \equiv ber_0(l_a)$. (Eq. (D13) is also easily deducible from the more

general expression involving the heat-transfer coefficient by permitting h_f to become infinitely large.) Note that the "drive" is in this instance $\eta_{2,M} \cos(\omega\theta - \varphi_2)$.

Differentiation of the above expression is merely tedious; the result is:

$$\frac{\partial \eta_1}{\partial(\alpha_1 r)} = \eta_{2,M} \left(\frac{\text{ber}_0'^2 + \text{bei}_0'^2}{\text{ber}_{0,a}^2 + \text{bei}_{0,a}^2} \right)^{1/2}$$

$$\cos \left[\omega\theta - \varphi_2 - \tan^{-1} \frac{(\text{bei}_{0,a}\, \text{ber}_0' - \text{ber}_{0,a}\, \text{bei}_0')}{(\text{ber}_{0,a}\, \text{bei}_0' + \text{bei}_{0,a}\, \text{bei}_0')} \right] \tag{D14}$$

The value of the derivative at r_a is then, obviously:

$$\left[\frac{\partial \eta_1}{\partial(\alpha_1 r)} \right]_{r_a} = \eta_{2,M} \left(\frac{\text{ber}_{0,a}'^2 + \text{bei}_{0,a}'^2}{\text{ber}_{0,a}^2 + \text{bei}_{0,a}^2} \right)^{1/2}$$

$$\cos \left[\omega\theta - \varphi_2 - \tan^{-1} \frac{(\text{bei}_{0,a}\, \text{ber}_{0,a}' - \text{ber}_{0,a}\, \text{bei}_{0,a}')}{(\text{ber}_{0,a}\, \text{ber}_{0,a}' + \text{bei}_{0,a}\, \text{bei}_{0,a}')} \right] \tag{D15a}$$

Note that

$$\text{ber}_0' = \frac{\sqrt{2}}{2} (\text{ber}_1 + \text{bei}_1)$$

and

$$\text{bei}_0' = \frac{\sqrt{2}}{2} (\text{bei}_1 - \text{ber}_1)$$

We write now

$$\left[\frac{\partial \eta_1}{\partial(\alpha_1 r)} \right]_{r_a} = \eta_{2,M}\, \Lambda_{0,a} \cos(\omega\theta - \varphi_2 - \Gamma_{0,a}) \tag{D15b}$$

where, by comparison with equation (D15a), the denotations of $\Lambda_{0,a}$ and $\Gamma_{0,a}$ will become clear. Note that the denotation of $\Gamma_{0,a}$, used only in this appendix, is not related in any way to the denotation of Γ or Γ^* as used throughout the balance of this report.

From (D1f) and (D15b) the following may be obtained:

$$\frac{\eta_{2,M}(1 - \beta^2)\sin(\omega\theta - \varphi_2)}{2Fo_{1,2}^{1/2}} = \left(\beta\sqrt{\frac{\rho_1 c_{p,1}}{\rho_2 c_{p,2}}}\right)\left[\eta_{2,M}\,\Lambda_{0,a}\cos(\omega\theta - \varphi_2 - \Gamma_{0,a})\right] - \qquad 2922$$

$$Ja_{1,2}\left[\cos(\omega\theta) - \eta_{2,M}\cos(\omega\theta - \varphi_2)\right] \qquad \text{(D16a)}$$

or, if we write

$$\xi \equiv \frac{(1 - \beta^2)}{2Fo_{1,2}^{1/2}}$$

and

$$\beta^* \equiv \beta\sqrt{\frac{\rho_1 c_{p,1}}{\rho_2 c_{p,2}}}$$

then

$$\xi\sin(\omega\theta - \varphi_2) = \beta^*\,\Lambda_{0,a}\cos(\omega\theta - \varphi_2 - \Gamma_{0,a}) -$$

$$Ja_{1,2}\left[\eta_{2,M}^{-1}\cos(\omega\theta) - \cos(\omega\theta - \varphi_2)\right] \qquad \text{(D16b)}$$

When the parenthetical expressions of equation (D16b) are expanded

$$\xi\sin(\omega\theta)\cos\varphi_2 - \xi\cos(\omega\theta)\sin\varphi_2$$

$$= \beta^*\,\Lambda_{0,a}(\cos\varphi_2\cos\Gamma_{0,a} - \sin\varphi_2\sin\Gamma_{0,a})\cos(\omega\theta) +$$

$$\beta^*\,\Lambda_{0,a}(\sin\varphi_2\cos\Gamma_{0,a} + \cos\varphi_2\sin\Gamma_{0,a})\sin(\omega\theta) -$$

$$Ja_{1,2}\left[\eta_{2,M}^{-1}\cos(\omega\theta) - \cos\varphi_2\cos(\omega\theta) - \sin\varphi_2\sin(\omega\theta)\right]$$

The last expression is equivalent to the two equations

$$\xi \cos \varphi_2 = \beta^* \Lambda_{0,a}(\sin \varphi_2 \cos \Gamma_{0,a} + \cos \varphi_2 \sin \Gamma_{0,a}) + Ja_{1,2} \sin \varphi_2$$

or

$$\xi = \beta^* \Lambda_{0,a} \cos \Gamma_{0,a} \tan \varphi_2 + \beta^* \Lambda_{0,a} \sin \Gamma_{0,a} + Ja_{1,2} \tan \varphi_2 \tag{D17}$$

and

$$-\xi \sin \varphi_2 = \beta^* \Lambda_{0,a}(\cos \varphi_2 \cos \Gamma_{0,a} - \sin \varphi_2 \sin \Gamma_{0,a}) + Ja_{1,2}(\cos \varphi_2 - \eta_{2,M}^{-1})$$

or

$$\xi \tan \varphi_2 = -\beta^* \Lambda_{0,a} \cos \Gamma_{0,a} + \beta^* \Lambda_{0,a} \sin \Gamma_{0,a} \tan \varphi_2 - Ja_{1,2} + Ja_{1,2} \eta_{2,M}^{-1} \sec \Phi_2 \tag{D18}$$

From equation (D17)

$$\varphi_2 = \tan^{-1} \frac{\xi - \beta^* \Lambda_{0,a} \sin \Gamma_{0,a}}{Ja_{1,2} + \beta^* \Lambda_{0,a} \cos \Gamma_{0,a}} \tag{D19a}$$

$$= \tan^{-1} \frac{\left[\dfrac{(1 - \beta^2)}{2Fo_{1,2}^{1/2}} - \beta\sqrt{\dfrac{\rho_1 c_{p,1}}{\rho_2 c_{p,2}}}\, \Lambda_{0,a} \sin \Gamma_{0,a}\right]}{\left(Ja_{1,2} + \beta\sqrt{\dfrac{\rho_1 c_{p,1}}{\rho_2 c_{p,2}}}\, \Lambda_{0,a} \cos \Gamma_{0,a}\right)} \tag{D19b}$$

while from equation (D18)

$$Ja_{1,2} \eta_{2,M}^{-1} \sec \varphi_2 = (\xi - \beta^* \Lambda_{0,a} \sin \Gamma_{0,a}) \tan \varphi_2 + Ja_{1,2} + \beta^* \Lambda_{0,a} \cos \Gamma_{0,a}$$

or

$$\eta_{2,M} = \frac{Ja_{1,2} \sec \varphi_2}{(\xi - \beta^* \Lambda_{0,a} \sin \Gamma_{0,a}) \tan \varphi_2 + Ja_{1,2} + \beta^* \Lambda_{0,a} \cos \Gamma_{0,a}} \tag{D20a}$$

or

$$\eta_{2,M} = \frac{Ja_{1,2} \sec \varphi_2}{\left[\frac{(1-\beta^2)}{2Fo_{1,2}^{1/2}} - \beta\sqrt{\frac{\rho_1 c_{p,1}}{\rho_2 c_{p,2}}}\,\Lambda_{0,a} \sin \Gamma_{0,a}\right] \tan \varphi_2 + Ja_{1,2} + \beta\sqrt{\frac{\rho_1 c_{p,1}}{\rho_2 c_{p,2}}}\,\Lambda_{0,a} \cos \Gamma_{0,a}} \tag{D20b}$$

2922

Note that φ_2 and $\eta_{2,M}$ are functions of the four parameters $Fo_{1,2}$, $Ja_{1,2}$, β, and $\frac{\rho_2 c_{p,2}}{\rho_1 c_{p,1}}$. The number of parameters is in accordance with the fact that a general two-material laminated-cylinder analysis requires a specification of five independent parameters; by specifying k_2 (here taken equal to infinity) we have reduced the number to four and greatly simplified the analysis. If $\frac{\rho_2 c_{p,2}}{\rho_1 c_{p,1}}$ is further limited to the value unity, it is necessary to consider only three parameters, of which β must take on only two or three values for design purposes. Thus, only $Fo_{1,2}$ and $Ja_{1,2}$ need take on extensive ranges of values.

Explicit expressions for $\Lambda_{0,a} \sin \Gamma_{0,a}$ and $\Lambda_{0,a} \cos \Gamma_{0,a}$ are obtained as follows:

Since

$$\Lambda_{0,a} = \left(\frac{ber_{0,a}^2 + bei_{0,a}^2}{ber_{0,a}^2 + bei_{0,a}^2}\right)^{1/2}$$

and

$$\Gamma_{0,a} = \tan^{-1} \frac{\mathrm{bei}_{0,a}\,\mathrm{ber}'_{0,a} - \mathrm{ber}_{0,a}\,\mathrm{bei}'_{0,a}}{\mathrm{ber}_{0,a}\,\mathrm{ber}'_{0,a} + \mathrm{bei}_{0,a}\,\mathrm{bei}'_{0,a}}$$

Then

$$A_{0,a} \sin \Gamma_{0,a} = \left(\frac{\mathrm{ber}'^{2}_{0,a} + \mathrm{bei}'^{2}_{0,a}}{\mathrm{ber}^{2}_{0,a} + \mathrm{bei}^{2}_{0,a}}\right)^{1/2} \times$$

$$\frac{\mathrm{bei}_{0,a}\,\mathrm{ber}'_{0,a} - \mathrm{ber}_{0,a}\,\mathrm{bei}'_{0,a}}{\left[\left(\mathrm{ber}_{0,a}\,\mathrm{ber}'_{0,a} + \mathrm{bei}_{0,a}\,\mathrm{bei}'_{0,a}\right)^{2} + \left(\mathrm{bei}_{0,a}\,\mathrm{ber}'_{0,a} - \mathrm{ber}_{0,a}\,\mathrm{bei}'_{0,a}\right)^{2}\right]^{1/2}}$$

$$= \left(\frac{\mathrm{ber}'^{2}_{0,a} + \mathrm{bei}'^{2}_{0,a}}{\mathrm{ber}^{2}_{0,a} + \mathrm{bei}^{2}_{0,a}}\right)^{1/2} \frac{\mathrm{bei}_{0,a}\,\mathrm{ber}'_{0,a} - \mathrm{ber}_{0,a}\,\mathrm{bei}'_{0,a}}{\left[\left(\mathrm{ber}^{2}_{0,a} + \mathrm{bei}^{2}_{0,a}\right)\left(\mathrm{ber}'^{2}_{0,a} + \mathrm{bei}'^{2}_{0,a}\right)\right]^{1/2}}$$

$$= \frac{\mathrm{bei}_{0,a}\,\mathrm{ber}'_{0,a} - \mathrm{ber}_{0,a}\,\mathrm{bei}'_{0,a}}{\mathrm{ber}^{2}_{0,a} + \mathrm{bei}^{2}_{0,a}}$$

Similarly,

$$A_{0,a} \cos \Gamma_{0,a} = \frac{\mathrm{ber}_{0,a}\,\mathrm{ber}'_{0,a} + \mathrm{bei}_{0,a}\,\mathrm{bei}'_{0,a}}{\mathrm{ber}^{2}_{0,a} + \mathrm{bei}^{2}_{0,a}}$$

APPENDIX E

CARD-PROGRAMMED CALCULATOR OPERATIONS AND INTERRELATIONS AMONG EQUATIONS USED FOR REDUCTION OF CPC INTEGRATIONS AND ANALYTICAL SOLUTION

Numerical Integrations

The exact analytical solution of the laminated-cylinder problem was given in appendix C. It was shown there (eqs. (C6) and (C7)) that

$$t_i = e^{i\omega\theta} \left(C_{i,1} \psi_{i,1} + C_{i,2} \psi_{i,2}\right) \tag{E1}$$

where

$$\frac{d^2\psi_i}{dr^2} + \frac{1}{r}\frac{d\psi_i}{dr} - i\alpha_i^2 \psi_i = 0 \tag{C8}$$

for the i^{th} region, and $\psi_{i,1}$ and $\psi_{i,2}$ are any two independent solutions of the zero order in the i^{th} region. Equation (E1) is based upon a temperature "drive" $t_e = t_{e,M} e^{i\omega\theta}$; if $t_e = t_{e,M} \cos \omega\theta$ is assumed, then only the real parts of t_1 and t_2 are of physical significance, that is, are to be associated with $t_{e,M} \cos \omega\theta$.

The notation

$$\left.\begin{aligned} R_i &= \text{Real part of } \left(C_{i,1} \psi_{i,1} + C_{i,2} \psi_{i,2}\right) \\ Im_i &= \text{Real coefficient of imaginary part of } \left(C_{i,1} \psi_{i,1} + C_{i,2} \psi_{i,2}\right) \end{aligned}\right\} \tag{E2}$$

is now employed. (Also, $l_i = \alpha_i r$ is used.) It follows that equation (C8) may be written (since ψ_i may be replaced by any linear combination of independent solutions) as follows:

$$\frac{d^2(R_i + i\ Im_i)}{dl_i^2} + \frac{1}{l_i}\frac{d(R_i + i\ Im_i)}{dl_i} + i(R_i + i\ Im_i) = 0 \tag{E3}$$

Equation (E3) is, of course, equivalent to the pair of equations:

$$\left.\begin{aligned} \frac{d^2R_i}{dl_i^2} + \frac{1}{l_i}\frac{dR_i}{dl_i} + Im_i = 0 \\ \frac{d^2Im_i}{dl_i^2} + \frac{1}{l_i}\frac{dIm_i}{dl_i} - R_i = 0 \end{aligned}\right\} \tag{E4}$$

Basically, the IBM procedure followed was that of numerical integration of these simultaneous equations outward from the center of the core to the outer surface, the change in material at the interface being taken into account in the following way:

The boundary conditions at the interface are as stated in appendix C (eqs. (C4) and (C5)). From those equations, it follows that the value of R at r_a in the oxide equals the R at r_a in the metal, and similarly for Im. Further, it follows that

$$\left(\frac{dR}{dr}\right)_{2,a} = \frac{k_1}{k_2}\left(\frac{dR}{dr}\right)_{1,a}$$

and similarly for the space derivatives of Im. Since R' is understood throughout this study to be $dR/d(\alpha_1 r)$, the following may be written:

$$\alpha_1 R'_{2,a} = \alpha_1 \frac{k_1}{k_2} R'_{1,a}$$

It follows that

$$R'_{2,a} = \frac{k_1}{k_2} R'_{1,a}$$

In other words, the starting values R'_a and Im'_a in the oxide at the interface must be multiplied by the reciprocal of k_2/k_1 before continuing the integration through the shell.

In practice, a substantial saving of time was achieved by avoiding integration of the equations (E4) between center and interface; this was accomplished by computing (on the CPC) all values of ber_0, bei_0, ber'_0, and bei'_0 at $l_a = \alpha_1 r_a$ and using these values (modified as indicated)

as starting values of the integration from interface to surface. In the case of small-argument ($l_a \leq 10$) values, the functions are given in several references at small intervals and to a large number of decimal places, so that values interpolated among tabulated values are available at the interface. Nevertheless, it was found more convenient to compute small-argument values as well as large-argument values; additional details are given herein.

It is to be noted that $\psi_{1,2}$ is identically zero, since only the solution ($J_0(\alpha_1 r i^{3/2})$) of the first kind may be used in region 1 ($(d\psi/dr)_{r=0} = 0$). This is tantamount to putting $\ker_0 r = \mathrm{kei}_0 r = 0$ for all $r \leq r_a$. However, $\psi_{2,2}$ is in general not equal to zero. When the surface is reached, the problem becomes that of matching the solution already obtained to the assumed surface conditions in effect, determining $C_{1,1}$, $C_{1,2}$, $C_{2,1}$, and $C_{2,2}$ as in appendix C. The details are given in the second part of this appendix.

The numerical integrations (from the interface outward through the shell) were performed by extrapolating successive values of the third derivatives of R and Im. The variable of integration remained $l_1 \equiv l$; equations (E4) accordingly became, explicitly, within the shell, the following (the subscript 2 on R and Im is omitted):

$$\left.\begin{aligned} \frac{d^2R}{dl^2} + \frac{1}{l}\frac{dR}{dl} + A\,\mathrm{Im} = 0 \\ \frac{d^2\mathrm{Im}}{dl^2} + \frac{1}{l}\frac{d\mathrm{Im}}{dl} - AR = 0 \end{aligned}\right\} \tag{E5}$$

where $A \equiv (\alpha_2/\alpha_1)^2$; note (e.g.) that $d\mathrm{Im}/dl = d\mathrm{Im}/d(\alpha_1 r)$, not $d\mathrm{Im}/d(\alpha_2 r)$.

From the first of these relations, the expression

$$R''' = -\left(\frac{2}{l}R'' + A\mathrm{Im}' + \frac{A}{l}\mathrm{Im}\right) \tag{E6}$$

is obtained by differentiation; the prime convention for differentiation has here been adopted.

2922

The subscript j will now be used to identify values at the j^{th} point of the numerical integration; the subscript $j+\frac{1}{2}$ identifies values at a point half way between j and $j+1$.

It follows that

$$R''_{j+(1/2)} \cong R''_j + \frac{1}{2}\Delta R''_j \tag{E7}$$

where Δ denotes the change between j and $j+1$. However, it is true that

$$\frac{1}{2}\Delta R''_j = \frac{\Delta l}{2} R'''_j \tag{E8}$$

It follows from equations (E6), (E7), and (E8) that

$$R''_{j+(1/2)} = R''_j - \left(\frac{2}{l_j} R''_j + A\mathrm{Im}'_j + \frac{A}{l_j}\mathrm{Im}_j\right)\frac{\Delta l}{2} = \left(\frac{l_j - \Delta l}{l_j}\right) R''_j - \left(\mathrm{Im}'_j + \frac{1}{l_j}\mathrm{Im}_j\right)\frac{A\Delta l}{2} \tag{E9}$$

Similarly, the following is true:

$$\mathrm{Im}''_{j+(1/2)} = \left(\frac{l_j - \Delta l}{l_j}\right)\mathrm{Im}''_j + \left(R'_j + \frac{1}{l_j} R_j\right)\frac{A\Delta l}{2} \tag{E10}$$

A special set of fixed-decimal-point wiring boards was used for these (and other similar) calculations. The values of $R = \left[\mathrm{ber}_0(l)\right]_{r_a}$, $\mathrm{Im} = \left[\mathrm{bei}_0(l)\right]_{r_a}$, $R' = \left[\mathrm{ber}_0(l)\right]_{r_a}$, $\mathrm{Im}' = \left[\mathrm{bei}_0(l)\right]_{r_a}$, $l_a = \alpha_1 r_a$, and $A = (\alpha_2/\alpha_1)^2 = (k_2/k_1)^{-1}$ (for these calculations, since $\rho_1 c_{p,1}$ was assumed equal to $\rho_2 c_{p,2}$) were entered into storage units. R''_a and Im''_a were then computed (eqs. (E5)). Equations (E9) and (E10) were then used to compute $R''_a + \frac{1}{2}\Delta l$ and $\mathrm{Im}''_a + \frac{1}{2}\Delta l$. $\Delta R'/2 = (R''_{a+(\Delta l/2)})\,\Delta l/2$ and $R'_{a+(\Delta l/2)} = R'_a + \Delta R'/2$ were computed in turn; corresponding relations were used for Im'.

The function values themselves were then estimated at the center of the first half-interval by using $\Delta R/2 = (R'_{a+(\Delta l/2)})\,\Delta l/2$ and $R_{a+(\Delta l/2)} = R_a + \Delta R/2$ and corresponding expressions for Im.

After the first half-interval was reached, the procedure was modified slightly. If the value of the symbol precisely at the end of a given interval is denoted by the symbol without a subscript, that at the end of a half-interval by the symbol with a "+" as a subscript, that at the end of the preceding half-interval by the symbol with a "-" as a subscript, and so forth, then the following indicate the arithmetic operations performed after the "a+" calculations were completed. Note that a "++" indicates evaluation at the end of a full-interval.

$$\Delta R'/2 = (R''_+)\,\frac{\Delta l}{2}$$

$$R'_+ = R'_- + (\Delta R'/2)_- + (\Delta R'/2)_+$$

$$\Delta R/2 = (R'_+)\,\frac{\Delta l}{2}$$

$$R_+ = R_- + (\Delta R/2)_+ + (\Delta R/2)_-$$

$$R'_{++} = R'_+ + \Delta R'_+/2$$

$$R_{++} = R_+ + \Delta R_+/2$$

Corresponding relations were used for $\frac{\Delta Im'}{2}$, Im'_+, and so forth.

In addition, the following relations were used:

$$R'_{++} = -\left(\frac{1}{l_{++}}\,R'_{++} + AIm_{++}\right)$$

$$Im'_{++} = -\left(\frac{1}{l_{++}}\,Im'_{++} - AR_{++}\right)$$

Finally, equations (E9) and (E10) were used to compute second derivatives at the half-interval.

The series used for computations of most of the starting values were the following:

$$R(l) = ber_0(l) = \frac{\sum_{j=0}^{\infty} (-1)^j (l/2)^{4j}}{\left[(2j!)\right]^2}$$

Continued on next page.

$$= \left[\left(\left\{\left[\frac{(l/2)^4}{(40\cdot39)^2}-1\right]\frac{(l/2)^4}{(38\cdot37)^2}+1\right\}\frac{(l/2)^4}{(36\cdot35)^2}-1\right)\frac{(l/2)^4}{(34\cdot33)^2}+1\right] \cdots$$

(E11)

$$\mathrm{Im}(l) = \mathrm{bei}_0(l) = \frac{\sum_{j=0}^{\infty}(-1)^j(l/2)^{4j+2}}{\left[(2j+1)!\right]^2}$$

$$= \left(\frac{l}{2}\right)^2\left[\left(\left\{\left[\frac{(l/2)^4}{(41\cdot40)^2}-1\right]\frac{(l/2)^4}{(39\cdot38)^2}+1\right\}\frac{(l/2)^4}{(37\cdot36)^2}-1\right)\frac{(l/2)^4}{(35\cdot34)^2}+1\right] \cdots$$

(E12)

$$\mathrm{R}'(l) = \mathrm{ber}_0'(l) = \frac{\sum_{j=1}^{\infty}(-1)^j(2j)(l/2)^{4j-1}}{\left[(2j)!\right]^2}$$

$$= -\left(\frac{l}{2}\right)^3\left(\frac{1}{2}\right)\left[\left(\left\{\left[\frac{(l/2)^4}{(42\cdot41^2\cdot40)}-1\right]\frac{(l/2)^4}{(40\cdot39^2\cdot38)}+1\right\}\frac{(l/2)^4}{(38\cdot37^2\cdot36)}-1\right)\frac{(l/2)^4}{(36\cdot35^2\cdot34)}+1\right]\cdots$$

(E13)

$$\mathrm{Im}'(l) = \mathrm{bei}_0(l) = \frac{\sum_{j=0}^{\infty}(-1)^j(2j+1)(l/2)^{4j+1}}{\left[(2j+1)!\right]^2}$$

$$= \left(\frac{l}{2}\right)\left[\left(\left\{\left[\frac{(l/2)^4}{(41\cdot40^2\cdot39)}-1\right]\frac{(l/2)^4}{(39\cdot38^2\cdot37)}+1\right\}\frac{(l/2)^4}{(37\cdot36^2\cdot35)}-1\right)\frac{(l/2)^4}{(35\cdot34^2\cdot33)}+1\right]\cdots$$

(E14)

Truncation errors were held to less than three units at the eighth significant figure by using more than $l_a/2$ terms in each case. Specifically, 20 terms were used for $1.5918 \leq l_a \leq 25.318$, and 40 terms for $25.318 < l_a$. It was later determined that the procedure had been an unnecessarily conservative one insofar as truncation errors were concerned. Round-off errors, however, reduced accuracy at the higher arguments to such an extent that for arguments greater than 45 it became necessary to use the well-known asymptotic series for these functions.

In table XIII the calculated values of $R_a = \mathrm{ber}_0(l_a)$, $Im_a = \mathrm{bei}_0(l_a)$, $R'_a = \mathrm{ber}'_0(l_a)$, and $Im'_a = \mathrm{bei}'_0(l_a)$ are listed as calculated for each of the 47 l_a values. Low-argument values (less than 10) checked against existing tables agreed with them to 8 figures. This order of accuracy, however, was not maintained throughout; the function values are believed correct to 6 figures or more in all cases. The accuracy of the integrations was enhanced by maintaining a nonzero initial digit in the absolutely largest number present at a given step. This was accomplished by using a right or left shift of all numbers being carried, as required.

Two or three different step sizes were used for certain large-argument cases, both for check purposes and in an effort to reduce total CPC time. As an example, integrations were performed for a particular case using standard intervals (Δl) of 0.16, 0.32, and 0.64. (In this instance, these results were later discarded because the starting values had been incorrectly computed.)

The following table exhibits the important results of the three integrations (which were, however, executed in the order 0.64, 0.32, and 0.16), including the first differences of the successive end-values of the functions.

Run number	Step		R_b	Im_b	R'_b	Im'_b
3	0.16		14,378,808	-11,893,246	1,330,416	796,851
		First Δ	418	542	176	-184
2	.32		14,379,226	-11,893,788	1,330,592	796,667
		First Δ	1796	2122	694	-732
1	.64		14,381,022	-11,895,910	1,331,286	795,935

Two facts are apparent: The errors increase as the square of the interval, and the residual errors of the 0.16 run are almost certainly smaller than 1 in 10^5. In addition, such multiple runs served as very convenient checks on final results when the otherwise supernumerary run (s) was (were) carried either to completion or essentially to completion.

Cases 1 through 21 were checked for smoothness by visual inspection of the R'' and Im'' entries of the original CPC listing. Additional tabulation and visual-inspection checks were used for cases 22 through 46. Case 47 was checked by using several step sizes. The results for cases 48, 49, and 50 were obtained solely by the use of the analytical theory developed in appendix C.

Reduction of Integration Results

Calculation of local and mean shell amplitudes and phase angles. - The following relations were used in the reduction of integration results to actual local and mean relative temperature amplitudes and phase shifts within the shell for cases 1 to 47; "floating" decimal-point wiring and operations were used (ref. 14):

Mean relative shell temperature amplitude and phase angle; derivatives at r_a are evaluated within the metal but with respect to $l = \alpha_1 r$:

$$\frac{\bar{t}_{2,M}}{t_{e,M}} = \bar{\eta}_{2,M} = \frac{2}{l_b(1 - \beta^2)} \left(\frac{\alpha_1}{\alpha_2}\right)^2 \frac{\left[(R_b' - \beta R_a')^2 + (Im_b' - \beta Im_a')^2\right]^{1/2}}{(\Phi_{R,b}^2 + \Phi_{I,b}^2)^{1/2}} \tag{E15}$$

$$\tan \bar{\varphi}_2 = \frac{1 + \dfrac{\Phi_{R,b}}{\Phi_{I,b}} \cdot \dfrac{(R_b' - \beta R_a')}{(Im_b' - \beta Im_a')}}{\dfrac{\Phi_{R,b}}{\Phi_{I,b}} - \dfrac{(R_b' - \beta R_a')}{(Im_b' - \beta Im_a')}} \tag{E16}$$

where

$$\Phi_{R,b} = Ja_2^{-1} \frac{\alpha_1}{\alpha_2} R_b' + R_b$$

$$\Phi_{I,b} = Ja_2^{-1} \frac{\alpha_1}{\alpha_2} Im_b' + Im_b$$

Local ("point") amplitude relative to mean amplitude, and local phase angle (lag) relative to mean phase angle (lag) are, respectively

$$\frac{(t_{2,M}/t_{e,M})}{(\bar{t}_{2,M}/t_{e,M})} = \frac{\eta_{2,M}}{\bar{\eta}_{2,M}}$$

$$= \left(\frac{\alpha_2}{\alpha_1}\right)^2 \frac{l_b(1 - \beta^2)}{2} \frac{\left[(R_b' - \beta R_a')^2 + (Im_b' - \beta Im_a')^2\right]^{1/2}}{(R^2 + Im^2)^{1/2}} \tag{E17}$$

$$\tan(\bar{\varphi}_2 - \varphi_2) = \frac{1 + \dfrac{R'_b - \beta R'_a}{Im'_b - Im'_a} \cdot \dfrac{R}{Im}}{\dfrac{R}{Im} - \dfrac{R'_b - \beta R'_a}{Im'_b - \beta Im'_a}} \tag{E18}$$

There are several ways of deriving the preceding equations. For example, they were originally obtained by assuming $t_2 = C\psi_2 \exp i\,(\omega\theta + \delta^*)$, where the undetermined constants C and δ^* are independent of the variable $\alpha_2 r$. This expression was then used with the surface boundary condition to determine C and δ^*.

This approach, although straightforward, sheds no light on the interrelations among $\eta_{2,C}$ and R, $\eta_{2,S}$ and Im, $ber_0(l_b)$ and R_b, $\eta_{2,C}$ and $C_{1,1}\,\psi_{1,1}$, and so forth.

A more illuminating derivation is now given:

The heat-flow equation for the shell region is written in the form

$$\frac{\partial^2 \eta_2}{\partial l^{*2}} + \frac{1}{l^*}\frac{\partial \eta_2}{\partial l^*} - \frac{\partial \eta_2}{\partial(\omega\theta)} = 0 \tag{E19}$$

Here, $l^* = \alpha_2 r$ as usual.

The solution

$$\eta_2 = \eta_{2,C} \cos \omega\theta + \eta_{2,S} \sin \omega\theta \tag{E20}$$

is assumed for $(t_e/t_{e,M}) = \cos \omega\theta$.

Equations (E19) and (E20) lead to the following relations:

$$\left.\begin{aligned} \frac{\partial^2 \eta_{2,C}}{\partial l^{*2}} + \frac{1}{l^*}\frac{\partial \eta_{2,C}}{\partial l^*} - \eta_{2,S} &= 0 \\ \frac{\partial^2 \eta_{2,S}}{\partial l^{*2}} + \frac{1}{l^*}\frac{\partial \eta_{2,S}}{\partial l^*} + \eta_{2,C} &= 0 \end{aligned}\right\} \tag{E21}$$

Equations (E21) can be combined into a single equation provided a new time-independent complex function (of $\alpha_2 r$) is defined:

$$\eta_2^* = \eta_{2,C} - i\eta_{2,S} \tag{E22}$$

When η_2^* is used, equations (E21) become the single equation

$$\frac{\partial^2 \eta_2^*}{\partial \zeta^{*2}} + \frac{1}{\zeta^*} \frac{\partial \eta_2^*}{\partial \zeta^*} - i\eta_2^* = 0 \tag{E23}$$

This relation is, however, formally identical with, for example, equation (C8), which is the modified Bessel's equation. It follows that $\eta_2^* = C\psi_2$, and that appropriate real solutions of equations (E21) may be obtained by properly combining real parts of conjugates of solutions of the first and second kinds of the modified Bessel's equation; the minus sign in equation (E22) should be noted. In other words, if ${}_1\psi_2 \equiv f_R + if_I$, for example, is one of a pair of independent solutions of the modified Bessel's equation (as denoted by the subscript to the left of ψ_2), then one solution of equation (E23) is $C\ {}_1\psi_2 \equiv {}_1\eta_2^* = C(f_R - if_I)$, where C remains arbitrary. Another independent solution is $C\ {}_2\psi_2 = {}_2\eta_2^* = C(F_R - iF_I)$. Since the constant C is arbitrary, additional solutions may be obtained by noting that $i\ {}_1\psi_2 = if_R - f_I$, and that the conjugate of $i\ {}_1\psi_2$ is $-f_I - if_R = -(f_I + if_R)$, and so forth. In this manner, it is possible to arrive at the following general solution of equations (E21)

$$\left.\begin{aligned} \eta_{2,C} &= C_3 R + C_4 \mathrm{Im} \\ \eta_{2,S} &= -C_3 \mathrm{Im} + C_4 R \end{aligned}\right\} \tag{E24}$$

where C_3 and C_4 are arbitrary undetermined real constants. These relations satisfy the differential equation, are linearly independent, automatically satisfy the interfacial boundary conditions because of the manner in which R and Im were computed, and can be made to satisfy the surface boundary conditions through selection of C_3 and C_4. They therefore fulfill all requirements.

The surface boundary condition is as given by equation (C3). This may by obvious manipulations be transformed into

$$-\left(\frac{\partial \eta_2}{\partial \zeta}\right)_b = \frac{\alpha_2}{\alpha_1} \mathrm{Ja}_2(\eta_{2,b} - \cos \omega\theta) \tag{E25}$$

If, now, relations (E24) are substituted into equation (E25), an expression in $\cos \omega\theta$ and $\sin \omega\theta$ is obtained which yields the equations

$$\left.\begin{aligned} C_3\left(\frac{\alpha_1}{\alpha_2} Ja_2^{-1} R_b' + R_b\right) + C_4\left(\frac{\alpha_1}{\alpha_2} Ja_2^{-1} Im_b' + Im_b\right) - 1 = 0 \\ C_4\left(\frac{\alpha_1}{\alpha_2} Ja_2^{-1} Im_b' + Im_b\right) - C_4\left(\frac{\alpha_1}{\alpha_2} Ja_2^{-1} R_b' + R_b\right) = 0 \end{aligned}\right\} \quad \text{(E26)}$$

(Note, again, that derivatives are taken with respect to $\zeta = \alpha_1 r$.) The expressions in parenthesis will, however, be recognized as $\Phi_{R,b}$ and $\Phi_{I,b}$. Accordingly, equations (E26) may be written

$$\left.\begin{aligned} C_3 \Phi_{R,b} + C_4 \Phi_{I,b} - 1 = 0 \\ C_3 \Phi_{I,b} - C_4 \Phi_{R,b} = 0 \end{aligned}\right\} \quad \text{(E27)}$$

The solution of equations (E27) is

$$\left.\begin{aligned} C_3 = \frac{\Phi_{R,b}}{\Phi_{R,b}^2 + \Phi_{R,b}^2} \\ C_4 = \frac{\Phi_{I,b}}{\Phi_{R,b}^2 + \Phi_{I,b}^2} \end{aligned}\right\} \quad \text{(E28)}$$

It follows from the latter relations and equations (E24) that

$$\left.\begin{aligned} \eta_{2,C} = \frac{\Phi_{R,b}\, R + \Phi_{I,b}\, Im}{\Phi_{R,b}^2 + \Phi_{I,b}^2} \\ \eta_{2,S} = \frac{\Phi_{I,b}\, R - \Phi_{R,b}\, Im}{\Phi_{R,b}^2 + \Phi_{I,b}^2} \end{aligned}\right\} \quad \text{(E29)}$$

Finally, the following relation is obtained by using equations (E20) and (E29):

$$\eta_2 = \eta_{2,M} \cos(\omega\theta - \varphi_2) \tag{E30}$$

in which

$$\left.\begin{aligned} \eta_{2,M} &= (\eta_{2,C}^2 + \eta_{2,S}^2)^{1/2} = \left(\frac{R^2 + Im^2}{\Phi_{R,b}^2 + \Phi_{I,b}^2}\right)^{1/2} \\ \varphi_2 &= \tan^{-1}\frac{\eta_{2,S}}{\eta_{2,C}} = \tan^{-1}\frac{\dfrac{R}{Im} - \dfrac{\Phi_{R,b}}{\Phi_{I,b}}}{\dfrac{\Phi_{R,b}}{\Phi_{I,b}}\dfrac{R}{Im} + 1} \end{aligned}\right\} \tag{E31}$$

The following observations may now be made:

(1) Equation (B15) (or eq. (9)) is merely a special case of (E30), since, in the case of a homogeneous cylinder, $R = ber_0$ and $Im = bei_0$.

(2) In addition, the following may be written:

$$\left.\begin{aligned} \eta_{2,C} &= C_2^* f_R(l^*) + G_2^* F_R(l^*) + D_2^* f_I(l^*) + E_2^* F_I(l^*) = C_3 R + C_4 Im \\ \eta_{2,S} &= D_2^* f_R(l^*) + E_2^* F_R(l^*) - C_2^* f_I(l^*) - G_2^* F_I(l^*) = C_4 R - C_3 Im \end{aligned}\right\} \tag{E32}$$

It follows that

$$\left.\begin{aligned} R &= (\Phi_{R,b}^2 + \Phi_{I,b}^2)(\Phi_{R,b}\,\eta_{2,C} + \Phi_{I,b}\,\eta_{2,S}) \\ Im &= (\Phi_{R,b}^2 + \Phi_{I,b}^2)(\Phi_{I,b}\,\eta_{2,C} - \Phi_{R,b}\,\eta_{2,S}) \end{aligned}\right\} \tag{E33}$$

or

$$R = (\Phi_{R,b}^2 + \Phi_{I,b}^2)\left[(\Phi_{R,b}\,C_2^* + \Phi_{I,b}\,D_2^*)\,f_R(l^*) + (\Phi_{R,b}\,G_2^* + \Phi_{I,b}\,E_2^*)\,F_R(l^*) + (\Phi_{R,b}\,D_2^* - \Phi_{I,b}\,C_2^*)\,f_I(l^*) + (\Phi_{R,b}\,E_2^* - \Phi_{I,b}\,G_2^*)\,F_I(l^*)\right]$$

$$Im = (\Phi_{R,b}^2 + \Phi_{I,b}^2)\left[(\Phi_{I,b}\,C_2^* - \Phi_{R,b}\,D_2^*)\,f_R(l^*) + (\Phi_{I,b}\,G_2^* - \Phi_{R,b}\,E_2^*)\,F_R(l^*) + (\Phi_{I,b}\,D_2^* + \Phi_{R,b}\,C_2^*)\,f_I(l^*) + (\Phi_{I,b}\,E_2^* + \Phi_{R,b}\,G_2^*)\,F_I(l^*)\right] \quad \text{(E34)}$$

Since, at l_a^*, $R_a = ber_{0,a} = f_R(l_a) = f_R(\alpha_1 r_a)$, these equations also furnish relations among R_a, Im_a, $f_R(l_a^*)$, and so forth. The significance of relations (E34) is that, in actuality, the right sides of these relations are independent of Ja.

(3) Because of the nature of the derivation, equations (E31) are valid for any number of layers. If extension of the analysis to a plurality of layers were desired, therefore, it would only be necessary to continue the integration outward through the succession of layers to the surface.

The additional relations (E15), and so forth, required are now obtainable as follows:

$$\bar{\eta} = \frac{1}{\pi(r_b^2 - r_a^2)} \int_{r_a}^{r_b} 2\pi r \eta \, dr$$

$$= \frac{2}{l_b^{*2}(1 - \beta^2)} \int_{l_a^*}^{l_b^*} \left(\frac{R^2 + Im^2}{\Phi_{R,b}^2 + \Phi_{I,b}^2}\right)^{1/2} \cos\left[\omega\theta - \left(\frac{\frac{R}{Im} - \frac{\Phi_{R,b}}{\Phi_{I,b}}}{\frac{\Phi_{R,b}}{\Phi_{I,b}}\frac{R}{Im} + 1}\right)\right] dl^*$$

In the execution of this integration, the following is used:

$$\int_{y_1}^{y_2} xR(x)\,dx = y_2 Im'(y_2) - y_1 Im'(y_1)$$

$$\int_{y_1}^{y_2} xIm(x)\,dx = -y_2 R'(y_2) + y_1 R'(y_1)$$

The result of the integration is the following with obvious details omitted:

$$\bar{\eta}_2 = \bar{\eta}_{2,M} \cos(\omega\theta - \bar{\varphi}) \tag{E35}$$

in which $\bar{\eta}_{2,M}$ is given by equation (E15) and is also equal to $(\bar{\eta}_{2,C}^2 + \bar{\eta}_{2,S}^2)^{1/2}$ of equation (C19), and $\bar{\varphi}$ is given by equation (E16) and is also equal to $\tan^{-1}(\bar{\eta}_{2,S}/\bar{\eta}_{2,C})$ of equation (C19). In this case, again, if $\beta \to 0$, R' becomes ber_0', Im' becomes bei_0', and $\bar{\eta}_{2,M}$ and $\bar{\varphi}_2$ reduce to the expressions contained in equation (B17). Note, however, that in this instance $\alpha_2/\alpha_1 = 1$ since the derivatives ber_0' and bei_0' would then be evaluated with respect to the outer material, that is, with respect to the variable $\alpha_2 r$ rather than $\alpha_1 r$, and, further, $l_b = \alpha_1 r_b$ would become $l_b^* = \alpha_2 r_b$.

The expressions (E17) and (E18) are then obtained in an obvious manner by performing the indicated division and subtraction, using equations (E15), (E16), and (E31). The point that $\eta_{2,M}/\bar{\eta}_{2,M}$ and $\tan(\bar{\varphi}_2 - \varphi_2)$ are dependent only upon the physical structure (β, r_b, and properties) of the laminated cylinder and upon frequency and are independent of the heat-transfer coefficient (i.e., Ja_2, provided the remaining physical variables of Ja_2 are constant), is of the greatest importance. That fact follows directly from the discussions in the text concerning $\omega\tau_{int,1}$ and $\omega\tau_{int,2}$, and enables calculation of the internal distribution of temperature without reference to mass-flow conditions.

APPENDIX F

HOLLOW-SHELL THEORY

The differential equation of heat flow (e.g., eq. (B1)) applies. As usual, the subscript "a" means that the quantity in question is to be evaluated at the interface (in this instance, the interior surface); "b" means that the quantity is to be evaluated at the outer surface.

The boundary conditions are:

$$\left(\frac{\partial \eta}{\partial l}\right)_b = Ja(\cos \omega\theta - \eta_b) \tag{F1}$$

$$\left(\frac{\partial \eta}{\partial l}\right)_a = 0 \tag{F2}$$

The expression (C13) is valid in the present case; it is necessary merely to evaluate the constants C*, G*, D*, and E*. This may be accomplished by using the right side of equation (C13) in equations (F1) and (F2). The resulting pair of equations in $\cos \omega\theta$ and $\sin \omega\theta$ is then split, as usual, into four relations.

Only the results are given. Certain auxiliary parameters are first defined ($l = \alpha r$, where α is characteristic of the shell material), and it should be noted that the denotations here assigned the quantities a, b, c, d, g, m, n, and p are restricted to the present appendix.

$$\left.\begin{aligned}
a \equiv \Phi_{R,b} &= \mathrm{ber}_0(l_b) + Ja^{-1}\,\mathrm{ber}_0'(l_b) \\
b \equiv \Phi_{I,b} &= \mathrm{bei}_0(l_b) + Ja^{-1}\,\mathrm{bei}_0'(l_b) \\
c &\equiv \mathrm{ker}_0(l_b) + Ja^{-1}\,\mathrm{ker}_0'(l_b) \\
d &\equiv \mathrm{kei}_0(l_b) + Ja^{-1}\,\mathrm{kei}_0'(l_b) \\
g &\equiv -\mathrm{ber}_0'(l_a) \\
m &\equiv -\mathrm{bei}_0'(l_a) \\
n &\equiv -\mathrm{ker}_0'(l_a) \\
p &\equiv -\mathrm{kei}_0'(l_a)
\end{aligned}\right\} \tag{F3}$$

The set of equations determining the constants is then the following:

$$\left.\begin{aligned} aC^* + bG^* + cD^* + dE^* &= 1 \\ -bC^* + aG^* - dD^* + cE^* &= 0 \\ gC^* + mG^* + nD^* + pE^* &= 0 \\ -mC^* + gG^* - pD^* + nE^* &= 0 \end{aligned}\right\} \tag{F4}$$

The simplicity and symmetry of this set of equations are such that it seemed worthwhile to obtain the explicit solutions. These solutions are the following:

The determinant Δ of the coefficients a, . . ., p is given by:

$$\Delta = (a^2 + b^2)(n^2 + p^2) + (g^2 + m^2)(c^2 + d^2) + 2[(am - bg)(dn - cp) - (ag + bm)(dp + cn)] \tag{F5}$$

The constants are then given by:

$$\left.\begin{aligned} C^* &= \Delta^{-1}[a(n^2 + p^2) + m(dn - cp) - g(dp + cn)] \\ D^* &= \Delta^{-1}[b(n^2 + p^2) - m(dp + cn) - g(dn - cp)] \\ G^* &= \Delta^{-1}[c(g^2 + m^2) - p(am - bg) - n(ag + bm)] \\ E^* &= \Delta^{-1}[d(g^2 + m^2) - p(ag + bm) + n(am - bg)] \end{aligned}\right\} \tag{F6}$$

The mean temperature amplitude and phase are given by the following, which were in part obtained from equations (C20) by putting $\zeta_b^* = \zeta_b$, $f_I = \mathrm{bei}_0$, and so forth:

$$\bar{\eta}_{a-b} = (\bar{\eta}_C^2 + \bar{\eta}_S^2)^{1/2} \cos\left(\omega\theta - \tan^{-1}\frac{\bar{\eta}_S}{\bar{\eta}_C}\right) \tag{F7}$$

where

$$\bar{\eta}_C = \frac{2}{l_b(1 - \beta^2)} [C^*(\mathrm{bei}_0'(l_b) - \beta\mathrm{bei}_0'(l_a)) + G^*(\mathrm{kei}_0'(l_b) - \beta\mathrm{kei}_0'(l_a)) - D^*(\mathrm{ber}_0'(l_b) - \beta\mathrm{ber}_0'(l_a)) - E^*(\mathrm{ker}_0'(l_b) - \beta\mathrm{ker}_0'(l_a))]$$

$$\bar{\eta}_S = \frac{2}{l_b(1 - \beta^2)} [D^*(\mathrm{bei}_0'(l_b) - \beta\mathrm{bei}_0'(l_a)) + E^*(\mathrm{kei}_0'(l_b) - \beta\mathrm{kei}_0'(l_a)) + G^*(\mathrm{ber}_0'(l_b) - \beta\mathrm{ber}_0'(l_a)) + G^*(\mathrm{ker}_0'(l_b) - \beta\mathrm{ker}_0'(l_b))] \quad (F8)$$

APPENDIX G

INTERPOLATION AMONG CALCULATED RESPONSE VALUES

The following discussion relates to the construction of the response curves of the real wires A and C discussed in the main text. It should first be observed that successive amplitude curves (fig. 8) corresponding to successive Biot numbers differing from one another by multiples of a single factor are uniformly spaced along the amplitude axis (ordinate) except at very large (~ 1) amplitudes. This uniformity, of course, exists only on a log-log plot. It follows that the correct ordinate of a point corresponding to a Biot number falling between two for which calculations were made is found by first establishing the ratio of the intermediate Biot number to the smaller of the two. The ratio is then considered to be some fraction of the common ratio existing between successive Biot numbers of the calculations, which is $10^{1/4} = 1.7782794+$. The fraction thus found is used to establish the ordinate of the point to be plotted in the manner to be now indicated; the method is actually a linear-logarithmic interpolation and is clarified by the following example (which concerns the oxide surface points for wire A):

The Biot number for wire A is 0.00064. Oxide surface calculations were available for all the combinations of Biot number, $\omega\tau_{int,2}$, and Ja_2^{-1} for which laminated-cylinder results were obtained, as well as for many additional points. At an $\omega\tau_{int,2}$ value of 0.1, the $Ja_2^{-1} = 2107.1+$ amplitude (for the Biot number 0.00045045) is 0.0031747. At the same $\omega\tau_{int,2}$ value of 0.1, the $Ja_2^{-1} = 1184.9+$ amplitude (for the Biot number 0.00080103) is 0.0056364. The ratio 0.00064/0.00045045 = 1.421 (slide rule). Using the relation, fractional (physical) distance (denoted by z) from 0.00045045 to 0.000640 $= 4 \log_{10}\left(\frac{0.00064}{0.00045045}\right) = 4 \log_{10}(1.421)$, z is found to be about 0.61_0. This means that on these log-log plots, points corresponding to a Biot number of 0.0064 will fall 0.61 times the actual vertical distance between 0.00045045 and 0.00080103 Biot number values above the 0.00045045 points (all at a given $\omega\tau_{int,2}$ value). In particular, the amplitude for the example cited should be about 0.0450; that figure is most easily obtained by using a Gerber variable scale (essentially, a good spring with a number of marked turns) to interpolate linearly on a log scale after marking points at 0.00564 (= 0.0056364) and 0.00317+ (= 0.0031747).

As a check on the relation given for the calculation of z, it should be noted that z is unity when $\log_{10}\left(\frac{\text{Biot number}}{0.00045045}\right) = 0.25$, that is, when the Biot number is 0.00080103.

Since complete $\beta = 0.90$ and 0.75 curves are available for the Biot numbers 0.00045045 and 0.00080103, the Gerber variable scale may be used more directly where the laminated-cylinder results are concerned by establishing a series of points lying 0.61 (in this example) of the vertical distance between the curves in question above the lower (0.00045045) curve. In this manner, a large number of points may be easily and accurately established either on the original sheet (fig. 8) or a new one (e.g., fig. 11). This procedure was followed for all of the surface points and $\beta = 0.90$ and 0.75 points of wires A and C. The accuracy of the procedure of course decreases where it is obvious by inspection that the increments (in terms of actual vertical distance on the log-log plot) of amplitude are no longer equal for successive pairs of Biot numbers differing by a common factor; this situation will generally exist at high amplitudes only and does not represent a serious limitation evidently.

REFERENCES

1. Willis, J. B.: Review of Hot Wire Anemometry. Rep. ACA-19, Australian Council Aero., Oct. 1945.

2. Shepard, Charles E., and Warshawsky, Isadore: Electrical Techniques for Compensation of Thermal Time Lag of Thermocouples and Resistance Thermometer Elements. NACA TN 2703, 1952.

3. Ossofsky, Eli: Constant Temperature Operation of the Hot-Wire Anemometer at High Frequency. Rev. Sci. Instr., vol. 19, no. 12, Dec. 1948, pp. 881-889.

4. Carslaw, H. S., and Jaeger, J. C.: Conduction of Heat in Solids. Univ. Press (Oxford), 1947.

5. Watson, G. N.: A Treatise on the Theory of Bessel Functions. Second ed., Cambridge Univ. Press, 1952.

6. Fletcher, Alan, Miller, J. C. P., and Rosenhead, L.: An Index of Mathematical Tables. McGraw-Hill Book Co., Inc., 1946.

7. Lamb, Horace: On the Induction of Electric Currents in Cylindrical and Spherical Conductors. Proc. London Math. Soc., vol. XV, Jan. 1884, pp. 139-149.

8. Thomson, J. J.: Recent Researches in Electricity and Magnetism. Clarendon Press (Oxford), 1893, p. 357.

9. Jakob, Max: Heat Transfer. Vol. I. John Wiley & Sons, Inc., 1949.

10. Gröber, Heinrich: Temperaturverlauf und Wärmeströmungen in periodisch Erwärmten Körpern. Forsch.-Arb., Heft 300, 1928, pp. 1-13.

11. Boelter, L. M. K., Cherry, V. H., Johnson, H. A., and Martinelli, R. C.: Heat Transfer Notes. Univ. Calif. Press (Berkeley and Los Angeles), 1948, particularly pp. VI-30 to VI-37.

12. Computation Laboratory, National Bureau Standards: Table of the Bessel Functions $J_0(z)$ and $J_1(z)$ for Complex Arguments. Second ed., Columbia Univ. Press, 1947.

13. Computation Laboratory, National Bureau Standards: Table of the Bessel Functions $Y_0(z)$ and $Y_1(z)$ for Complex Arguments. Columbia Univ. Press, 1950.

14. Berger, Kathleen, Turner, L. Richard, and Patton, Norman A.: General-Purpose Floating Point Control Panels for the IBM Card-Programmed Electronic Calculator. International Business Machine Corp., 1951. (Reprinted from Proc., Computation Seminar, Dec. 1949.)

15. Lowell, Herman H.: Response of Two-Material Laminated Cylinder to Simple Harmonic Environment Temperature Change. Jour. Appl. Phys., vol. 24, no. 12, Dec. 1953, pp. 1473-1478.

16. Scadron, Marvin D., and Warshawsky, Isidore: Experimental Determination of Time Constants and Nusselt Numbers for Bare-Wire Thermocouples in High-Velocity Air Streams and Analytic Approximation of Conduction and Radiation Errors. NACA TN 2599, 1952.

17. Whitehead, C. S.: On a Generalization of the Functions ber x, bei x, ker x, kei x. Quart. Jour. Pure and Appl. Math., vol. 42, 1911, pp. 316-342.

18. Russel, Alexander: The Effective Resistance and Inductance of a Concentric Main, and Methods of Computing the Ber and Bei and Allied Functions. Phil. Mag., ser. 7, vol. 17, 1909, pp. 524-552.

TABLE I. - VALUES OF bei, ber, bei', ber', AND RELATED FUNCTIONS

$\omega\tau_{int}$	αr	$(\alpha r)^2$	ber(αr)		bei(αr)		ber'(αr)		bei'(αr)	
			Correct	Gröber	Correct	Gröber	Correct	Gröber	Correct	Gröber
0	0	0	1	1	0	0	0	0	0	0
.00444	.2	.04	.99998	1.000	.01000	.010	-.00049	-.0005	.10000	.100
.02775	.5	.25	.99902	.999	.06249	[a].063	-.00781	-.0078	.24992	.250
.111	1	1	.98438	.984	.24957	.250	-.06244	[a]-.0625	.49740	.497
.444	2	4	.75173	.752	.97229	.972	-.49307	-.493	.91702	.917
.999	3	9	-.22138	-.221	1.93759	1.938	-1.56984	-1.570	.88048	.880
1.776	4	16	-2.56342	-2.563	2.29269	2.293	-3.13465	-3.13	-.49114	[a]-.496
2.775	5	25	-6.23008	-6.230	.11603	.116	-3.84534	[a]-3.85	-4.35414	[a]-4.369
3.996	6	36	-8.85832	-8.86	-7.33475	-7.33	-.29308	[a]-.27	-10.84623	[a]-10.86
5.439	7	49	-3.63293	[a]-3.59	-21.23940	[a]-21.23	12.76452	[a]13.0	-16.04150	[a]-15.1
7.104	8	64	20.97396	[a]21.4	-35.01673	[a]-34.89	38.31133	[a]38.5	-7.66031	[a]-8.05
8.991	9	81	73.93573	[a]75.4	-24.71278	[a]-25.0	65.60077	[a]67.5	36.29938	[a]25.8
11.1	10	100	138.84047	[a]146	56.37046	[a]55.4	51.19526	[a]52.5	135.30930	[a]122

ber^2 (Correct)	bei^2 (Correct)	$ber^2 + bei^2$ (Correct)	$(ber^2+bei^2)^{\frac{1}{2}}$ (Correct)	[b]$(ber^2 + bei^2)^{-0.5}$		ber_1 (Correct)	bei_1 (Correct)	$ber_1 + bei_1$ (Correct)	$bei_1 - ber_1$ (Correct)
				Correct	Gröber				
1.000	0	1.000	1.0000	1.0000	1.000	0	0	0	0
.99996	.00010	1.00006	1.0000300	.99997000	1.000	-.07106	.07036	-.00070	.14142
.99804	.003905	1.001945	1.0009718	.99902914	.999	-.18224	.17120	-.01104	.35344
.96900	.062285	1.031285	1.0155220	.98471525	[a].987	-.039587	.30756	-.08831	.70343
.56510	.94334784	1.5104478	1.2290027	.81366786	[a].775	-.99708	.29978	-.69730	1.29686
.04901	3.7542550	3.803265	1.9501961	.51276895	.513	-1.73264	-.48745	2.22009	1.24519
6.57112	5.2564274	11.827547	3.4391200	.29077206	.291	-1.86925	-2.56382	-4.43307	-.69457
38.81390	.01346296	38.827363	6.2311606	.16048375	[a].161	.35978	-5.79791	-5.43813	-6.15769
78.46985	53.798558	132.26839	11.500799	.08695048	.087	7.46220	-7.87668	-.41448	-15.33888
13.19818	451.11211	464.31029	21.547860	.04640832	[a].047	20.36893	-2.31717	18.05176	-22.68610
439.90700	1226.1714	1,666.0784	40.817623	.02449922	[a].025	32.50686	21.67354	54.18040	-10.83332
5,466.4922	610.72150	6,077.2137	77.956486	.01282767	.013	20.71921	72.05429	92.77350	51.33508
19,276.676	3177.6288	22,454.305	149.84761	.00667345	[a].006	-59.47761	131.87864	72.40103	191.35625

[a]Incorrect values.

[b]$(ber^2 + bei^2)^{-0.5} = \chi_{0m}$ in Gröber's notation.

TABLE II. - CONVERSION FACTORS AND CONSTANTS

(a) Conversion factors

$Ja^{*2} = {}^{a}(h^2 a t_0)$	$Ja^2 = \frac{{}^{a}(h^2 a t_0)}{2\pi}$	$Ja_2 = \sqrt{\frac{{}^{a}(h^2 a t_0)}{2\pi}}$	$Fo^* = {}^{a}\left(\frac{at_0}{R2}\right)$	Fo^{-1}
0	0	0	0	∞
.001	.00015915494	.012615663	.2	31.41593
.002	.00031830986	.017841240	.5	12.56637
.005	.00079577466	.028209478		
.01	.0015915494	.039894229	1	6.283185
.002	.0031830986	.056418955	2	3.141593
.005	.0079577466	.089206203	5	1.256637
.1	.015915494	.12615663	10	.6283185
.2	.031830986	.17841240	20	.3141593
.5	.079577466	.28209478	50	.1256637
1	.15915494	.39894229	100	.06283185
2	.31830986	.56418955	200	.03141593
5	.79577466	.89206203		
			∞	0
10	1.5915494	1.2615663		
20	3.1830986	1.7841240		
50	7.9577466	2.8209478		
100	15.915494	3.9894229		
200	31.830986	5.6418955		
500	79.577466	8.9206203		
1000	159.15494	12.615663		
∞	∞	∞		

$Fo^* \equiv {}^{a}\left(\frac{at_0}{2}\right)$	$Fo = \frac{1}{2\pi}\,{}^{a}\left(\frac{at_0}{2}\right)$	$\omega\tau_{int} = \frac{\lambda}{Fo} = \frac{2\pi\lambda}{Fo}$	$\alpha_2 r_b = Fo^{-0.5} = 3.00150(\omega\tau_{int})^{0.5}$
0	0	∞	∞
.1	.015915494	6.97434	7.92665
.2	.031830986	3.48717	5.60499
.5	.079577466	1.394867	3.54491
1	.15915494	.697434	2.50663
2	.31830986	.348717	1.772454
5	.79577466	.1394867	1.120998
10	1.5915494	.0697434	.792665
20	3.1830986	.0348717	.560499
50	7.9577466	.01394867	.354491
100	15.915494	.00697434	.250663
200	31.830986	.00348717	.1772454
∞	∞	0	0

[a]Gröber's notation.

TABLE II. - Concluded. CONVERSION FACTORS AND CONSTANTS

(b) Constants

$2\pi = 6.2831853$	$\lambda = 0.111$ (Definition)
$\pi/2 = 1.5707963$	$0.111^{-1} = 9.0090090$
$\pi/4 = 0.78539816$	$0.111^{1/2} = 0.33316662$
$\sqrt{\pi} = 1.7724539$	$0.111^{-1/2} = 3.0015011$
$\sqrt{2\pi} = 2.5066283$	$0.111^{1/2}/2 = 0.16658331$
$\pi^{-1} = 0.31830989$	$(2\times0.111)^{-1} = 4.5045045$
$(2\pi)^{-1} = 0.15915494$	$(4\times0.111)^{-1} = 2.2522523$
$\sqrt{\pi/2} = 1.2533141$	$(4\times0.111)^{1/2} = 0.66633325$
$e^{-1} = 0.36787944$	$(4\times0.111)^{-1/2} = 1.5007506$
$1-e^{-1} = 0.63212056$	$2\pi\times0.111 = 0.69743357$
$\sqrt{2} = 1.4142136$	$(2\pi\times0.111)^{1/2} = 0.83512488$
$\sqrt{2}/2 = 0.70710678$	$(2\pi\times0.111)^{-1} = 1.4338283$
$2^{1/4} = 0.84089642$	$2\pi(4\times0.111)^{-1} = 14.151318$
$\sqrt{5} = 2.2360680$	$(2\pi/4\times0.111)^{1/2} = 3.7618238$
$\sqrt{10} = 3.1622777$	
$10^{1/4} = 1.7782794$	
$10^{3/4} = 5.6234133$	$\sqrt{1/5} = 0.44721360$
$\sqrt{20} = 4.4721360$	$\sqrt{1/10} = 0.31622777$
$\sqrt{40} = 6.3245553$	$\sqrt{1/20} = 0.22360680$
$\sqrt{80} = 8.9442719$	$\sqrt{1/40} = 0.15811388$
	$\sqrt{1/80} = 0.11180340$

TABLE III. - GROBER'S TABLE OF SURFACE AMPLITUDES AND PHASE SHIFTS FOR INFINITELY THICK SLABS

h^2at_0 [Ja*2]	η_0 [η_b]	ε_0 [φ_b]	h^2at_0 [Ja*2]	η_0 [η_b]	ε_0 [φ_b]
0	0	45°00'	1	0.304	32°40'
.001	.012	44°30'	2	.388	29°05'
.002	.017	44°20'	5	.510	23°50'
.005	.028	43°55'	10	.603	19°50'
.01	.039	43°30'	20	.689	15°50'
.02	.054	42°50	50	.784	11°50'
.05	.084	41°40'	100	.843	8°35'
.1	.116	40°20'	200	.883	6°20'
.2	.159	38°40'	500	.925	4°20'
.5	.232	35°35'	1000	.945	3°00'

TABLE IV. - REDUCTION FACTOR $\eta_0[\eta_b]$, DEPENDENT UPON

$h^2at_0[Ja^{*2}]$ AND $\frac{at_0}{R^2}[Fo^*]$

h^2at_0 $[Ja^{*2}]$	$\frac{at_0}{R^2}$ $[Fo^*]$											
	0	0.2	0.5	1	2	5	10	20	50	100	200	∞
0.000	0	0	0	0	0	0	0	0	0	0	0	----
.001	.01	.01	.01	.01	.01	.02	.03	.04	.06	.09	.13	1.00
.002	.02	.02	.02	.02	.02	.03	.04	.06	.10	.13	.19	1.00
.005	.03	.03	.03	.03	.04	.05	.07	.10	.16	.23	.31	1.00
.01	.04	.04	.04	.04	.05	.08	.10	.14	.22	.30	.43	1.00
.02	.05	.05	.05	.05	.06	.10	.14	.20	.30	.41	.55	1.00
.05	.08	.08	.08	.08	.09	.16	.22	.30	.45	.58	.70	1.00
.1	.12	.12	.12	.12	.14	.21	.30	.40	.57	.70	.81	1.00
.2	.16	.16	.16	.17	.19	.28	.40	.53	.69	.80	.89	1.00
.5	.23	.23	.25	.26	.30	.41	.56	.69	.83	.91	.94	1.00
1	.30	.31	.32	.33	.39	.53	.68	.80	.90	.94	.98	1.00
2	.39	.40	.41	.43	.50	.64	.78	.88	.94	.97	.99	1.00
5	.51	.52	.54	.57	.65	.79	.89	.96	.98	1.00	1.00	1.00
10	.60	.61	.64	.67	.73	.86	.94	.98	.99	1.00		
20	.69	.70	.72	.75	.81	.91	.95	.99	1.00			
50	.78	.79	.80	.83	.88	.95	.97	1.00				
100	.84	.85	.86	.88	.93	.97	1.00					
200	.88	.89	.90	.92	.95	.99	1.00					
500	.93	.93	.94	.96	.97	1.00						
1000	.95	.96	.97	.99	.99	1.00						
∞	1.00	1.00	1.00	1.00	1.00							

TABLE V. - PHASE SHIFT $\varepsilon_0[\varphi_b]$ DEPENDENT UPON $h^2at_0[Ja^{*2}]$ AND $\frac{at_0}{R^2}[Fo^*]$

h^2at_0 $[Ja^{*2}]$	$\frac{at_0}{R^2}[Fo^*]$											
	0	0.2	0.5	1	2	5	10	20	50	100	200	∞
0	45°	45°	50.5°	58.5°	68°	80.5°	86.5°	88°	88.5°	89°	89°	--
.001	45°	45°	50°	57.5°	66.5°	78.5°	83°	85°	84°	83°	81°	0°
.002	44°	45°	50°	57°	66°	78°	82.5°	84°	82°	81°	78°	0°
.005	44°	44.5°	49°	57°	65.5°	77°	81.5°	82°	77.5°	74°	70°	0°
.01	44°	44°	48.5°	56.5°	65°	75°	79°	79°	73.5°	69°	65°	0°
.02	43°	43.5°	48°	55.5°	63.5°	73°	77.5°	76°	68.5°	63.5°	57°	0°
.05	42°	43°	47°	53.5°	62°	71°	73°	70°	60°	52.5°	45°	0°
.1	40°	42°	45°	52°	60°	67.5°	68°	63.5°	53°	44°	35.5°	0°
.2	39°	40.5°	42.5°	49°	57°	63°	62°	55°	43°	34°	26°	0°
.5	36°	37.5°	39°	45.5°	52.5°	55°	52.5°	43.5°	32°	23.5°	16°	0°
1	33°	34.5°	36.5°	41°	47.0°	47.5°	42.5°	35°	24°	17.5°	11.5°	0°
2	29°	31°	32°	36°	42°	40°	33°	26°	17°	12°	8°	0°
5	24°	25.5°	26.5°	29.5°	32.5°	28.5°	23°	17°	11.5°	7.5°	4.5°	0°
10	20°	21°	22°	23.5°	25°	22°	16.5°	12.5°	7.5°	5°	2°	0°
20	16°	16.5°	17°	18°	20°	16.5°	12°	8°	4°	3°	2°	0°
50	12°	12°	12°	12.5°	13°	10.5°	7.5°	6°	3°	2°	1°	0°
100	9°	9°	9°	9°	9°	7°	5°	3°	2°	1°	1°	0°
200	6°	6°	6°	6°	6°	5°	4°	2°	1°	1°	0°	0°
500	4°	4°	4°	4°	4°	4°	3°	2°	1°	1°	0°	0°
1000	3°	3°	3°	3°	3°	3°	3°	2°	1°	1°	0°	0°
∞	0°	0°	0°	0°	0°	0°	0°	0°	0°	0°	0°	0°

TABLE VI. - MEAN RESPONSE OF HOMOGENEOUS CYLINDER FOR THE CASE OF SURFACE TEMPERATURE DRIVE

$\omega\tau_{int}$	$\overline{\eta}_M/\eta_{b,M}$	$\tan(\overline{\varphi}-\varphi_b)$	$\overline{\varphi}-\varphi_b$, radian
0.001	0.999999	0.00112613	0.00112610
.00316228	.999989	.00356124	.00356120
.01	.999897	.0112606	.0112601
.0316228	.998944	.0355885	.0355735
.1	.989627	.111904	.111441
.316228	.910910	.335156	.323390
1.0	.614989	.721615	.625086
3.16228	.350850	.859119	.709764
10.	.203056	.922660	.745194
31.6228	.116041	.957212	.763540
100.	.0658531	.976170	.773340
316.228	.0372233	.986665	.778686
1000.	.0209930	.992523	.781645

TABLE VII. - LAMINATED-CYLINDER CALCULATION

CASE NUMBERS

$a_2 r_b$	$\omega\tau_{int,2}$	Case numbers for $\beta = 0.90$ and k_2/k_1 of					Case numbers for $\beta = 0.75$ and k_2/k_1 of				
		5	10	20	40	80	5	10	20	40	80
		Group letter					Group letter				
		A	B	C	D	E	F	G	H	I	J
0.94916	0.1	2	4	8	13	19	1	3	6	10	16
1.6879	$0.1\sqrt{10}$	7	11	17	23	29	5	9	14	20	26
3.0015	1.	15	21	27	33	39	12	18	24	30	36
5.3375	$1.\sqrt{10}$	25	31	37	42	46	22	28	34	40	44
9.4916	10.	35	41	45	48	50	32	38	43	47	49

TABLE VIII. - LIMITS OF VARIABLES FOR 50 SHELL CASES

Case number	l_a, $\alpha_1 r_a$	l_b, $\alpha_1 r_b$	l^*_a, $\alpha_2 r_a$	l^*_b, $\alpha_2 r_b$	Case number	l_a, $\alpha_1 r_a$	l_b, $\alpha_1 r_b$	l^*_a, $\alpha_2 r_a$	l^*_b, $\alpha_2 r_b$
F1	1.5918	2.1224	0.71187	0.94916	J26	11.3228	15.0970	1.2659	1.6879
A2	1.9101	2.1224	.85424	.94916	C27	12.0808	13.4231	2.7014	3.0015
G3	2.2511	3.0015	.71187	.94916	G28	12.6590	16.8787	4.0031	5.3375
B4	2.7014	3.0015	.85424	.94916	E29	13.5873	15.0970	1.5191	1.6879
F5	2.8307	3.7743	1.2659	1.6879	I30	14.2373	18.9832	2.2511	3.0015
H6	3.1836	4.2448	.71187	.94916	B31	15.1908	16.8787	4.8038	5.3375
A7	3.3968	3.7743	1.5191	1.6879	F32	15.9179	21.2239	7.1187	9.4916
C8	3.8203	4.2448	.85424	.94916	D33	17.0848	18.9832	2.7014	3.0015
G9	4.0032	5.3376	1.2659	1.6879	H34	17.9025	23.8700	4.0031	5.3375
I10	4.5023	6.0030	.71187	.94916	A35	19.1015	21.2239	8.5424	9.4916
B11	4.8038	5.3376	1.5191	1.6879	J36	20.1347	26.8462	2.2511	3.0015
F12	5.0337	6.7116	2.2511	3.0015	C37	21.4830	23.8700	4.8038	5.3375
D13	5.4027	6.0030	.85424	.94916	G38	22.5113	30.0151	7.1187	9.4916
H14	5.6614	7.5485	1.2659	1.6879	E39	24.1616	26.8462	2.7014	3.0015
A15	6.0404	6.7116	2.7014	3.0015	I40	25.3180	33.7573	4.0031	5.3375
J16	6.3672	8.4895	.7187	.94916	B41	27.0136	30.0151	8.5424	9.4916
C17	6.7937	7.5485	1.5191	1.6879	D42	30.3816	33.7573	4.8038	5.3375
G18	7.1187	9.4916	2.2511	3.0015	E43	31.8358	42.4477	7.1187	9.4916
E19	7.6406	8.4895	.85424	.94916	J44	35.8050	47.7401	4.0031	5.3375
I20	8.0064	10.6752	1.2659	1.6879	C45	38.2030	42.4477	8.5424	9.4916
B21	8.5424	9.4916	2.7014	3.0015	E46	42.9660	47.7401	4.8038	5.3375
F22	8.9513	11.9350	4.0031	5.3375	I47	45.023	60.0301	7.1187	9.4916
D23	9.6077	10.6752	1.5191	1.6879	D48	54.027	60.0301	8.5424	9.4916
H24	10.0673	13.4231	2.2511	3.0015	J49	63.672	84.8955	7.1187	9.4916
A25	10.7415	11.9350	4.8038	5.3375	E50	76.406	84.8955	8.5424	9.4916

TABLE IX . - VALUES OF $\omega\tau_{ext,2}$ AND Bi_2 FOR VARIOUS VALUES OF Ja_2 AND $\omega\tau_{int,2}$

$\omega\tau_{int,2}$	0.1			$0.1\times10^{0.5} = 0.316228$		1		$1\times10^{0.5} = 3.16228$		10	
$(\omega\tau_{int,2})^{0.5}$	0.316228			0.562342		1		1.77828		3.16228	
a_2r_b	0.84916			1.6879		3.0015		5.3375		9.4916	
Fo	1.11			0.351013		0.111		0.0351013		0.0111	
Fo*	6.97434			2.20548		.697434		0.220548		0.0697434	
Ja_2	Ja_2^{-1}	$\omega\tau_{ext,2}$		Bi_2 (a)	$\omega\tau_{ext,2}$ (a)	Bi_2 (a)	$\omega\tau_{ext,2}$ (a)	Bi_2 (a)	$\omega\tau_{ext,2}$ (a)	Bi_2 (a)	$\omega\tau_{ext,2}$ (a)	Bi_2 (a)
0.000150075	6665.34	3162.28	$1000\times10^{0.5}$	1.42×10^{-4}	[b]5623	$[b]0.265\times10^{-3}$	10,000	0.450×10^{-3}	17,780	0.801×10^{-3}	31,620	1.42×10^{-3}
.00026688	3747.00	1778.28	$1000\times10^{0.25}$	$.253\times10^{-3}$	[b]3162	$[b].450\times10^{-3}$	5,623	$.801\times10^{-3}$	10,000	1.42×10^{-3}	17,780	2.53×10^{-3}
.00047458	2107.13	1000.00	1000	$.450\times10^{-3}$	[b]1778	$[b].801\times10^{-3}$	3,162	1.42×10^{-3}	5,623	2.53×10^{-3}	10,000	4.50×10^{-3}
.00084394	1184.92	562.34	$100\times10^{0.75}$	$.801\times10^{-3}$	[b]1000	$[b]1.42\times10^{-3}$	1,778	2.53×10^{-3}	3,162	4.50×10^{-3}	5,623	.00801
.00150075	666.334	316.228	$100\times10^{0.5}$	1.42×10^{-3}	[b]562	$[b]2.53\times10^{-3}$	1,000	4.50×10^{-3}	1,778	.00801	3,162	.0142
0.0026688	374.700	177.828	$100\times10^{0.25}$	2.53×10^{-3}	[b]316	$[b]4.50\times10^{-3}$	562	0.00801	1,000	0.0142	1,778	0.0253
.0047458	210.713	100.000	100	4.50×10^{-3}	[b]178	[b].00801	316	.0142	562	.0253	1,000	.0450
.0084394	118.492	[c]56.234	$[c]10\times10^{0.75}$	[c].00801	[b,c]100	[b,c].0142	[c]178	[c].0253	[c]316	[c].0450	[c]562	[c].0801
.0150075	666.334	31.6228	$10\times10^{0.50}$	.0142	[b]56.2	[b].0253	100	.0450	178	.0801	316	.142
.026688	37.4700	[d]17.7828	$[d]10\times10^{0.25}$	[d].0253	[b]31.6	[b].0450	56.2	.0801	100	.142	178	.253
0.047458	21.0713	10.0000	10	0.0450	[b,d]17.8	[b,d]0.0801	31.6	0.142	56.2	0.253	100	0.450
.084394	11.8492	5.6234	$1\times10^{0.75}$	.0801	[b]10.0	[b].142	[d]17.8	[d].253	31.6	.450	56.2	.801
.150075	6.66334	3.16228	$1\times10^{0.50}$	.142	[b]5.62	[b].253	10.0	.450	[d]17.8	[d].801	31.6	1.42
.26688	3.74700	1.77828	$1\times10^{0.25}$	.253	[b]3.16	[b].450	5.62	.801	10.0	1.42	[d]17.8	[d]2.53
.47458	2.10713	1.00000	1	.450	[b]1.78	[b].801	3.16	1.42	5.62	2.53	10.0	4.50
0.84394	1.18492	0.56234	$0.1\times10^{0.75}$	0.801	[b]1.00	[b]1.42	1.78	2.53	3.16	4.50	[e]5.62	[e]8.01
1.50075	.666334	.316228	$.1\times10^{0.50}$	1.42	[b].562	[b]2.53	1.00	4.50	[e]1.78	[e]8.01	3.16	14.2
2.6688	.374700	.177828	$.1\times10^{0.25}$	2.53	[b].316	[b]4.50	[e].562	[e]8.01	1.00	14.2	1.78	25.3
4.7458	.210713	.100000	.1	4.50	[b,e].178	[b,e]8.01	.316	14.2	.562	25.3	1.00	45.0

[a]Approximate values.
[b]Increasing heat-transfer coefficient. Read from top to bottom.
[c]Increasing surface radius r_b. Read from left to right.
[d]Increasing thermal conductivity level of entire cylinder. Read along diagonal from left to right.
[e]Increasing ω, ρ, c_p, $\omega\rho$, ωc_p, or $\omega\rho c_p$. Read along diagonal from left to right.

TABLE X. - SAMPLE IBM BLOCK INDICATING DENOTATION OF TABLE ENTRIES

$\omega\tau_{ext,2}$	Homogeneous cylinder	β	Laminated cylinder									
			k_2/k_1									
			5		10		20		40		80	
	Exact											
-1 1.000	$\overline{\eta}_{2,M}$ -1 9.7425	1.00	$\eta_{b,1,M}$	-1 9.6890	-1 9.6418		-1 9.7846		-1 9.7946		-1 9.8485	
	$\tan \overline{\Phi}_2$ -1 2.1149		$\tan \Phi_{b,1}$	-2 7.1037	-2 4.8138		-2 3.8689		-2 3.3180		-2 1.6442	
	$\overline{\Phi}_2$ .2084		$\Phi_{b,1}$	.0709	.0481		.0326		.0232		.0164	
		.90	$\overline{\eta}_{2,M}$	-1 9.6857	-1 9.6087		-1 9.6881		-1 9.7680		-1 9.8873	
			$\tan \overline{\Phi}_2$	-2 9.7118	-2 7.4636		-2 6.7013		-2 4.6700		-2 3.9506	
			$\overline{\Phi}_2$	.097	.075		.057		.047		.040	
	First order											
	η_2 -1 9.9504	.75	$\overline{\eta}_{2,M}$	-1 9.6489	-1 9.5991		-1 9.6461		-1 9.7894		-1 9.7947	
	μ, db -2 4.3214		$\tan \overline{\Phi}_2$	-1 1.3353	-1 1.1586		-2 9.6865		-2 8.5318		-2 7.8046	
	Φ_2 -2 9.9669		$\overline{\Phi}_2$	.133	.115		.097		.085		.078	

Symbols:

$\omega\tau_{int,2}$ product of angular frequency and internal time constant in homogeneous cylinder having properties of material 2 (the shell material in the case of the laminated cylinder)

$\omega\tau_{ext,2}$ product of angular frequency and external (conventional) time constant in homogeneous cylinder having volumetric specific heat equal to that of either material; the volumetric specific heats of materials 1 and 2 are assumed equal in this work

β ratio of core to over-all radius

k_2/k_1 ratio of thermal conductivity of material 2 to that of material 1

$\overline{\eta}_{2,M}$ relative mean amplitude in homogeneous material 2 cylinder or in material 2 shell of laminated cylinder

$\tan \overline{\Phi}_2$ tangent of phase shift (lag) angle in cylinder or shell in which amplitude is $\overline{\eta}_{2,M}$

$\overline{\Phi}_2$ phase shift (lag) angle in cylinder of shell in which amplitude is $\overline{\eta}_{2,M}$, radians

η_2 relative amplitude in homogeneous cylinder having volumetric specific heat of either material and infinitely great thermal conductivity; the volumetric specific heats of materials 1 and 2 are assumed equal in this work

μ, db attenuation, decibels, in cylinder in which amplitude is η_2 (note tangent of phase lag angle in this case equals $\omega\tau_{ext,2}$)

Φ_2 phase shift (lag) angle in cylinder in which amplitude is η_2, radians

$\eta_{b,1,M}$ relative amplitude at surface of material 1 cylinder

$\tan \Phi_{b,1}$ tangent of phase shift (lag) angle at surface of material 1 cylinder

$\Phi_{b,1}$ phase shift (lag) angle at surface of material 1 cylinder, radians

TABLE X. - RESPONSES OF CYLINDERS

[The number to the left of each entry denotes the power of ten by which each entry as printed is to be multiplied. Example: -1 9.7420 is actually equal to 0.97420.]

(a) $\omega\tau_{int,2} = 0.1$

$\omega\tau_{ext,2}$	Homogeneous cylinder: Exact / First order	β	Laminated cylinder k_2/k_1 = 5	= 10	= 20	= 40	= 80
-1 1.000	-1 9.7425 -1 2.1149 .2084	1.00	-1 9.6290 -2 7.1027 .0709	-1 9.6415 -2 4.8138 .0481	-1 9.7246 -2 3.2629 .0326	-1 9.7946 -2 2.3180 .0232	-1 9.8485 -2 1.6442 .0164
		.90	-1 9.6257 -2 9.7118 .097	-1 9.6087 -2 7.4636 .075	-1 9.6881 -2 5.7013 .057	-1 9.7680 -2 4.6700 .047	-1 9.8273 -2 3.9506 .040
	-1 9.9504 -2 4.3214 -2 9.9669	.75	-1 9.6489 -1 1.3353 .133	-1 9.5991 -1 1.1586 .115	-1 9.6461 -2 9.6865 .097	-1 9.7294 -2 8.5318 .085	-1 9.7947 -2 7.8046 .078
-1 1.778	-1 9.5666 -1 2.8899 .2813	1.00	-1 9.3293 -1 1.2299 .1224	-1 9.3661 -2 8.3348 .0832	-1 9.5141 -2 5.6828 .0568	-1 9.6371 -2 4.0579 .0406	-1 9.7320 -2 2.8900 .0289
		.90	-1 9.3592 -1 1.5629 .155	-1 9.3516 -1 1.2005 .120	-1 9.4857 -2 9.2298 .092	-1 9.6158 -2 7.6135 .076	-1 9.7132 -2 6.4788 .065
	-1 9.8455 -1 1.3581 -1 1.7599	.75	-1 9.4219 -1 2.0094 .198	-1 9.3657 -1 1.7431 .173	-1 9.4468 -1 1.4665 .146	-1 9.5733 -1 1.3018 .130	-1 9.6719 -1 1.1983 .119
-1 3.162	-1 9.1587 -1 4.2681 .4034	1.00	-1 8.7901 -1 2.0894 .2060	-1 8.8896 -1 1.4159 .1407	-1 9.1493 -2 9.7487 .0972	-1 9.3627 -2 7.0223 .0701	-1 9.5281 -2 5.0359 .0503
		.90	-1 8.8548 -1 2.5575 .250	-1 8.8876 -1 1.9595 .194	-1 9.1208 -1 1.5196 .158	-1 9.3382 -1 1.2652 .126	-1 9.5086 -1 1.0848 .108
	-1 9.5346 -1 4.1393 -1 3.0628	.75	-1 8.9585 -1 3.1665 .307	-1 8.9132 -1 2.7369 .267	-1 9.0615 -1 2.3163 .228	-1 9.2661 -1 2.0750 .205	-1 9.4233 -1 1.9242 .190
-1 5.623	-1 8.2656 -1 6.7189 .5916	1.00	-1 7.8664 -1 3.4423 .3315	-1 8.0995 -1 2.3324 .2291	-1 8.5365 -1 1.6311 .1617	-1 8.8946 -1 1.1918 .1186	-1 9.1763 -2 8.6457 .0868
		.90	-1 7.9413 -1 4.1636 .395	-1 8.0797 -1 3.1743 .307	-1 8.4761 -1 2.4923 .244	-1 8.8346 -1 2.1040 .207	-1 9.1115 -1 1.8242 .181
	-1 8.7163 1.1933 -1 5.1227	.75	-1 8.0525 -1 5.1021 .472	-1 8.0654 -1 4.3734 .412	-1 8.3349 -1 3.7240 .357	-1 8.6618 -1 3.3770 .326	-1 8.9136 -1 3.1689 .306
1.000	-1 6.6729 1.1077 .8365	1.00	-1 6.4700 -1 5.4133 .4962	-1 6.9040 -1 3.6673 .3515	-1 7.5701 -1 2.6246 .2567	-1 8.1307 -1 1.9603 .1936	-1 8.5877 -1 1.4485 .1438
		.90	-1 6.5003 -1 6.5969 .583	-1 6.8101 -1 4.9898 .463	-1 7.4133 -1 3.9890 .380	-1 7.9592 -1 3.4378 .331	-1 8.4002 -1 3.0316 .293
	-1 7.3711 3.0103 -1 7.8540	.75	-1 6.5469 -1 8.2040 .687	-1 6.6730 -1 6.9301 .606	-1 7.0939 -1 5.9448 .536	-1 7.5592 -1 5.4866 .502	-1 7.9860 -1 5.2148 .481
1.778	-1 4.6711 1.8827 1.0825	1.00	-1 4.7686 -1 7.9841 .6738	-1 5.3638 -1 5.4076 .4957	-1 6.2171 -1 3.9920 .3798	-1 6.9870 -1 3.0755 .2984	-1 7.6613 -1 2.3353 .2294
		.90	-1 4.7246 -1 9.9495 .783	-1 5.1667 -1 7.4425 .640	-1 5.9078 -1 6.0970 .548	-1 6.6064 -1 5.4113 .496	-1 7.2138 -1 4.8934 .455
	-1 4.9016 6.1933 1.0585	.75	-1 4.6752 1.2849 .910	-1 4.8914 1.0614 .815	-1 5.3837 -1 9.1916 .743	-1 5.9075 -1 8.6994 .716	-1 6.3337 -1 8.4515 .708

TABLE X. - Continued. RESPONSES OF CYLINDERS

[The number to the left of each entry denotes the power of ten by which each entry as printed is to be multiplied. Example: -1 9.7420 is actually equal to 0.97420.]

(a) Continued. $\omega\tau_{int,2} = 0.1$

$\omega\tau_{ext,2}$	Homogeneous cylinder: Exact / First order	β	Laminated cylinder, k_2/k_1 = 5	k_2/k_1 = 10	k_2/k_1 = 20	k_2/k_1 = 40	k_2/k_1 = 80
3.162	-1 2.9196 3.2609 1.2732	1.00	-1 3.1661 1.0893 .8281	-1 3.7640 -1 7.3762 .6355	-1 4.6363 -1 5.6463 .5140	-1 5.5075 -1 4.5824 .4247	-1 6.3564 -1 3.5618 .3488
		.90	-1 3.0818 1.4011 .951	-1 3.5158 1.0341 .802	-1 4.2160 -1 8.7351 .717	-1 4.9144 -1 8.0406 .677	-1 5.5748 -1 7.5247 .645
	-1 3.0151 1 1.0414 1.2645	.75	-1 2.9875 1.9141 1.089	-1 3.2024 1.5348 .993	-1 3.6890 1.3447 .931	-1 4.0721 1.3159 .921	-1 4.4407 1.3183 .922
5.623	-1 1.7173 5.7117 1.3975	1.00	-1 1.9522 1.3701 .9403	-1 2.4248 -1 9.2747 .7478	-1 3.1437 -1 7.3618 .6346	-1 3.9369 -1 6.1490 .5513	-1 4.8056 -1 5.0544 .4680
		.90	-1 1.8721 1.8229 1.069	-1 2.2027 1.3870 .925	-1 2.7333 1.1545 .857	-1 3.2846 1.1094 .837	-1 3.8383 1.0819 .825
	-1 1.7508 1 1.5135 1.3948	.75	-1 1.7860 2.6604 1.211	-1 1.9463 2.0608 1.119	-1 2.2453 1.8290 1.071	-1 2.5487 1.8614 1.078	-1 2.8015 1.9382 1.095
1 1.000	-2 9.8404 1 1.0070 1.4718	1.00	-1 1.1530 1.6023 1.0128	-1 1.4741 1.0844 .8259	-1 1.9798 -1 8.8787 .7261	-1 2.5803 -1 7.7082 .6567	-1 3.3044 -1 6.6127 .5843
		.90	-1 1.0946 2.1965 1.144	-1 1.3126 1.5798 1.007	-1 1.6631 1.4122 .955	-1 2.0384 1.4123 .955	-1 2.4161 1.4378 .963
	-2 9.9504 1 2.0043 1.4711	.75	-1 1.0336 3.4173 1.286	-1 1.1372 2.5592 1.198	-1 1.3242 2.2992 1.161	-1 1.5099 2.4340 1.181	-1 1.6635 2.6436 1.209
1 1.778	-2 5.5793 1 1.7820 1.5147	1.00	-2 6.6552 1.7711 1.0568	-2 8.6582 1.1985 .8754	-1 1.1882 1.0048 .7875	-1 1.5890 -1 8.9900 .7323	-1 2.1045 -1 7.9296 .6747
		.90	-2 6.2798 2.4833 1.188	-2 7.6127 1.7698 1.057	-2 9.7467 1.6155 1.017	-1 1.2023 1.6691 1.031	-1 1.4410 1.7636 1.055
	-2 5.6145 1 2.5014 1.5146	.75	-2 5.8942 4.0729 1.330	-2 6.5192 2.9646 1.246	-2 7.6263 2.6902 1.215	-2 8.7093 2.9464 1.244	-2 9.5958 3.3282 1.279
1 3.162	-2 3.1495 1 3.1602 1.5392	1.00	-2 3.7956 1.8826 1.0825	-2 4.9877 1.2738 .9053	-2 6.9313 1.0841 .8257	-2 9.4117 -1 9.9175 .7813	-1 1.2787 -1 9.0694 .7366
		.90	-2 3.5686 2.6805 1.214	-2 4.3525 1.8984 1.086	-2 5.6057 1.7580 1.054	-2 6.9449 1.8596 1.077	-2 8.3538 2.0822 1.112
	-2 3.1607 1 3.0004 1.5392	.75	-2 3.3379 4.5672 1.355	-2 3.7026 3.2555 1.273	-2 4.3417 2.9757 1.247	-2 4.9603 3.3434 1.280	-2 5.4632 3.8974 1.320
1 5.623	-2 1.7744 1 5.6110 1.5530	1.00	-2 2.1509 1.9517 1.0973	-2 2.8427 1.3805 .9227	-2 3.9786 1.1349 .8485	-2 5.4497 1.0588 .8111	-2 7.4591 -1 9.8068 .7756
		.90	-2 2.0182 2.8059 1.228	-2 2.4699 1.9793 1.103	-2 3.1918 1.8499 1.075	-2 3.9681 1.9871 1.105	-2 4.7737 2.2040 1.145
	-2 1.7780 1 3.5001 1.5530	.75	-2 1.8840 4.9024 1.370	-2 2.0932 3.4461 1.288	-2 2.4575 3.1648 1.265	-2 2.8079 3.6180 1.301	-2 3.0915 4.3188 1.343

TABLE X. - Continued. RESPONSES OF CYLINDERS

[The number to the left of each entry denotes the power of ten by which each entry as printed is to be multiplied. Example: -1 9.7420 is actually equal to 0.97420.]

(a) Concluded. $\omega\tau_{int,2} = 0.1$

$\omega\tau_{ext,2}$	Homogeneous cylinder: Exact / First order	β	Laminated cylinder, k_2/k_1 = 5	k_2/k_1 = 10	k_2/k_1 = 20	k_2/k_1 = 40	k_2/k_1 = 80
2 1.000	-3 9.9883 1 9.9693 1.5608	1.00	-2 1.2147 1.9928 1.1057	-2 1.6106 1.3483 .9326	-2 2.2638 1.1656 .8617	-2 3.1153 1.0906 .8287	-2 4.2935 1.0277 .7990
		.90	-2 1.1384 2.6817 1.237	-2 1.3959 2.0280 1.113	-2 1.8067 1.9059 1.088	-2 2.2456 2.0669 1.120	-2 2.7077 2.3215 1.164
	-3 9.9995 1 4.0000 1.5608	.75	-2 1.0616 5.1136 1.378	-2 1.1805 3.5635 1.297	-2 1.3869 3.2823 1.275	-2 1.5846 3.7933 1.313	-2 1.7442 4.5880 1.356
2 1.778	-3 5.6198 2 1.7719 1.5652	1.00	-3 6.8473 2.0167 1.1105	-3 9.0952 1.3645 .9383	-2 1.2809 1.1836 .8693	-2 1.7681 1.1131 .8388	-2 2.4463 1.0561 .8127
		.90	-3 6.4189 2.9262 1.242	-3 7.8716 2.0564 1.118	-2 1.0198 1.9389 1.095	-2 1.2683 2.1146 1.129	-2 1.5299 2.3932 1.175
	-3 5.6233 1 4.5000 1.5652	.75	-3 5.9763 5.2407 1.383	-3 6.6492 3.6331 1.302	-3 7.8144 3.3523 1.281	-3 8.9285 3.8997 1.320	-3 9.8263 4.7589 1.364
2 3.162	-3 3.1611 2 3.1501 1.5676	1.00	-3 3.8556 2.0304 1.1132	-3 5.1265 1.3737 .9416	-3 7.2298 1.1940 .8736	-3 9.9939 1.1261 .8446	-2 1.3858 1.0728 .8305
		.90	-3 3.6096 2.9518 1.244	-3 4.4333 2.0728 1.121	-3 5.7466 1.9580 1.099	-3 7.1493 2.1425 1.134	-3 8.6256 2.4385 1.181
	-3 3.1623 1 5.0000 1.5676	.75	-3 3.3627 5.3150 1.385	-3 3.7483 3.6735 1.305	-3 4.3990 3.3930 1.284	-3 5.0861 3.9622 1.324	-3 5.5310 4.8607 1.368
2 5.623	-3 1.7779 2 5.6009 1.5690	1.00	-3 2.1698 2.0382 1.1147	-3 2.8867 1.3790 .9434	-3 4.0736 1.1999 .8760	-3 5.6364 1.1336 .8479	-3 7.8251 1.0885 .8250
		.90	-3 2.0310 2.9664 1.246	-3 2.4952 2.0821 1.123	-3 3.2354 1.9689 1.101	-3 4.0258 2.1585 1.137	-3 4.8576 2.4600 1.185
	-3 1.7783 1 5.5000 1.5690	.75	-3 1.8916 5.3577 1.386	-3 2.1058 3.6966 1.307	-3 2.4753 3.4163 1.286	-3 2.8281 3.9982 1.326	-3 3.1120 4.9200 1.370
3 1.000	-4 9.9988 2 9.9592 1.5698	1.00	-3 1.2807 2.0426 1.1155	-3 1.6245 1.3819 .9444	-3 2.2933 1.2033 .8774	-3 3.1747 1.1378 .8498	-3 4.4106 1.0880 .8275
		.90	-3 1.1424 2.9747 1.247	-3 1.4039 2.0873 1.124	-3 1.8206 1.9751 1.102	-3 2.2656 2.1676 1.139	-3 2.7338 2.4740 1.187
	-3 1.0000 1 6.0000 1.5698	.75	-3 1.0639 5.3881 1.387	-3 1.1844 3.7097 1.308	-3 1.3984 3.4296 1.287	-3 1.5909 4.0187 1.327	-3 1.7506 4.9539 1.372
3 1.778	-4 5.6230 3 1.7710 1.5702	1.00	-4 6.8660 2.0481 1.1160	-4 9.1392 1.3836 .9450	-3 1.2905 1.2051 .8782	-3 1.7869 1.1402 .8508	-3 2.4835 1.0911 .8289
		.90	-4 6.4255 2.9794 1.247	-4 7.8967 2.0903 1.125	-3 1.0242 1.9786 1.103	-3 1.2746 2.1727 1.140	-3 1.5381 2.4819 1.188
	-4 5.6234 1 6.5000 1.5702	.75	-4 5.9837 5.3958 1.388	-4 6.6612 3.7171 1.308	-4 7.8318 3.4371 1.288	-4 8.9480 4.0304 1.328	-4 9.8459 4.9732 1.378
3 3.162	-4 3.1628 3 3.1491 1.5705	1.00	-4 3.8615 2.0465 1.1163	-4 5.1405 1.3846 .9453	-4 7.2594 1.2062 .8786	-3 1.0054 1.1416 .8514	-3 1.3976 1.0928 .8297
		.90	-4 3.6136 2.9820 1.247	-4 4.4413 2.0920 1.125	-4 5.7604 1.9805 1.103	-4 7.1691 2.1756 1.140	-4 8.6513 2.4864 1.188
	-4 3.1623 1 7.0000 1.5705	.75	-4 3.3650 5.4036 1.388	-4 3.7462 3.7213 1.308	-4 4.4045 3.4413 1.288	-4 5.0323 4.0370 1.328	-4 5.5372 4.9841 1.373

TABLE X. - Continued. RESPONSES OF CYLINDERS

[The number to the left of each entry denotes the power of ten by which each entry as printed is to be multiplied. Example: -1 9.7420 is actually equal to 0.97420.]

(b) $\omega\tau_{int,2}$ = 0.316228

$\omega\tau_{ext,2}$	Homogeneous cylinder: Exact	Homogeneous cylinder: First order	β	Laminated cylinder, k_2/k_1 = 5	k_2/k_1 = 10	k_2/k_1 = 20	k_2/k_1 = 40	k_2/k_1 = 80
-1 1.778	-1 8.5722	-1 8.5728	1.00	-1 9.4635	-1 9.5994	-1 9.7025	-1 9.7824	-1 9.8485
	-1 5.0600	-1 5.0600		-2 6.4140	-2 4.5475	-2 3.2433	-2 2.3081	-2 1.6408
	.4684	.4684		.0641	.0454	.0324	.0231	.0164
			.90	-1 9.2936	-1 9.4696	-1 9.5994	-1 9.7055	-1 9.7836
				-1 1.1772	-2 9.5679	-2 8.0887	-2 7.0094	-2 6.2397
				.117	.095	.081	.700	.062
	-1 9.8455	-1 9.8455	.75	-1 8.9793	-1 9.2497	-1 9.4180	-1 9.5464	-1 9.6449
	-1 1.3581	-1 1.3581		-1 2.0713	-1 1.8306	-1 1.6819	-1 1.5733	-1 1.4942
	-1 1.7599	-1 1.7599		.204	.181	.167	.156	.148
-1 3.162	-1 8.0956	-1 8.0956	1.00	-1 9.0618	-1 9.2972	-1 9.4765	-1 9.6161	-1 9.7215
	-1 6.3897	-1 6.3897		-1 1.0964	-2 7.8481	-2 5.6390	-2 4.0368	-2 2.8827
	.5686	.5686		.1092	.0783	.0563	.0403	.0288
			.90	-1 8.8953	-1 9.1647	-1 9.3661	-1 9.5288	-1 9.6505
				-1 1.7896	-1 1.4715	-1 1.2561	-1 1.0977	-2 9.8256
				.177	.146	.125	.109	.098
	-1 9.5346	-1 9.5346	.75	-1 8.5653	-1 8.9067	-1 9.1351	-1 9.3109	-1 9.4467
	-1 4.1393	-1 4.1393		-1 2.8858	-1 2.5783	-1 2.3917	-1 2.2545	-1 2.1544
	-1 3.0628	-1 3.0628		.281	.252	.238	.222	.212
-1 5.623	-1 7.2286	-1 7.2286	1.00	-1 8.3908	-1 8.7839	-1 9.0880	-1 9.3576	-1 9.5102
	-1 8.7541	-1 8.7541		-1 1.8243	-1 1.3260	-2 9.6462	-2 6.9746	-2 5.0191
	.7191	.7191		.1804	.1318	.0962	.0696	.0501
			.90	-1 8.2053	-1 8.6209	-1 8.9394	-1 9.1976	-1 9.3946
				-1 2.7807	-1 2.3231	-1 2.0091	-1 1.7752	-1 1.6033
				.271	.228	.198	.176	.159
	-1 8.7163	-1 8.7163	.75	-1 7.8241	-1 8.2682	-1 8.5861	-1 8.8357	-1 9.0311
	-1 1.1933	-1 1.1933		-1 4.2275	-1 3.8308	-1 3.5976	-1 3.4253	-1 3.2994
	-1 5.1227	-1 5.1227		.400	.366	.345	.330	.319
1.000	-1 5.8692	-1 5.8692	1.00	-1 7.3483	-1 7.9547	-1 8.4431	-1 8.8389	-1 9.1469
	1.2959	1.2959		-1 2.9109	-1 2.1660	-1 1.6066	-1 1.1806	-2 8.6053
	.9136	.9136		.2833	.2133	.1593	.1175	.0858
			.90	-1 7.1010	-1 7.7000	-1 8.1813	-1 8.5828	-1 8.8992
				-1 4.8876	-1 3.6637	-1 3.2287	-1 2.8983	-1 2.6512
				.405	.351	.312	.282	.259
	-1 7.3711	-1 7.3711	.75	-1 6.6838	-1 7.1689	-1 7.5836	-1 7.9199	-1 8.1895
	3.0103	3.0103		-1 6.3852	-1 5.8395	-1 5.5804	-1 5.3876	-1 5.2480
	-1 7.8540	-1 7.8540		.564	.529	.509	.494	.483
1.778	-1 4.2226	-1 4.2226	1.00	-1 5.9283	-1 6.7383	-1 7.4435	-1 8.0494	-1 8.5425
	2.0436	2.0436		-1 4.3770	-1 3.3645	-1 2.5675	-1 1.9339	-1 1.4385
	1.1157	1.1157		.4126	.3846	.3513	.1910	.1429
			.90	-1 5.5921	-1 6.3237	-1 6.9566	-1 7.5159	-1 7.9813
				-1 6.3742	-1 5.6175	-1 5.0849	-1 4.6719	-1 4.3564
				.568	.512	.470	.437	.411
	-1 4.9016	-1 4.9016	.75	-1 5.0325	-1 5.5947	-1 6.0428	-1 6.4203	-1 6.7317
	6.1933	6.1933		-1 9.3509	-1 8.8553	-1 8.6710	-1 8.5485	-1 8.4612
	1.0585	1.0585		.752	.725	.714	.707	.702
3.162	-1 2.7306	-1 2.7306	1.00	-1 4.3331	-1 5.2151	-1 6.0730	-1 6.8842	-1 7.5988
	3.3738	3.3738		-1 6.1065	-1 4.8842	-1 3.8686	-1 3.0161	-1 2.3117
	1.3826	1.3826		.5482	.4543	.3691	.2929	.2278
			.90	-1 3.9534	-1 4.6605	-1 5.3289	-1 5.9518	-1 6.5118
				-1 8.9181	-1 8.1667	-1 7.6591	-1 7.2687	-1 6.9706
				.788	.685	.654	.629	.609
	-1 3.0151	-1 3.0151	.75	-1 3.4178	-1 3.8779	-1 4.2533	-1 4.5773	-1 4.8491
	1 1.0414	1.0414		1.3844	1.2955	1.3109	1.3290	1.3492
	1.2645	1.2645		.924	.913	.919	.926	.933

TABLE X. - Continued. RESPONSES OF CYLINDERS

[The number to the left of each entry denotes the power of ten by which each entry as printed is to be multiplied. Example: -1 9.7420 is actually equal to 0.97420.]

(b) Continued. $\omega\tau_{int,2} = 0.316228$

$\omega\tau_{ext,2}$	Homogeneous cylinder: Exact / First Order	β	Laminated cylinder, k_2/k_1 = 5	k_2/k_1 = 10	k_2/k_1 = 20	k_2/k_1 = 40	k_2/k_1 = 80
5.623	-1 1.6495 5.7377 1.3962	1.00	-1 2.8872 -1 7.8511 .6656	-1 3.6603 -1 6.5474 .5797	-1 4.5042 -1 5.4107 .4960	-1 5.4004 -1 4.4011 .4146	-1 6.2888 -1 3.5097 .3375
		.90	-1 2.5498 1.1579 .858	-1 3.0981 1.1053 .835	-1 3.6419 1.0804 .824	-1 4.1876 1.0679 .818	-1 4.7008 1.0635 .816
	-1 1.7508 1 1.5135 1.3948	.75	-1 2.1329 1.7578 1.054	-1 2.4473 1.7837 1.060	-1 2.7030 1.8784 1.082	-1 2.9246 1.9768 1.103	-1 3.1103 2.0766 1.128
1 1.000	-2 9.6142 9.9424 1.4706	1.00	-1 1.7960 -1 9.3538 .7520	-1 2.3648 -1 8.0979 .6807	-1 3.0446 -1 6.9737 .6090	-1 3.8469 -1 5.9333 .5355	-1 4.7353 -1 4.9532 .4599
		.90	-1 1.5474 1.3952 .949	-1 1.9133 1.3840 .945	-1 2.2867 1.4101 .954	-1 2.6717 1.4571 .969	-1 3.0482 1.5178 .988
	-2 9.9504 1 2.0043 1.4711	.75	-1 1.2668 2.1689 1.139	-1 1.4602 2.2813 1.158	-1 1.6156 2.5057 1.191	-1 1.7494 2.7519 1.222	-1 1.8605 3.0153 1.251
1 1.778	-2 5.5060 1 1.7480 1.5135	1.00	-1 1.0697 1.0482 .8089	-1 1.4425 -1 9.3481 .7514	-1 1.9158 -1 8.3263 .6943	-1 2.5169 -1 7.3776 .6356	-1 3.2495 -1 6.4434 .5724
		.90	-2 9.0687 1.5786 1.006	-1 1.1315 1.6145 1.016	-1 1.3633 1.7048 1.040	-1 1.6042 1.8360 1.072	-1 1.8371 2.0004 1.107
	-2 5.6145 1 2.5014 1.5146	.75	-2 7.3297 2.5040 1.191	-2 8.4626 2.7141 1.218	-2 9.3623 3.0966 1.258	-1 1.0131 3.5459 1.296	-1 1.0762 4.0642 1.330
1 3.162	-2 3.1261 1 3.0716 1.5383	1.00	-2 6.2128 1.1845 .8439	-2 8.4956 1.0225 .7965	-1 1.1493 -1 9.3457 .7516	-1 1.5490 -1 8.5476 .7073	-1 2.0676 -1 7.7554 .6596
		.90	-2 5.2155 1.7051 1.040	-2 6.5370 1.7822 1.060	-2 7.9054 1.9328 1.093	-2 9.3885 2.1518 1.136	-1 1.0701 2.4388 1.182
	-2 3.1607 1 3.0004 1.5392	.75	-2 4.1847 2.7447 1.221	-2 4.8341 3.0416 1.253	-2 5.3454 3.5749 1.298	-2 5.7794 4.2398 1.339	-2 6.1334 5.0632 1.376
1 5.623	-2 1.7670 1 5.4361 1.5524	1.00	-2 3.5572 1.1724 .8646	-2 4.9030 1.0800 .8838	-2 6.7051 1.0037 .7872	-2 9.1741 -1 9.3846 .7537	-1 1.2500 -1 8.7584 .7193
		.90	-2 2.9693 1.7858 1.060	-2 3.7302 1.8930 1.084	-2 4.5188 2.0905 1.125	-2 5.3380 2.3888 1.174	-2 6.1850 2.7825 1.226
	-2 1.7780 1 3.5001 1.5530	.75	-2 2.3726 2.9034 1.239	-2 2.7412 3.3643 1.274	-2 3.0298 3.9168 1.321	-2 3.2738 4.7671 1.364	-2 3.4719 5.8798 1.402
2 1.000	-3 9.9645 1 9.6408 1.5604	1.00	-2 2.0206 1.2013 .8766	-2 2.7976 1.1153 .8398	-2 3.8494 1.0472 .8085	-2 5.3185 -1 9.9314 .7820	-2 7.3257 -1 9.4453 .7569
		.90	-2 1.6811 1.8346 1.072	-2 2.1146 1.9617 1.099	-2 2.5638 2.1910 1.143	-2 3.0299 2.5361 1.195	-2 3.4763 3.0222 1.251
	-3 9.9995 1 4.0000 1.5608	.75	-2 1.3402 2.9997 1.249	-2 1.5485 3.4048 1.285	-2 1.7111 4.1402 1.334	-2 1.8481 5.1266 1.378	-2 1.9591 6.4681 1.417

TABLE X. - Continued. RESPONSES OF CYLINDERS

[The number to the left of each entry denotes the power of ten by which each entry as printed is to be multiplied. Example: -1 9.7420 is actually equal to 0.97420.]

(b) Concluded. $\omega\tau_{int,2} = 0.316228$

$\omega\tau_{ext,2}$	Homogeneous cylinder: Exact / First order	β	Laminated cylinder, k_2/k_1 = 5	10	20	40	80
2 1.778	-3 5.6122 2 1.7118 1.5650	1.00	-2 1.1427 1.2181 .8834	-2 1.5861 1.1360 .8490	-2 2.1900 1.0734 .8208	-2 3.0371 1.0268 .7986	-2 4.2168 -1 9.8810 .7794
		.90	-3 9.4894 1.8633 1.078	-2 1.1944 2.0026 1.108	-2 1.4488 2.2520 1.153	-2 1.7124 2.6313 1.208	-2 1.9645 3.1762 1.266
	-3 5.6233 1 4.5000 1.5652	.75	-3 7.5553 3.0574 1.255	-3 8.7297 3.4895 1.292	-3 9.6443 4.2775 1.341	-2 1.0415 5.3540 1.386	-2 1.1037 6.8543 1.426
2 3.162	-3 3.1587 2 3.0414 1.5675	1.00	-3 6.4465 1.2278 .8873	-3 8.9605 1.1481 .8542	-2 1.2396 1.0887 .8278	-2 1.7838 1.0467 .8082	-2 2.4026 1.0144 .7926
		.90	-3 5.3477 1.8799 1.082	-3 6.7335 2.0264 1.112	-3 8.1694 2.2879 1.159	-3 9.6568 2.6881 1.215	-2 1.1077 3.2699 1.274
	-3 3.1623 1 5.0000 1.5676	.75	-3 4.2546 3.0909 1.258	-3 4.9160 3.5390 1.295	-3 5.4305 4.3589 1.345	-3 5.8634 5.4911 1.391	-3 6.2129 7.0927 1.431
2 5.623	-3 1.7771 2 5.4059 1.5689	1.00	-3 3.6315 1.2333 .8895	-3 5.0518 1.1550 .8572	-3 6.9964 1.0975 .8318	-3 9.7442 1.0583 .8137	-2 1.3611 1.0298 .8001
		.90	-3 3.0107 1.8893 1.084	-3 3.7917 2.0400 1.115	-3 4.6009 2.3085 1.162	-3 5.4387 2.7212 1.219	-3 6.2383 3.3252 1.279
	-3 1.7783 1 5.5000 1.5690	.75	-3 2.3944 3.1100 1.260	-3 2.7666 3.5675 1.298	-3 3.0559 4.4061 1.348	-3 3.2993 5.5714 1.393	-3 3.4957 7.2348 1.434
3 1.000	-4 9.9963 2 9.6106 1.5698	1.00	-3 8.0442 1.2364 .8907	-3 8.8450 1.1589 .8589	-3 9.9425 1.1025 .8341	-3 5.4957 1.0649 .8168	-3 7.6858 1.0387 .8044
		.90	-3 1.6942 1.8947 1.085	-3 2.1339 2.0477 1.117	-3 2.5895 2.3203 1.164	-3 3.0611 2.7401 1.221	-3 3.5110 3.3570 1.281
	-3 1.0000 1 6.0000 1.5698	.75	-3 1.3471 3.1209 1.261	-3 1.5564 3.5837 1.299	-3 1.7192 4.4331 1.349	-3 1.8560 5.6176 1.395	-3 1.9664 7.3164 1.435
3 1.778	-4 5.6222 3 1.7088 1.5708	1.00	-3 1.1502 1.2382 .8914	-3 1.6011 1.1611 .8598	-3 2.2196 1.1054 .8354	-3 3.0955 1.0687 .8186	-3 4.3321 1.0436 .8068
		.90	-4 9.5307 1.8977 1.086	-3 1.2005 2.0521 1.117	-3 1.4568 2.3270 1.165	-3 1.7222 2.7509 1.222	-3 1.9753 3.3752 1.283
	-4 5.6234 1 6.5000 1.5708	.75	-4 7.5769 3.1270 1.261	-4 8.7547 3.5929 1.299	-4 9.6697 4.4484 1.350	-3 1.0439 5.6439 1.395	-3 1.1060 7.3634 1.436
3 3.162	-4 3.1619 3 3.0385 1.5705	1.00	-4 6.4708 1.2392 .8918	-4 9.0081 1.1624 .8603	-3 1.2490 1.1070 .8361	-3 1.7484 1.0708 .8196	-3 2.4394 1.0467 .8082
		.90	-4 5.3607 1.8994 1.086	-4 6.7527 2.0546 1.118	-4 8.1948 2.3307 1.166	-4 9.6874 2.7570 1.223	-3 1.1111 3.3855 1.284
	-4 3.1623 1 7.0000 1.5705	.75	-4 4.2614 3.1305 1.262	-4 4.9239 3.5981 1.300	-4 5.4384 4.4571 1.350	-4 5.8710 5.6588 1.396	-4 6.2199 7.3901 1.436
3 5.623	-4 1.7781 3 5.4034 1.5706	1.00	-4 3.6390 1.2397 .8920	-4 5.0668 1.1631 .8606	-4 7.0261 1.1079 .8365	-4 9.8030 1.0780 .8201	-3 1.3727 1.0483 .8090
		.90	-4 3.0149 1.9004 1.086	-4 3.7978 2.0559 1.118	-4 4.6089 2.3329 1.166	-4 5.4484 2.7604 1.223	-4 6.2488 3.3914 1.284
	-4 1.7783 1 7.5000 1.5706	.75	-4 2.3965 3.1325 1.263	-4 2.7691 3.6010 1.300	-4 3.0584 4.4620 1.350	-4 3.3017 5.6672 1.396	-4 3.4979 7.4052 1.437

TABLE X. - Continued. RESPONSES OF CYLINDERS

[The number to the left of each entry denotes the power of ten by which each entry as printed is to be multiplied. Example: -1 9.7420 is actually equal to 0.97420.]

(c) $\omega\tau_{int,2} = 1.0$

$\omega\tau_{ext,2}$	Homogeneous cylinder: Exact / First order	β	Laminated cylinder, k_2/k_1 = 5	= 10	= 20	= 40	= 80
-1 3.162	-1 5.4670 -1 9.6144 .7657	1.00	-1 9.4203 -2 6.3121 .0630	-1 9.5730 -2 4.5224 .0452	-1 9.6898 -2 3.2323 .0323	-1 9.7757 -2 2.3045 .0230	-1 9.8391 -2 1.6396 .0164
		.90	-1 9.0210 -1 1.6693 .165	-1 9.2601 -1 1.4627 .145	-1 9.4456 -1 1.3071 .130	-1 9.5865 -1 1.1909 .119	-1 9.6902 -1 1.1055 .110
	-1 9.5346 -1 4.1393 -1 3.0628	.75	-1 8.2598 -1 3.5275 .339	-1 8.6172 -1 3.4655 .334	-1 8.7974 -1 3.3031 .318	-1 8.9868 -1 3.2237 .312	-1 9.1312 -1 3.1623 .306
-1 5.623	-1 4.9811 1.1461 .8548	1.00	-1 8.9924 -1 1.0755 .1071	-1 9.2533 -2 7.7890 .0777	-1 9.4541 -2 5.6142 .0561	-1 9.6047 -2 4.0384 .0403	-1 9.7157 -2 2.8798 .0288
		.90	-1 8.5657 -1 2.3941 .235	-1 8.8978 -1 2.1261 .210	-1 9.1601 -1 1.9215 .190	-1 9.3619 -1 1.7671 .175	-1 9.5122 -1 1.6524 .164
	-1 8.7163 1.1933 -1 5.1227	.75	-1 7.7191 -1 4.5787 .429	-1 8.1105 -1 4.5298 .425	-1 8.3394 -1 4.3676 .412	-1 8.5627 -1 4.2914 .405	-1 8.7347 -1 4.2316 .400
1.000	-1 4.2459 1.4800 .9766	1.00	-1 8.2877 -1 1.7802 .1762	-1 8.7150 -1 1.3118 .1304	-1 9.0516 -2 9.5875 .0956	-1 9.3085 -2 6.9541 .0694	-1 9.5003 -2 5.0118 .0501
		.90	-1 7.7860 -1 3.5588 .342	-1 8.2486 -1 3.2185 .311	-1 8.6264 -1 2.9531 .287	-1 8.9245 -1 2.7494 .268	-1 9.1516 -1 2.5957 .254
	-1 7.3711 3.0103 -1 7.8540	.75	-1 6.8121 -1 6.2969 .562	-1 7.2278 -1 6.3030 .562	-1 7.5072 -1 6.1702 .553	-1 7.7649 -1 6.1223 .549	-1 7.9665 -1 6.0833 .547
1.778	-1 3.2986 8.0702 1.1308	1.00	-1 7.2141 -1 8.8186 .2747	-1 7.8565 -1 2.1318 .2100	-1 8.3879 -1 1.5925 .1579	-1 8.8086 -1 1.1754 .1170	-1 9.1307 -2 8.5864 .0857
		.90	-1 6.5776 -1 5.3101 .488	-1 7.1691 -1 4.9248 .458	-1 7.6791 -1 4.6166 .433	-1 8.0994 -1 4.3736 .412	-1 8.4317 -1 4.1859 .396
	-1 4.9016 6.1933 1.0585	.75	-1 5.4928 -1 8.9499 .730	-1 5.8875 -1 9.1355 .740	-1 6.1818 -1 9.1166 .739	-1 6.4450 -1 9.1790 .743	-1 6.6540 -1 9.8262 .745
3.162	-1 2.3148 3.1199 1.2606	1.00	-1 5.7842 -1 4.1945 .3972	-1 6.6181 -1 3.2877 .3176	-1 7.3693 -1 2.5348 .2482	-1 8.0054 -1 1.9211 .1898	-1 8.5176 -1 1.4337 .1484
		.90	-1 5.0193 -1 7.6970 .656	-1 5.6478 -1 7.3833 .636	-1 6.2255 -1 7.1313 .620	-1 6.7293 -1 6.9283 .606	-1 7.1477 -1 6.7673 .595
	-1 3.0151 1 1.0414 1.2645	.75	-1 3.9644 1.2707 .904	-1 4.2775 1.3309 .926	-1 4.5238 1.3667 .939	-1 4.7402 1.4062 .953	-1 4.9133 1.4386 .963
5.623	-1 1.4912 4.9864 1.3729	1.00	-1 4.2091 -1 5.7816 .5242	-1 5.0949 -1 4.7398 .4418	-1 5.9893 -1 3.7987 .3630	-1 6.8886 -1 2.9867 .2902	-1 7.5643 -1 2.2997 .2260
		.90	-1 3.4485 1.0549 .812	-1 3.9732 1.0541 .812	-1 4.4857 1.0585 .814	-1 4.9536 1.0647 .817	-1 5.3584 1.0710 .820
	-1 1.7508 1 1.5135 1.3948	.75	-1 2.5905 1.7428 1.050	-1 2.8000 1.8896 1.084	-1 2.9666 2.0113 1.109	-1 3.1110 2.1340 1.133	-1 3.2259 2.2408 1.151

TABLE X. - Continued. RESPONSES OF CYLINDERS

[The number to the left of each entry denotes the power of ten by which each entry as printed is to be multiplied. Example: -1 9.7420 is actually equal to 0.97420.]

(c) Continued. $\omega\tau_{int,2} = 1.0$

$\omega\tau_{ext,2}$	Homogeneous cylinder: Exact / First order	β	Laminated cylinder, k_2/k_1 = 5	10	20	40	80
1 1.000	-2 9.0657 6.3055 1.4510	1.00	-1 2.7992 -1 7.3445 .6335	-1 3.5630 -1 6.2785 .5606	-1 4.4276 -1 5.2789 .4857	-1 5.3426 -1 4.3406 .4095	-1 6.8485 -1 3.4888 .3351
		.90	-1 2.1720 1.3466 .932	-1 2.5437 1.4051 .952	-1 2.9107 1.4751 .975	-1 3.2823 1.5490 .998	-1 3.5526 1.6907 1.018
	-2 9.9504 1 2.0043 1.4711	.75	-1 1.5821 2.2523 1.153	-1 1.7085 2.5404 1.196	-1 1.8078 2.8208 1.230	-1 1.8930 3.1135 1.260	-1 1.9602 3.3864 1.284
1 1.778	-2 5.3246 1 1.4208 1.5005	1.00	-1 1.7410 -1 8.6610 .7138	-1 2.2981 -1 7.6954 .6559	-1 2.9870 -1 6.7608 .5944	-1 3.7982 -1 5.8255 .5275	-1 4.6967 -1 4.9006 .4557
		.90	-1 1.3008 1.6011 1.012	-1 1.5336 1.7374 1.049	-1 1.7644 1.9058 1.088	-1 1.9792 2.0962 1.186	-1 2.1677 2.2967 1.160
	-2 5.6145 1 2.5014 1.5146	.75	-2 9.2974 2.7223 1.219	-1 1.0025 3.1879 1.267	-1 1.0588 3.6968 1.307	-1 1.1067 4.2653 1.341	-1 1.1441 4.8488 1.367
1 3.162	-2 3.0674 1 2.4704 1.5303	1.00	-1 1.0374 -1 9.6319 .7666	-1 1.4011 -1 8.8140 .7284	-1 1.8774 -1 8.0268 .6764	-1 2.4823 -1 7.2131 .6249	-1 3.2193 -1 6.3554 .5661
		.90	-2 7.5681 1.7943 1.062	-2 8.9461 2.0078 1.109	-1 1.0309 2.2855 1.158	-1 1.1571 2.6232 1.207	-1 1.2669 3.0108 1.250
	-2 3.1607 1 3.0004 1.5392	.75	-2 5.3529 3.0956 1.258	-2 5.7643 3.7385 1.309	-2 6.0791 4.5044 1.352	-2 6.3457 5.4832 1.388	-2 6.5526 6.4536 1.417
1 5.623	-2 1.7483 1 4.3369 1.5477	1.00	-2 6.0278 1.0280 .7992	-2 8.2516 -1 9.5986 .7649	-1 1.1263 -1 8.9721 .7313	-1 1.5271 -1 8.3288 .6945	-1 2.0472 -1 7.6290 .6517
		.90	-2 4.3352 1.9259 1.092	-2 5.1300 2.2018 1.146	-2 5.9132 2.5761 1.201	-2 6.6341 3.0585 1.255	-2 7.2570 3.6536 1.304
	-2 1.7780 1 3.5001 1.5530	.75	-2 3.0489 3.3587 1.281	-2 3.2804 4.1478 1.334	-2 3.4562 5.1461 1.379	-2 3.6046 6.4175 1.416	-2 3.7193 7.9561 1.446
2 1.000	-3 9.9049 1 7.6561 1.5577	1.00	-2 3.4525 1.0684 .8185	-2 4.7627 1.0104 .7906	-2 6.5712 -1 9.6085 .7654	-2 9.0430 -1 9.1288 .7395	-1 1.8374 -1 8.5979 .7108
		.90	-2 2.4627 2.0091 1.109	-2 2.9154 2.3288 1.165	-2 3.3603 2.7753 1.225	-2 3.7681 3.3746 1.283	-2 4.1187 4.1543 1.335
	-3 9.9995 1 4.0000 1.5608	.75	-2 1.7266 3.5288 1.295	-2 1.8567 4.4284 1.348	-2 1.9550 5.5984 1.394	-2 2.0378 7.1620 1.432	-2 2.1017 9.1661 1.462
2 1.778	-3 5.5933 2 1.3558 1.5634	1.00	-2 1.9616 1.0986 .8296	-2 2.7178 1.0413 .8056	-2 3.7728 1.0008 .7858	-2 5.2365 -1 9.6386 .7670	-2 7.3513 -1 9.2598 .7470
		.90	-2 1.3927 2.0592 1.119	-2 1.6490 ------ ----	-2 1.9004 2.9017 1.239	-2 2.1303 3.5838 1.299	-2 2.3873 4.5018 1.352
	-3 5.6233 1 4.5000 1.5652	.75	-3 9.7471 3.6327 1.302	-2 1.0478 4.5943 1.357	-2 1.1029 5.8910 1.403	-2 1.1493 7.6644 1.441	-2 1.1850 1 1.0088 1.471

TABLE X. - Continued. RESPONSES OF CYLINDERS

[The number to the left of each entry denotes the power of ten by which each entry as printed is to be multiplied. Example: -1 9.7420 is actually equal to 0.97420.]

(c) Concluded. $\omega\tau_{int,2} = 1.0$

$\omega\tau_{ext,2}$	Homogeneous cylinder: Exact / First order	β	Laminated cylinder, k_2/k_1 = 5	= 10	= 20	= 40	= 80
2 3.162	-3 3.1528 2 2.4055 1.5666	1.00	-2 1.1095 1.1066 .8360	-2 1.5410 1.0595 .8143	-2 2.1465 1.0247 .7976	-2 2.9937 -1 9.9555 .7832	-2 4.1739 -1 9.6778 .7690
		.90	-3 7.8560 2.0885 1.184	-3 9.3026 2.4535 1.184	-2 1.0720 2.9781 1.247	-2 1.2014 3.7125 1.308	-2 1.3121 4.7243 1.362
	-3 3.1623 1 5.0000 1.5676	.75	-3 5.4930 3.6941 1.306	-3 5.9041 4.6973 1.361	-3 6.2132 6.0699 1.408	-3 6.4734 7.9800 1.446	-3 6.6736 1 1.0589 1.477
2 5.683	-3 1.7753 2 4.2720 1.5685	1.00	-3 6.8596 1.1147 .8396	-3 8.7059 1.0700 .8192	-2 1.2150 1.0387 .8044	-2 1.6992 1.0143 .7925	-2 2.3788 -1 9.9302 .7819
		.90	-3 4.4256 2.1054 1.127	-3 5.2407 2.4804 1.188	-3 6.0390 3.0329 1.251	-3 6.7670 3.7894 1.313	-3 7.3889 4.8594 1.368
	-3 1.7783 1 5.5000 1.5690	.75	-3 3.0928 3.7296 1.309	-3 3.3239 4.7573 1.364	-3 3.4975 6.1755 1.410	-3 3.6436 8.1695 1.449	-3 3.7559 1 1.0934 1.480
3 1.000	-4 9.9905 2 7.5911 1.5695	1.00	-3 3.5864 1.1193 .8416	-3 4.9083 1.0760 .8220	-3 6.8576 1.0467 .8082	-3 9.6051 1.0252 .7978	-2 1.3473 1.0078 .7893
		.90	-3 2.4911 2.1150 1.129	-3 2.9500 2.4958 1.190	-3 3.3992 3.0486 1.254	-3 3.8087 3.8341 1.316	-3 4.1583 4.9389 1.371
	-3 1.0000 1 6.0000 1.5698	.75	-3 1.7403 3.7499 1.310	-3 1.8703 4.7918 1.365	-3 1.9678 6.2365 1.418	-3 2.0499 8.2802 1.461	-3 2.1130 1 1.1138 1.481
3 1.778	-4 5.6204 3 1.3493 1.5701	1.00	-3 1.9851 1.1219 .8428	-3 2.7642 1.0794 .8236	-3 3.8644 1.0513 .8104	-3 5.4173 1.0314 .8008	-3 7.6078 1.0163 .7935
		.90	-3 1.4016 2.1205 1.130	-3 1.6598 2.5045 1.191	-3 1.9126 3.0633 1.255	-3 2.1428 3.8596 1.317	-3 2.3394 4.9848 1.373
	-4 5.6234 1 6.5000 1.5702	.75	-4 9.7905 3.7614 1.311	-3 1.0521 4.8846 1.369	-3 1.1069 6.3714 1.413	-3 1.1531 8.3437 1.458	-3 1.1885 1 1.1856 1.488
3 3.162	-4 3.1613 3 2.3991 1.5704	1.00	-3 1.1170 1.1234 .8434	-3 1.5557 1.0813 .8245	-3 2.1756 1.0538 .8116	-3 3.0514 1.0349 .8025	-3 4.2882 1.0218 .7959
		.90	-4 7.8843 2.1236 1.131	-4 9.3368 2.5095 1.192	-3 1.0758 3.0717 1.256	-3 1.2053 3.8742 1.318	-3 1.3159 5.0109 1.374
	-4 3.1623 1 7.0000 1.5705	.75	-4 5.5067 3.7679 1.311	-4 5.9176 4.8225 1.366	-4 6.2259 6.3912 1.413	-4 6.4852 8.3799 1.458	-4 6.6846 1 1.1323 1.483
3 5.623	-4 1.7780 3 4.2655 1.5706	1.00	-4 6.8832 1.1242 .8438	-4 8.7525 1.0824 .8250	-3 1.2243 1.0553 .8123	-3 1.7175 1.0369 .8035	-3 2.4146 1.0239 .7972
		.90	-4 4.4345 2.1253 1.131	-4 5.2515 2.5123 1.192	-4 6.0509 3.0764 1.257	-4 6.7793 3.8824 1.319	-4 7.4007 5.0258 1.374
	-4 1.7783 1 7.5000 1.5706	.75	-4 3.0971 3.7716 1.311	-4 3.3281 4.8288 1.367	-4 3.5015 6.3024 1.413	-4 3.6473 8.4004 1.458	-4 3.7594 1 1.1362 1.483
4 1.000	-5 9.9991 3 7.5861 1.5707	1.00	-4 3.5339 1.1247 .8440	-4 4.9231 1.0830 .8252	-4 6.8869 1.0561 .8127	-4 9.6633 1.0380 .8040	-3 1.3588 1.0255 .7980
		.90	-4 2.4939 2.1263 1.131	-4 2.9534 2.5138 1.192	-4 3.4030 3.0790 1.257	-4 3.8185 3.8871 1.319	-4 4.1680 5.0341 1.375
	-4 1.0000 1 8.0000 1.5707	.75	-4 1.7417 3.7736 1.311	-4 1.8716 4.8323 1.367	-4 1.9691 6.3087 1.414	-4 2.0511 8.4130 1.453	-4 2.1141 1 1.1383 1.483

TABLE X. - Continued. RESPONSES OF CYLINDERS

[The number to the left of each entry denotes the power of ten by which each entry as printed is to be multiplied. Example: -1 9.7420 is actually equal to 0.97420.]

(d) $\omega\tau_{int,2} = 3.16228$

$\omega\tau_{ext,2}$	Homogeneous cylinder: Exact / First order	β	Laminated cylinder, k_2/k_1 = 5	10	20	40	80
-1 5.623	-1 3.0818 1.1192 .8416	1.00	-1 9.3921 -2 6.2768 .0627	-1 9.5585 -2 4.5104 .0451	-1 9.6819 -2 3.2281 .0323	-1 9.7720 -2 2.3030 .0230	-1 9.8372 -2 1.6390 .0164
		.90	-1 8.4988 -1 2.6988 .264	-1 8.8224 -1 2.5291 .248	-1 9.0767 -1 2.3897 .235	-1 9.2709 -1 2.2796 .224	-1 9.4159 -1 2.1952 .216
	-1 8.7163 1.1933 -1 5.1227	.75	-1 6.5800 -1 6.3660 .567	-1 6.8205 -1 6.5587 .581	-1 7.0830 -1 6.7115 .591	-1 7.1932 -1 6.8170 .598	-1 7.3852 -1 6.8977 .604
1.000	-1 2.7909 1.3217 .9231	1.00	-1 8.9471 -1 1.0672 .1063	-1 9.2295 -2 7.7599 .0774	-1 9.4417 -2 5.6038 .0560	-1 9.5983 -2 4.0247 .0408	-1 9.7124 -2 2.8784 .0288
		.90	-1 7.9604 -1 3.6206 .347	-1 8.3571 -1 3.4384 .331	-1 8.6760 -1 3.2845 .317	-1 8.9241 -1 3.1605 .306	-1 9.1120 -1 3.0640 .297
	-1 7.3711 3.0103 -1 7.8540	.75	-1 5.9817 -1 7.7497 .659	-1 6.2097 -1 8.0343 .677	-1 6.4020 -1 8.2668 .691	-1 6.5646 -1 8.4347 .701	-1 6.6909 -1 8.5653 .708
1.778	-1 3.3641 1.6817 1.0343	1.00	-1 8.2205 -1 1.7605 .1743	-1 8.6778 -1 1.3045 .1297	-1 9.0315 -2 9.5608 .0953	-1 9.2979 -2 6.9448 .0693	-1 9.4948 -2 5.0082 .0500
		.90	-1 7.0624 -1 5.0967 .471	-1 7.5384 -1 4.9319 .458	-1 7.9349 -1 4.7844 .446	-1 8.2524 -1 4.6605 .436	-1 8.4988 -1 4.5610 .428
	-1 4.9016 6.1933 1.0585	.75	-1 5.0776 1.0017 .786	-1 5.2753 1.0495 .810	-1 5.4420 1.0897 .828	-1 5.5838 1.1206 .842	-1 5.6939 1.1450 .853
3.162	-1 1.8297 2.3218 1.1641	1.00	-1 7.1264 -1 2.7739 .2706	-1 7.8036 -1 2.1143 .2084	-1 8.3575 -1 1.5857 .1573	-1 8.7917 -1 1.1738 .1167	-1 9.1816 -2 8.5766 .0856
		.90	-1 5.7497 -1 7.3043 .631	-1 6.2591 -1 7.2559 .628	-1 6.7019 -1 7.1959 .624	-1 7.0693 -1 7.1356 .620	-1 7.3684 -1 7.0809 .616
	-1 3.0151 1 1.0414 1.2645	.75	-1 3.9207 1.3531 .934	-1 4.0693 1.4416 .964	-1 4.1939 1.5194 .989	-1 4.3004 1.5826 1.007	-1 4.3825 1.6338 1.022
5.623	-1 1.2842 3.4602 1.2895	1.00	-1 5.6891 -1 4.1013 .3892	-1 6.5537 -1 3.2482 .3141	-1 7.3285 -1 2.5184 .2467	-1 7.9810 -1 1.9146 .1892	-1 8.5036 -1 1.4311 .1421
		.90	-1 4.2018 1.0290 .800	-1 4.6495 1.0585 .814	-1 5.0515 1.0825 .825	-1 5.3946 1.1015 .834	-1 5.6750 1.1161 .840
	-1 1.7508 1 1.5135 1.3948	.75	-1 2.7329 1.8536 1.076	-1 2.8287 2.0239 1.112	-1 2.9081 2.1820 1.141	-1 2.9761 2.3168 1.164	-1 3.0280 2.4341 1.181
1 1.000	-2 8.2968 5.4846 1.3904	1.00	-1 4.1259 -1 5.6115 .5114	-1 5.0307 -1 4.6508 .4353	-1 5.9432 -1 3.7630 .3599	-1 6.7979 -1 2.9712 .2888	-1 7.5451 -1 2.3932 .2254
		.90	-1 2.7771 1.3824 .945	-1 3.0994 1.4828 .978	-1 3.3920 1.5778 1.001	-1 3.6439 1.6634 1.030	-1 3.8511 1.7368 1.048
	-2 9.9504 1 2.0043 1.4711	.75	-1 1.7508 2.4867 1.188	-1 1.8062 2.8036 1.228	-1 1.8516 3.1186 1.261	-1 1.8904 3.4117 1.286	-1 1.9198 3.6727 1.305

TABLE X. - Continued. RESPONSES OF CYLINDERS

[The number to the left of each entry denotes the power of ten by which each entry as printed is to be multiplied. Example: -1 9.7420 is actually equal to 0.97420.]

(d) Continued. $\omega\tau_{int,2} = 3.16228$

$\omega\tau_{ext,2}$	Homogeneous cylinder: Exact / First order	β	Laminated cylinder, k_2/k_1 = 5	= 10	= 20	= 40	= 80
1 1.778	-2 5.0610 9.0845 1.4612	1.00	-1 2.7387 -1 7.0768 .6159	-1 3.5111 -1 6.1423 .5508	-1 4.3855 -1 5.2114 .4804	-1 5.3108 -1 4.3085 .4068	-1 6.2200 -1 3.4683 .3338
		.90	-1 1.7098 1.7400 1.049	-1 1.9139 1.9500 1.097	-1 2.0963 2.1705 1.139	-1 2.2533 2.3902 1.175	-1 2.3816 2.5972 1.203
	-2 5.6145 1 2.5014 1.5146	.75	-1 1.0603 3.1776 1.266	-1 1.0908 3.7149 1.308	-1 1.1156 4.2919 1.348	-1 1.1368 4.8746 1.368	-1 1.1588 5.4331 1.389
1 3.162	-2 2.9806 1 1.5486 1.5063	1.00	-1 1.7021 -1 8.2948 .6925	-1 2.2632 -1 7.4937 .6431	-1 2.9552 -1 6.6508 .5869	-1 3.7713 -1 5.7683 .5232	-1 4.6753 -1 4.8780 .4534
		.90	-1 1.0098 2.0490 1.117	-1 1.1294 2.3884 1.174	-1 1.2366 2.7778 1.225	-1 1.3274 3.2045 1.268	-1 1.4008 3.6473 1.303
	-2 3.1607 1 3.0004 1.5392	.75	-2 6.2129 3.8199 1.315	-2 6.3799 4.6247 1.358	-2 6.5144 5.5573 1.393	-2 6.6296 6.5835 1.420	-2 6.7156 7.6537 1.441
1 5.623	-2 1.7202 1 2.6870 1.5336	1.00	-1 1.0141 -1 9.1837 .7439	-1 1.3787 -1 8.5518 .7075	-1 1.8564 -1 7.8739 .6670	-1 2.4631 -1 7.1262 .6191	-1 3.8025 -1 6.3078 .5627
		.90	-2 5.8306 2.2817 1.158	-2 6.5159 2.7420 1.221	-2 7.1851 3.3086 1.277	-2 7.6369 3.9823 1.325	-2 8.0477 4.7473 1.363
	-2 1.7780 1 3.5001 1.5530	.75	-2 3.5742 4.3340 1.344	-2 3.6659 5.4011 1.388	-2 3.7395 6.7204 1.423	-2 3.8025 8.2888 1.451	-2 3.8494 1 1.0069 1.472
2 1.000	-3 9.8155 1 4.7114 1.5496	1.00	-2 5.8928 -1 9.7726 .7739	-2 8.1191 -1 9.2893 .7486	-1 1.1135 -1 8.7820 .7206	-1 1.5149 -1 8.2134 .6876	-1 2.0358 -1 7.5606 .6474
		.90	-2 3.3263 2.4392 1.182	-2 3.7147 2.9941 1.249	-2 4.0579 3.7120 1.308	-2 4.3448 4.6197 1.359	-2 4.5737 5.7295 1.398
	-3 9.9995 1 4.0000 1.5608	.75	-2 2.0355 4.6983 1.361	-2 2.0863 5.9796 1.405	-2 2.1269 7.6420 1.441	-2 2.1617 9.7432 1.469	-2 2.1875 1 1.2307 1.490
2 1.778	-3 5.5649 1 8.3113 1.5588	1.00	-2 3.3754 1.0138 .7923	-2 4.6862 -1 9.7628 .7734	-2 6.4961 -1 9.3911 .7540	-2 8.9700 -1 8.9843 .7319	-1 1.2303 -1 8.5114 .7052
		.90	-2 1.8854 2.5384 1.196	-2 2.1045 3.1585 1.264	-2 2.2975 3.9871 1.325	-2 2.4581 5.0797 1.376	-2 2.5860 6.4891 1.418
	-3 5.6233 1 4.5000 1.5652	.75	-2 1.1527 4.9349 1.371	-2 1.1810 6.3685 1.415	-2 1.2036 8.2903 1.451	-2 1.2229 1 1.0827 1.479	-2 1.2373 1 1.4093 1.500
2 3.162	-3 3.1437 2 1.4713 1.5640	1.00	-2 1.9179 1.0356 .8029	-2 2.6743 1.0051 .7879	-2 3.7296 -1 9.7723 .7739	-2 5.1940 -1 9.4848 .7590	-2 7.2097 -1 9.1590 .7415
		.90	-2 1.0649 2.5981 1.203	-2 1.1883 3.2595 1.273	-2 1.2968 4.1611 1.335	-2 1.3869 5.3822 1.387	-2 1.4584 7.0138 1.429
	-3 3.1623 1 5.0000 1.5676	.75	-3 6.5078 5.0798 1.376	-3 6.6659 6.6123 1.421	-3 6.7920 8.7090 1.456	-3 6.9002 1 1.1555 1.485	-3 6.9804 1 1.5357 1.506

TABLE X. - Continued. RESPONSES OF CYLINDERS

[The number to the left of each entry denotes the power of ten by which each entry as printed is to be multiplied. Example: -1 9.7420 is actually equal to 0.97420.]

(d) Concluded. $\omega\tau_{int,2} = 3.16228$

$\omega\tau_{ext,2}$	Homogeneous cylinder: Exact	Homogeneous cylinder: First order	β	Laminated cylinder: k_2/k_1 = 5	= 10	= 20	= 40	= 80
2 5.623	-3 1.7734	2 8.6097 1.5670	1.00	-2 1.0848 1.0483 .8090	-2 1.5163 1.0281 .7963	-2 2.1220 1.0001 .7854	-2 2.9694 -1 9.7916 .7749	-2 4.1499 -1 9.5684 .7633
			.90	-3 6.0031 2.6329 1.308	-3 6.6974 3.3193 1.278	-3 7.3071 4.2660 1.341	-3 7.8131 5.5690 1.393	-3 8.2144 7.3485 1.436
	-3 1.7783	1 5.5000 1.5690	.75	-3 3.6677 5.1655 1.380	-3 3.7563 6.7584 1.424	-3 3.8269 8.9648 1.460	-3 3.8875 1 1.2011 1.488	-3 3.9324 1 1.6176 1.509
3 1.000	-4 9.9815	2 4.6341 1.5686	1.00	-3 6.1205 1.0555 .8124	-3 8.5666 1.0318 .8011	-2 1.2011 1.0134 .7920	-2 1.6854 -1 9.9730 .7840	-2 2.3645 -1 9.8151 .7761
			.90	-3 3.3805 2.6530 1.210	-3 3.7711 3.3539 1.281	-3 4.1138 4.3275 1.344	-3 4.3981 5.6800 1.397	-3 4.6234 7.5514 1.439
	-3 1.0000	1 6.0000 1.5698	.75	-3 2.0651 5.2152 1.381	-3 2.1148 6.8436 1.426	-3 2.1544 9.1157 1.462	-3 2.1885 1 1.2284 1.490	-3 2.2136 1 1.6677 1.511
3 1.778	-4 5.6175	2 8.2339 1.5696	1.00	-3 3.4481 1.0597 .8144	-3 4.8298 1.0374 .8038	-3 6.7794 1.0210 .7958	-3 9.5274 1.0078 .7893	-2 1.3395 -1 9.9595 .7834
			.90	-3 1.9024 2.6644 1.212	-3 2.1221 3.3737 1.283	-3 2.3148 4.3628 1.346	-3 2.4746 5.7444 1.399	-3 2.6011 7.6706 1.441
	-4 5.6234	1 6.5000 1.5702	.75	-3 1.1621 5.2435 1.382	-3 1.1900 6.8926 1.427	-3 1.2183 9.2029 1.463	-3 1.2314 1 1.2444 1.491	-3 1.2455 1 1.6973 1.512
3 3.162	-4 3.1604	3 1.4636 1.5701	1.00	-3 1.9410 1.0620 .8155	-3 2.7200 1.0406 .8053	-3 3.8203 1.0253 .7979	-3 5.3734 1.0138 .7923	-3 7.5641 1.0043 .7875
			.90	-3 1.0703 2.6709 1.213	-3 1.1938 3.3850 1.284	-3 1.3028 4.3829 1.347	-3 1.3980 5.7813 1.400	-3 1.4631 7.7393 1.442
	-4 3.1623	1 7.0000 1.5705	.75	-4 6.5374 5.2596 1.383	-4 6.6944 6.9204 1.427	-4 6.8194 9.2538 1.463	-4 6.9268 1 1.2535 1.491	-4 7.0063 1 1.7145 1.513
3 5.623	-4 1.7777	3 8.6018 1.5704	1.00	-3 1.0922 1.0633 .8161	-3 1.5308 1.0424 .8068	-3 2.1508 1.0278 .7991	-3 3.0367 1.0173 .7939	-3 4.2635 1.0090 .7899
			.90	-4 6.0201 2.6745 1.213	-4 6.7148 3.3913 1.284	-4 7.3848 4.3944 1.347	-4 7.8291 5.8038 1.400	-4 8.2290 7.7785 1.443
	-4 1.7783	1 7.5000 1.5706	.75	-4 3.6770 5.2687 1.383	-4 3.7653 6.9368 1.428	-4 3.8356 9.2811 1.464	-4 3.8959 1 1.2588 1.492	-4 3.9406 1 1.7243 1.513
4 1.000	-5 9.9982	3 4.6265 1.5706	1.00	-4 6.1438 1.0641 .8164	-4 8.6127 1.0434 .8066	-3 1.2103 1.0292 .7998	-3 1.7036 1.0191 .7949	-3 2.4007 1.0117 .7912
			.90	-4 3.3859 2.6766 1.213	-4 3.7766 3.3949 1.284	-4 4.1192 4.4008 1.347	-4 4.4031 5.8141 1.401	-4 4.6280 7.8007 1.443
	-4 1.0000	1 8.0000 1.5707	.75	-4 2.0680 5.2738 1.383	-4 2.1177 6.9451 1.428	-4 2.1572 9.2970 1.464	-4 2.1911 1 1.2617 1.492	-4 2.2162 1 1.7298 1.513
4 1.778	-5 5.6288	3 8.2258 1.5707	1.00	-4 3.4555 1.0645 .8166	-4 4.8444 1.0440 .8069	-4 6.8084 1.0300 .8002	-4 9.5851 1.0202 .7954	-3 1.3510 1.0138 .7920
			.90	-4 1.9041 2.6777 1.213	-4 2.1238 3.3969 1.285	-4 2.3165 4.4044 1.348	-4 2.4761 5.8208 1.401	-4 2.6026 7.8152 1.444
	-5 5.6234	1 8.5000 1.5707	.75	-4 1.1630 5.2767 1.384	-4 1.1909 6.9501 1.428	-4 1.2131 9.3061 1.464	-4 1.2322 1 1.2634 1.492	-4 1.2463 1 1.7330 1.513

TABLE X. - Continued. RESPONSES OF CYLINDERS

[The number to the left of each entry denotes the power of ten by which each entry as printed is to be multiplied. Example: -1 9.7420 is actually equal to 0.97420.]

(e) $\omega\tau_{int,2} = 10.$

$\omega\tau_{ext,2}$	Homogeneous cylinder: Exact / First order	β	Laminated cylinder, k_2/k_1 = 5	k_2/k_1 = 10	k_2/k_1 = 20	k_2/k_1 = 40	k_2/k_1 = 80
1.000	-1 1.7696 1.1989 .8756	1.00	-1 9.3766 -2 6.2621 .0625	-1 9.5505 -2 4.5050 .0450	-1 9.6778 -2 3.2262 .0323	-1 9.7699 -2 2.3023 .0230	-1 9.8362 -2 1.6388 .0164
		.90	-1 7.3758 -1 4.7603 .444	-1 7.7218 -1 4.7784 .446	-1 8.0103 -1 4.7731 .445	-1 8.2416 -1 4.7571 .444	-1 8.4204 -1 4.7378 .443
	-1 7.3711 3.0103 -1 7.8540	.75	-1 4.1897 1.0006 .786	-1 4.2047 1.0492 .809	-1 4.2187 1.0918 .829	-1 4.2309 1.1273 .845	-1 4.2413 1.1558 .858
1.778	-1 1.5953 1.4140 .9552	1.00	-1 8.9222 -1 1.0635 .1059	-1 9.2163 -2 7.7459 .0773	-1 9.4347 -2 5.5988 .0559	-1 9.5947 -2 4.0229 .0402	-1 9.7106 -2 2.8778 .0288
		.90	-1 6.7507 -1 5.9678 .538	-1 7.1097 -1 6.0514 .544	-1 7.4189 -1 6.0965 .548	-1 7.6589 -1 6.1178 .549	-1 7.8510 -1 6.1255 .550
	-1 4.9016 6.1933 1.0585	.75	-1 3.7672 1.1768 .866	-1 3.7770 1.2352 .890	-1 3.7866 1.2872 .910	-1 3.7951 1.3310 .927	-1 3.8024 1.3663 .939
3.162	-1 1.3438 1.7963 1.0688	1.00	-1 8.1836 -1 1.7513 .1734	-1 8.6571 -1 1.3009 .1294	-1 9.0203 -2 9.5473 .0952	-1 9.2980 -2 6.9392 .0693	-1 9.4917 -2 5.0064 .0500
		.90	-1 5.7810 -1 7.9050 .669	-1 6.1284 -1 8.1421 .683	-1 6.4265 -1 8.3123 .694	-1 6.6716 -1 8.4316 .701	-1 6.8652 -1 8.5136 .705
	-1 3.0151 1 1.0414 1.2645	.75	-1 3.1617 1.4727 .974	-1 3.1658 1.5523 .999	-1 3.1703 1.6835 1.019	-1 3.1745 1.6842 1.035	-1 3.1784 1.7336 1.048
5.623	-1 1.0345 2.4763 1.1870	1.00	-1 7.0784 -1 2.7517 .2685	-1 7.7744 -1 2.1053 .2075	-1 8.3406 -1 1.5822 .1569	-1 8.7824 -1 1.1715 .1166	-1 9.1166 -2 8.5715 .0855
		.90	-1 4.5026 1.0811 .824	-1 4.7951 1.1394 .851	-1 5.0486 1.1868 .871	-1 5.2587 1.2241 .886	-1 5.4858 1.2525 .897
	-1 1.7508 1 1.5135 1.3948	.75	-1 2.4237 1.9554 1.098	-1 2.4232 2.0778 1.122	-1 2.4235 2.1886 1.142	-1 2.4243 2.2853 1.158	-1 2.4253 2.3655 1.171
1 1.000	-2 7.2349 3.6855 1.3058	1.00	-1 5.6372 -1 4.0545 .3853	-1 6.5182 -1 3.2275 .3122	-1 7.3059 -1 2.5097 .2459	-1 7.9674 -1 1.9110 .1888	-1 8.4959 -1 1.4297 .1420
		.90	-1 3.1572 1.4757 .976	-1 3.3645 1.6050 1.014	-1 3.5439 1.7204 1.044	-1 3.6924 1.8190 1.068	-1 3.8103 1.8995 1.086
	-2 9.9504 1 2.0043 1.4711	.75	-1 1.6885 2.6958 1.216	-1 1.6858 2.9038 1.239	-1 1.6842 3.1006 1.259	-1 1.6832 3.2768 1.275	-1 1.6827 3.4366 1.287
1 1.778	-2 4.6663 5.8357 1.4011	1.00	-1 4.0803 -1 3.5254 .5048	-1 4.9955 -1 4.6092 .4319	-1 5.9178 -1 3.7439 .3582	-1 6.7809 -1 2.9629 .2880	-1 7.5345 -1 2.2897 .2251
		.90	-1 2.0280 1.9451 1.096	-1 2.1564 2.1981 1.144	-1 2.2664 2.4457 1.183	-1 2.3566 2.6757 1.213	-1 2.4278 2.8785 1.236
	-2 5.6145 1 2.5014 1.5146	.75	-1 1.0861 3.7342 1.309	-1 1.0833 4.1094 1.332	-1 1.0813 4.4815 1.351	-1 1.0800 4.8296 1.367	-1 1.0791 5.1376 1.379

TABLE X. - Continued. RESPONSES OF CYLINDERS

[The number to the left of each entry denotes the power of ten by which each entry as printed is to be multiplied. Example: -1 9.7420 is actually equal to 0.97420.]

(e) Continued. $\omega\tau_{int,2} = 10$.

$\omega\tau_{ext,2}$	Homogeneous cylinder: Exact / First order	β	Laminated cylinder, k_2/k_1 = 5	10	20	40	80
1 3.162	-2 2.8450 9.6595 1.4676	1.00	-1 2.7055 -1 6.9418 .6068	-1 3.4824 -1 6.0707 .5456	-1 4.3623 -1 5.1752 .4776	-1 5.2930 -1 4.2911 .4053	-1 6.2075 -1 3.4603 .3331
		.90	-1 1.2890 2.4228 1.179	-1 1.3030 2.8507 1.233	-1 1.3658 3.3091 1.277	-1 1.4168 3.7758 1.312	-1 1.4567 4.2243 1.338
	-2 3.1607 1 3.0004 1.5392	.75	-2 6.6102 5.0217 1.374	-2 6.5892 5.6842 1.397	-2 6.5740 6.3822 1.415	-2 6.5632 7.0756 1.430	-2 6.5561 7.7844 1.443
1 5.623	-2 1.6755 1 1.6459 1.5101	1.00	-1 1.6806 -1 8.1109 .6815	-1 2.2424 -1 7.3879 .6363	-1 2.9376 -1 6.5923 .5828	-1 3.7563 -1 5.7373 .5209	-1 4.6634 -1 4.8564 .4521
		.90	-2 7.2009 2.8379 1.232	-2 7.6169 3.4634 1.290	-2 7.9665 4.1888 1.337	-2 8.2487 4.9970 1.373	-2 8.4680 5.8503 1.408
	-2 1.7780 1 3.5001 1.5630	.75	-2 3.8891 6.3940 1.416	-2 3.8754 7.4693 1.438	-2 3.8653 8.6816 1.456	-2 3.8581 9.9757 1.471	-2 3.8532 1 1.1269 1.482
2 1.000	-3 9.6709 1 2.8551 1.5358	1.00	-1 1.0011 -1 8.9594 .7306	-1 1.3663 -1 8.4147 .6995	-1 1.8447 -1 7.7928 .6619	-1 2.4525 -1 7.0791 .6160	-1 3.1931 -1 6.2817 .5609
		.90	-2 4.1416 3.1516 1.264	-2 4.3739 3.9555 1.323	-2 4.5682 4.9537 1.372	-2 4.7243 6.1537 1.410	-2 4.8449 7.3337 1.439
	-3 9.9995 1 4.0000 1.5608	.75	-2 2.2435 7.6406 1.441	-2 2.2352 9.1949 1.463	-2 2.2290 1 1.1066 1.481	-2 2.2245 1 1.3219 1.495	-2 2.2215 1 1.5566 1.507
2 1.778	-3 5.5186 1 5.0054 1.5508	1.00	-2 5.8172 -1 9.5194 .7608	-2 8.0455 -1 9.1281 .7398	-1 1.1064 -1 8.6807 .7149	-1 1.5081 -1 8.1510 .6839	-1 2.0295 -1 7.5233 .6450
		.90	-2 2.3582 3.3648 1.282	-2 2.4880 4.3070 1.343	-2 2.5962 5.5323 1.398	-2 2.6828 7.0937 1.431	-2 2.7497 9.0200 1.460
	-3 5.6233 1 4.5000 1.5652	.75	-2 1.2799 8.6186 1.455	-2 1.2750 1 1.0685 1.477	-2 1.2713 1 1.3175 1.495	-2 1.2687 1 1.6310 1.510	-2 1.2669 1 1.9996 1.521
2 3.162	-3 3.1890 1 8.8291 1.5595	1.00	-2 3.3321 -1 9.8662 .7787	-2 4.6437 -1 9.5851 .7642	-2 6.4543 -1 9.2755 .7478	-2 8.9291 -1 8.9096 .7278	-1 1.2364 -1 8.4641 .7024
		.90	-2 1.3353 3.4993 1.292	-2 1.4080 4.5360 1.354	-2 1.4684 5.9257 1.404	-2 1.5168 7.7679 1.443	-2 1.5540 1 1.0159 1.473
	-3 3.1623 1 5.0000 1.5676	.75	-3 7.2554 9.3014 1.464	-3 7.2272 1 1.1665 1.485	-3 7.2062 1 1.4793 1.503	-3 7.1911 1 1.8838 1.518	-3 7.1806 1 2.3906 1.529
2 5.623	-3 1.7677 2 1.5629 1.5644	1.00	-2 1.8934 1.0073 .7890	-2 2.6500 -1 9.8627 .7785	-2 3.7056 -1 9.6471 .7674	-2 5.1703 -1 9.4017 .7546	-2 7.1865 -1 9.1043 .7385
		.90	-3 7.5379 3.5802 1.298	-3 7.9457 4.6767 1.360	-3 8.2844 6.1740 1.410	-3 8.5548 8.2093 1.450	-3 8.7631 1 1.0940 1.480
	-3 1.7783 1 5.5000 1.5690	.75	-3 4.0986 9.7402 1.468	-3 4.0825 1 1.2353 1.490	-3 4.0706 1 1.5904 1.508	-3 4.0619 1 2.0660 1.523	-3 4.0559 1 2.6097 1.534

TABLE X. - Concluded. RESPONSES OF CYLINDERS

[The number to the left of each entry denotes the power of ten by which each entry as printed is to be multiplied. Example: -1 9.7420 is actually equal to 0.97420.]

(e) Concluded. $\omega\tau_{int,2} = 10.$

$\omega\tau_{ext,2}$	Homogeneous Cylinder: Exact	Homogeneous Cylinder: First order	Laminated cylinder: β	Laminated cylinder: k_2/k_1 = 5	k_2/k_1 = 10	k_2/k_1 = 20	k_2/k_1 = 40	k_2/k_1 = 80
3 1.000	-4 9.9666 2 2.7720 1.5672		1.00	-2 1.0709 1.0192 .7949	-2 1.5085 1.0026 .7867	-2 2.1083 -1 9.8695 .7788	-2 2.9558 -1 9.7031 .7703	-2 4.1365 -1 9.5087 .7602
			.90	-3 4.2480 3.6876 1.302	-3 4.4770 4.7600 1.364	-3 4.6670 6.3235 1.414	-3 4.8187 8.4811 1.453	-3 4.9354 1 1.1436 1.484
	-3 1.0000 1 6.0000 1.5698		.75	-3 2.3107 1 1.0007 1.471	-3 2.3016 1 1.2780 1.493	-3 2.2948 1 1.6610 1.511	-3 2.2899 1 2.1857 1.526	-3 2.2865 1 2.8948 1.536
3 1.778	-4 5.6128 2 4.9223 1.5668		1.00	-3 6.0422 1.0261 .7983	-3 8.4888 1.0120 .7914	-2 1.1934 -1 9.9998 .7854	-2 1.6777 -1 9.8812 .7794	-2 2.3569 -1 9.7523 .7729
			.90	-3 2.3918 3.6549 1.304	-3 2.5204 4.8082 1.366	-3 2.6271 6.4110 1.416	-3 2.7122 8.6424 1.456	-3 2.7778 1 1.1736 1.486
	-4 5.6234 1 6.5000 1.5702		.75	-3 1.3013 1 1.0165 1.473	-3 1.2961 1 1.3034 1.494	-3 1.2923 1 1.7037 1.512	-3 1.2895 1 2.2596 1.527	-3 1.2876 1 3.0248 1.538
3 3.162	-4 3.1589 2 8.7460 1.5697		1.00	-3 3.4040 1.0300 .8008	-3 4.7860 1.0174 .7940	-3 6.7357 1.0074 .7891	-3 9.4838 -1 9.9843 .7846	-2 1.3352 -1 9.8949 .7801
			.90	-3 1.3459 3.6704 1.305	-3 1.4182 4.8358 1.367	-3 1.4782 6.4613 1.417	-3 1.5260 8.7359 1.457	-3 1.5628 1 1.1912 1.487
	-4 3.1623 1 7.0000 1.5705		.75	-4 7.3233 1 1.0256 1.474	-4 7.2943 1 1.3182 1.495	-4 7.2728 1 1.7288 1.513	-4 7.2571 1 2.3035 1.527	-4 7.2463 1 3.1036 1.539
3 5.623	-4 1.7772 3 1.5546 1.5702		1.00	-3 1.9162 1.0322 .8013	-3 2.6953 1.0205 .7955	-3 3.7956 1.0116 .7912	-3 5.3488 1.0043 .7876	-3 7.5396 -1 9.9769 .7842
			.90	-4 7.5714 3.6792 1.305	-4 7.9779 4.8515 1.368	-4 8.3150 6.4900 1.418	-4 8.5838 8.7894 1.458	-4 8.7907 1 1.2013 1.488
	-4 1.7783 1 7.5000 1.5706		.75	-4 4.1201 1 1.0308 1.474	-4 4.1038 1 1.3266 1.496	-4 4.0916 1 1.7432 1.513	-4 4.0828 1 2.3389 1.528	-4 4.0767 1 3.1496 1.539
4 1.000	-5 9.9966 3 2.7635 1.5704		1.00	-3 1.0782 1.0335 .8019	-3 1.5170 1.0222 .7964	-3 2.1369 1.0140 .7923	-3 3.0128 1.0077 .7892	-3 4.2497 1.0024 .7866
			.90	-4 4.2586 3.6841 1.306	-4 4.4872 4.8603 1.368	-4 4.6767 6.5062 1.418	-4 4.8278 8.8197 1.458	-4 4.9441 1 1.2071 1.488
	-4 1.0000 1 8.0000 1.5707		.75	-4 2.3175 1 1.0337 1.474	-4 2.3083 1 1.3314 1.496	-4 2.3015 1 1.7514 1.514	-4 2.2965 1 2.3435 1.528	-4 2.2931 1 3.1763 1.539
4 1.778	-5 5.6223 3 4.9137 1.5706		1.00	-4 6.0652 1.0342 .8022	-4 8.5345 1.0231 .7968	-3 1.2035 1.0153 .7930	-3 1.6958 1.0096 .7902	-3 2.3930 1.0050 .7879
			.90	-4 2.3951 3.6869 1.306	-4 2.5836 4.8653 1.368	-4 2.6302 6.5154 1.419	-4 2.7151 8.8370 1.458	-4 2.7805 1 1.2104 1.488
	-5 5.6234 1 8.5000 1.5707		.75	-4 1.3034 1 1.0354 1.474	-4 1.2983 1 1.3341 1.496	-4 1.2944 1 1.7561 1.514	-4 1.2916 1 2.3516 1.528	-4 1.2897 1 3.1914 1.540
4 3.162	-5 3.1619 3 8.7368 1.5707		1.00	-4 3.4113 1.0346 .8024	-4 4.8005 1.0237 .7971	-4 6.7645 1.0161 .7934	-4 9.5412 1.0106 .7907	-3 1.3466 1.0065 .7886
			.90	-4 1.3469 3.6885 1.306	-4 1.4192 4.8682 1.368	-4 1.4791 6.5205 1.419	-4 1.5269 8.8467 1.458	-4 1.5637 1 1.2122 1.489
	-5 3.1683 1 9.0000 1.5708		.75	-5 7.3301 1 1.0363 1.475	-5 7.3011 1 1.3367 1.496	-5 7.2795 1 1.7587 1.514	-5 7.2637 1 2.3564 1.528	-5 7.2529 1 3.1999 1.540

TABLE XI. - THERMAL RESPONSES OF CYLINDERS TO SINUSOIDAL ENVIRONMENT TEMPERATURE CHANGE

(a) Parameter values for various combinations of cylinders and conditions at $\beta = 0.90$

Item	$\frac{k_2}{k_1}$	$\omega\tau_{ext}$	$\omega\tau_{int,2}$	Ja_2	$\alpha_1 r_a$	$\alpha_1 r_b$	$\alpha_2 r_a$	$\alpha_2 r_b$
I	40	10	0.1	0.047458	5.4027	6.0030	0.854244	0.94916
II	5	100	.1	.0047458	1.9101	2.1224	.854244	.94916
III	40	100	.1	.0047458	5.4027	6.0030	.854244	.94916
IV	40	100	1.0	.0150075	17.0848	18.9832	2.70135	3.0015
V	5	1000	1.0	.00150075	6.0404	6.7116	2.70135	3.0015
VI	40	1000	1.0	.00150075	17.0848	18.9832	2.70135	3.0015

(b) Relative amplitude η (or mean relative amplitude $\overline{\eta}$) and relative phase lag φ (or mean relative phase lag $\overline{\varphi}$), radians

Item	$\frac{k_2}{k_1}$	$\omega\tau_{ext}$	$\omega\tau_{int,2}$	Homogeneous metallic cylinder: exact solution		Homogeneous metallic cylinder: "first-order" solution		Metallic shell over oxide core			
								Shell thickness 0.1 r_b ($\beta = 0.90$)		Oxide surface value - equivalent to limiting case of zero shell thickness ($r_a = r_b$, β = unity)	
				$\overline{\eta}_2$	$\overline{\varphi}_2$	η_2	φ_2	$\overline{\eta}_2$	$\overline{\varphi}_2$	$\eta_{b,1}$	$\varphi_{b,1}$
I	40	10	0.1	0.098405	1.4718	0.099504	1.4711	0.20317 [a].20324	0.95513 [a].95468	0.25804	0.65689
II	5	100	0.1	0.0099883	1.5608	0.0099995	1.5608	0.011381 [a].011384	1.2366 [a]1.2370	0.012147	1.1057
III	40	100	0.1	0.0099883	1.5608	0.0099995	1.5608	0.022457 [a].022456	1.1202 [a]1.1200	0.031153	0.82871
IV	40	100	1.0	0.0099049	1.5577	0.0099995	1.5608	0.037680 [a].037681	1.2826 [a]1.2827	0.090430	0.73953
V	5	1000	1.0	0.00099905	1.5695	0.0010000	1.5698	0.0024910 [a].0024911	1.1291 [a]1.1290	0.0035264	0.84163
VI	40	1000	1.0	0.00099905	1.5695	0.0010000	1.5698	0.0038086 [a].0038087	1.3156 [a]1.3160	0.0096051	0.79782

[a]Numerical integration (all others analytical).

2922

CE-15

TABLE XII. - VALUES OF $\zeta \equiv \left[\frac{R_b'^2 + Im_b'^2}{(R_b' - \beta R_a')^2 + (Im_b' - \beta Im_a')^2} \right]^{1/2}$ AND ζ^{-1}

Case	β	$\frac{k_2}{k_1}$	R_b'	R_a'	Im_b'	Im_a'	$R_b'^2 + Im_b'^2$	ζ	ζ^{-1}
F1	0.75	5	-0.1001238	-0.0501360	0.1972549	0.1638661	0.0489264	2.14781	0.465591
A2	.90	5	-.1142315	-.0861063	.1916053	.1778131	.0497614	4.80519	.217146
Q3	.75	10	-.1344043	-.0697109	.1104311	.0976019	.0302595	1.92925	.518338
B4	.90	10	-.1534562	-.1175460	.0930813	.0981243	.0322129	3.74875	.266898
F5	.75	5	-.5086399	-.2678285	.1179808	.1899874	.270604	1.69584	.589678
H6	.75	20	-.1665920	-.0919382	.0007614	.0381408	.0277535	1.64082	.609451
A7	.90	5	-.5518770	-.4340794	.0255682	.1122606	.305222	5.10384	.322182
C8	.90	20	-.1756350	-.1427320	-.0458629	-.0046331	.0529321	2.88849	.346202
G9	.75	10	-.4899351	-.3139479	-.3687887	-.0498961	.376100	1.48771	.681534
I10	.75	40	-.1230785	-.0938909	-.1827518	-.0515370	.0485465	1.43814	.696511
B11	.90	10	-.3894454	-.3900846	-.5850827	-.3360279	.493989	2.46396	.405851
F12	.75	5	-.1692727	-.7641985	-2.709533	-.9072630	7.37022	1.31222	.762067
D13	.90	40	-.0411520	-.0799780	-.2613120	-.188450	.0699758	2.52086	.430875
H14	.75	20	-.3019220	-.1140320	-1.0083820	-.4233160	1.10799	1.32886	.752525
A15	.90	5	1.104770	.0026245	-3.118111	-2.226103	10.9451	2.11012	.473907
J16	.75	80	.308578	.0389140	-.3161320	-.1666440	.195036	1.30521	.766180
C17	.90	20	1.0626750	.4522930	-.8998850	-.7760490	1.93907	2.03031	.492536
Q18	.75	10	6.378515	1.516443	-.759680	-1.610672	41.2625	1.22114	.818907
E19	.90	80	.627734	.348538	-.0576120	-.188192	.397444	1.92319	.519969
I20	.75	40	2.744700	.9628220	1.229091	-.1879810	9.04404	1.23097	.812367
B21	.90	10	7.960020	5.466126	5.358710	1.015498	92.0777	1.78186	.561211
F22	.75	5	8.00200	12.94182	53.69394	6.59280	2919.06	1.10510	.904895
D23	.90	40	1.136920	1.663180	4.96095	2.24385	25.9054	1.71747	.582252
H24	.75	20	-11.82507	2.337990	25.76922	7.191500	798.860	1.16071	.861542
A25	.90	5	-58.27108	-7.55090	72.66964	46.63922	8,676.40	1.55421	.643414
J26	.75	80	-16.47183	-2.344390	5.781670	3.656750	304.749	1.16194	.860630
C27	.90	20	-59.76051	-25.71639	-.711380	12.94568	3,571.83	1.54645	.646842
Q28	.75	10	-257.0458	-84.6018	-332.3518	4.96680	166,648	1.07921	.926604
E29	.90	80	-20.6658	-16.3352	-38.5983	-11.0839	1,916.91	1.49747	.667793
I30	.75	40	76.1981	-30.16050	-292.3260	-83.1688	91,261.9	1.11432	.897408
B31	.90	10	754.1098	72.6934	-836.9125	-459.3737	126,911x10	1.39343	.717654
F32	.75	5	8,390.457	944.5842	8,103.892	-1,191.768	$136,073 \times 10^5$	.985974	1.01425
D33	.90	40	986.683	417.9770	487.1490	-32.1250	117,179x10	1.38033	.724464
H34	.75	20	392.3760	1,281.862	9,305.473	710.498	$887,458 \times 10^2$	1.05948	.943877
A35	.90	5	-20,285.685	2,927.539	33,414.525	12,894.371	$152,796 \times 10^4$	1.23554	.809383
J36	.75	80	-10,745.53	-811.430	2,916.75	1,462.41	$123,973 \times 10^3$	1.08110	.924984
C37	.90	20	-44,798.10	-16,712.10	-25,644.79	1,875.01	$268,453 \times 10^4$	1.27755	.782748
Q38	.75	10	440,812.4	-55,567.20	510,100.1	-59,254.37	$454,518 \times 10^6$	.931447	1.07360
E39	.90	80	63,322.3	5,501.90	-60,142.1	-25,803.9	$762,678 \times 10^4$	1.26446	.790851
I40	.75	40	879,842.3	99,993.3	477,428.2	-60,423.2	$100,206 \times 10^7$	1.04305	.958727
B41	.90	10	626,180	1,191,050	5,650.294	914,338.3	$392,133 \times 10^6$	.672674	1.48660
D42	.90	40	-1,267,653x10	-381,291x10	-829,584x10	40,742.5x10	$234,626 \times 10^9$	1.19520	.836680
E43	.75	20	23,345,160x10	-1,267,319x10	$1,436,595 \times 10^2$	-1,669,166x10	$751,376 \times 10^{11}$	.949083	1.05367
J44	.75	80	$-628,110 \times 10^2$	$682,222 \times 10^2$	$9,540,037 \times 10^2$	$452,373 \times 10^2$	$914,068 \times 10^{12}$	1.03124	.969706
C45	.90	20	$-8,577,456 \times 10^3$	$-1,126,706 \times 10^3$	$207,809 \times 10^3$	$1,310,798 \times 10^3$	$736,160 \times 10^{14}$	1.12515	.888770
E46	.90	80	$6,268,041 \times 10^4$	$953,051 \times 10^4$	$514,665 \times 10^4$	$-702,917 \times 10^4$	$395,532 \times 10^{16}$	1.13715	.879391
I47	.75	40	$-13,785,600 \times 10^5$	$678,425 \times 10^5$	$10,592,840 \times 10^5$	$722,760 \times 10^5$	$302,251 \times 10^{19}$	.994984	1.00504

TABLE XIII. - STARTING VALUES (IN OXIDE) AT OUTER SURFACE OF CORE

Case	$\frac{k_2}{k_1}$	t_a	$ber_0(t_a)$	$bei_0(t_a)$	$ber_0'(t_a)$	$bei_0'(t_a)$
F1	5	1.5918000	0.89986264	0.62640318	-0.25088018	0.76833041
A2	5	1.9101000	.79320681	.89108512	-.43053440	.88906846
G3	10	2.2611000	.60322862	1.2108103	-.69710873	.97601858
B4	10	2.7014000	.18708164	1.6571163	-1.1754803	.98124266
F5	5	2.8807000	.024614150	1.7821648	-1.3391427	.94993695
H6	20	3.1836000	-.63401710	2.0891683	-1.6387842	.78281854
A7	5	3.5988000	-.96108570	2.3516554	-2.1703972	.56130320
G8	20	3.8203000	-2.0250431	2.5439610	-2.8546399	-.082882905
G9	10	4.0032000	-2.6734553	2.2911081	-3.1394784	-4.9896065
I10	40	4.6023000	-4.3077222	1.6812860	-3.7566553	-2.0614812
B11	10	4.8038000	-5.4678889	.87082219	-3.9008481	-3.3602792
F12	5	5.0337000	-6.3592734	-.033762432	-3.8209915	-4.5364152
D13	40	5.4027000	-7.6780416	-2.1028540	-3.1891027	-6.7372095
H14	20	5.8814000	-8.3947422	-4.0686271	-2.2806450	-8.4663171
A15	5	6.0404000	-8.6640244	-7.7788811	.013121627	-11.130516
J16	80	6.3672000	-8.3845046	-11.782229	3.1131431	-13.331511
G17	20	6.7937000	-5.8728343	-17.975771	9.0458523	-15.820984
G18	10	7.1167000	-1.9772332	-23.149306	15.164426	-16.106716
E19	80	7.8406000	9.1089205	-31.103218	27.883047	-13.455300
I20	40	8.0064000	21.219767	-35.065301	38.504871	-7.5192302
B21	10	8.8424000	46.227720	-34.906988	54.661277	10.164955
F22	5	8.9513000	70.762339	-26.398782	64.709098	32.863999
D23	40	9.6077000	115.20995	12.474972	66.527187	89.753947
H24	20	10.067300	142.14002	55.762511	46.759828	143.82992
A25	5	10.741500	149.88051	192.82162	-37.754512	253.19608
J26	80	11.322800	88.192778	347.45310	-187.55133	292.83841
G27	20	12.080600	-188.37218	586.44555	-514.32770	258.91324
G28	10	12.659000	-559.49376	866.06885	-846.01828	49.868415
E29	80	13.587300	-1,582.8642	348.42370	-1,308.8137	-868.71066
I30	40	14.237300	-2,432.6108	-803.76951	-1,205.4119	-2,126.7538
B31	10	15.190800	-2,891.8055	-3,781.2411	728.83428	-4,593.7369
F32	5	15.917800	-1,072.7101	-7,898.5880	4,722.9209	-8,858.8402
D33	40	17.084600	10,858.251	-13,253.929	16,719.075	-1,265.0130
H34	20	17.902500	28,429.264	-8,957.4132	26,837.236	14,029.811
A35	5	19.101600	57,661.627	34,798.781	14,637.696	84,471.856
J36	80	20.134700	38,852.688	130,200.01	-64,914.115	118,983.17
G37	20	21.485000	-208,728.47	270,808.71	-354,242.06	37,500.148
G38	10	22.511300	-678,958.72	128,341.07	-555,671.98	-392,343.67
E39	80	24.161800	-1,192,335.6	-1,779,250.8	440,155.59	-2,084,314.8
I40	40	25.318000	1,068,715.8	-4,616,828.3	3,999,731.8	-2,416,926.2
B41	10	27.013600	15,055,163.0	-2,184,881.0	11,910,503.0	9,143,363.0
D42	40	30.381600	-95,995,861.0	1.2191870×10^{8}	-1.5251648×10^{8}	16,299,812.0
E43	20	31.835800	-4.2055305×10^{8}	-5.2677622×10^{7}	-2.5346385×10^{8}	-3.3383324×10^{8}
J44	80	35.805000	6.4891290×10^{9}	-1.3786472×10^{9}	5.4577720×10^{9}	3.6189811×10^{9}
G45	20	38.205000	2.9581886×10^{9}	3.4756858×10^{10}	-2.2534126×10^{10}	2.6215890×10^{10}
E46	80	42.986000	1.3488547×10^{11}	-9.4545525×10^{11}	7.6244061×10^{11}	-5.6233336×10^{11}
I47	40	45.025000	3.9906180×10^{12}	9.8129759×10^{10}	2.7056988×10^{12}	2.8910383×10^{12}

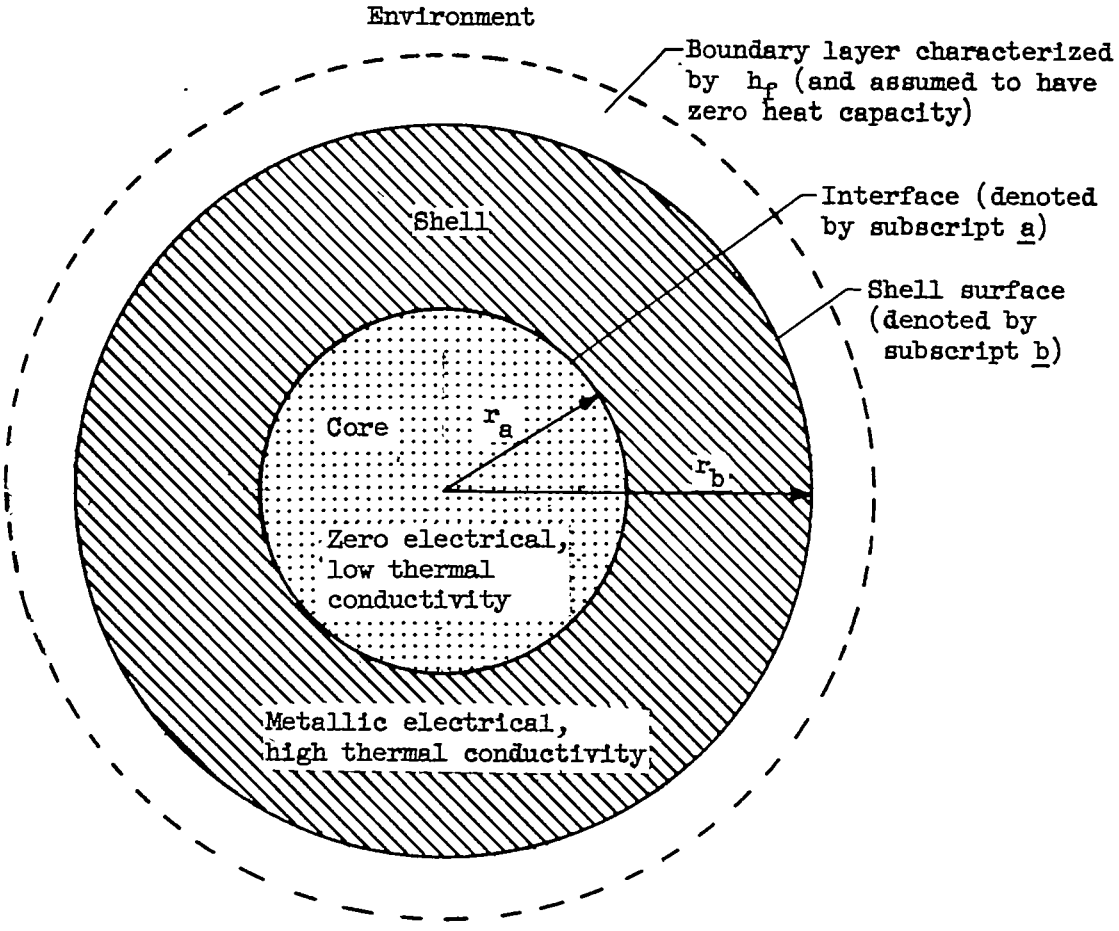

Figure 1. - Laminated cylinder.

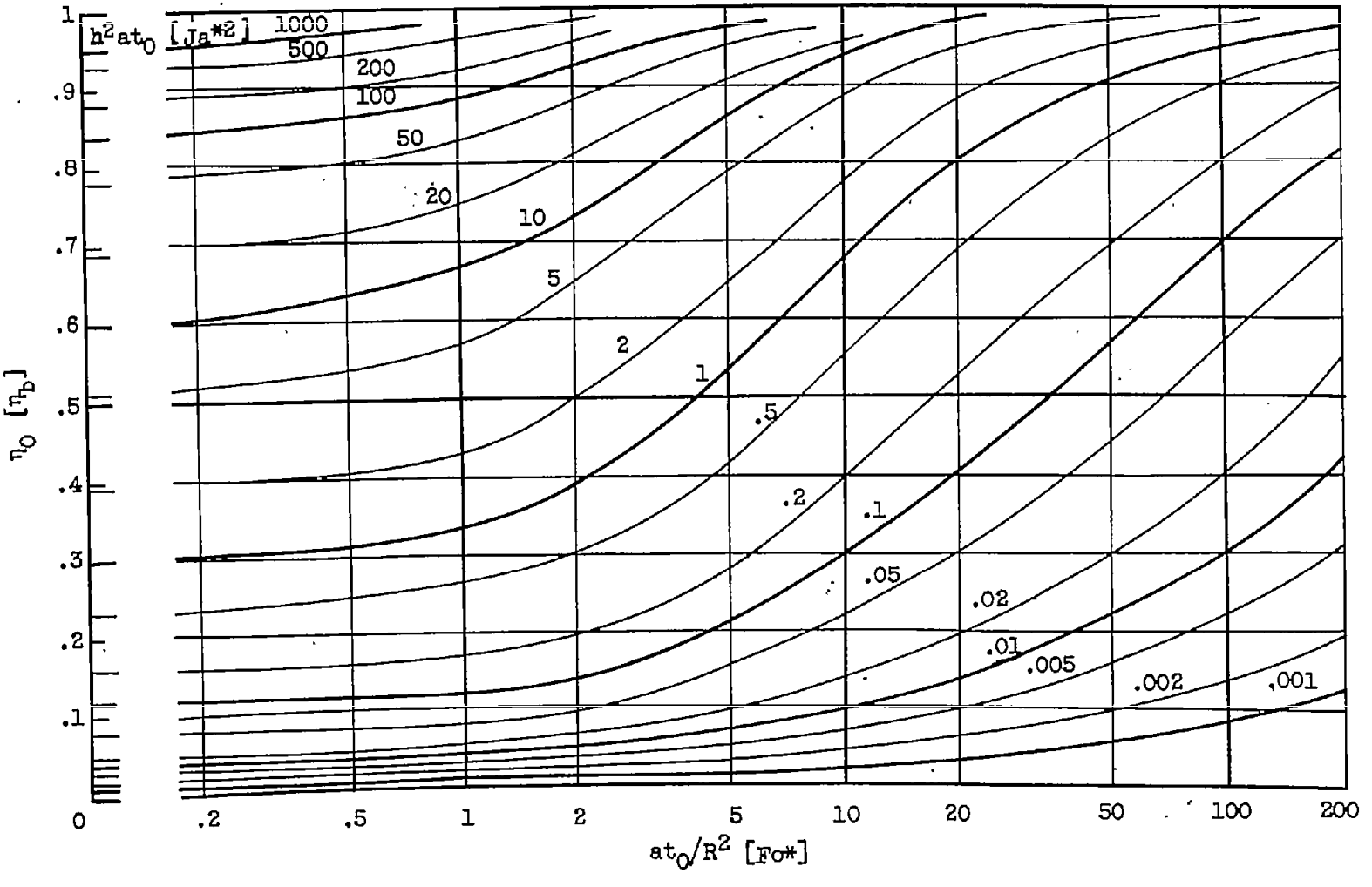

Figure 2. - Reduction factor η_0 [η_b].

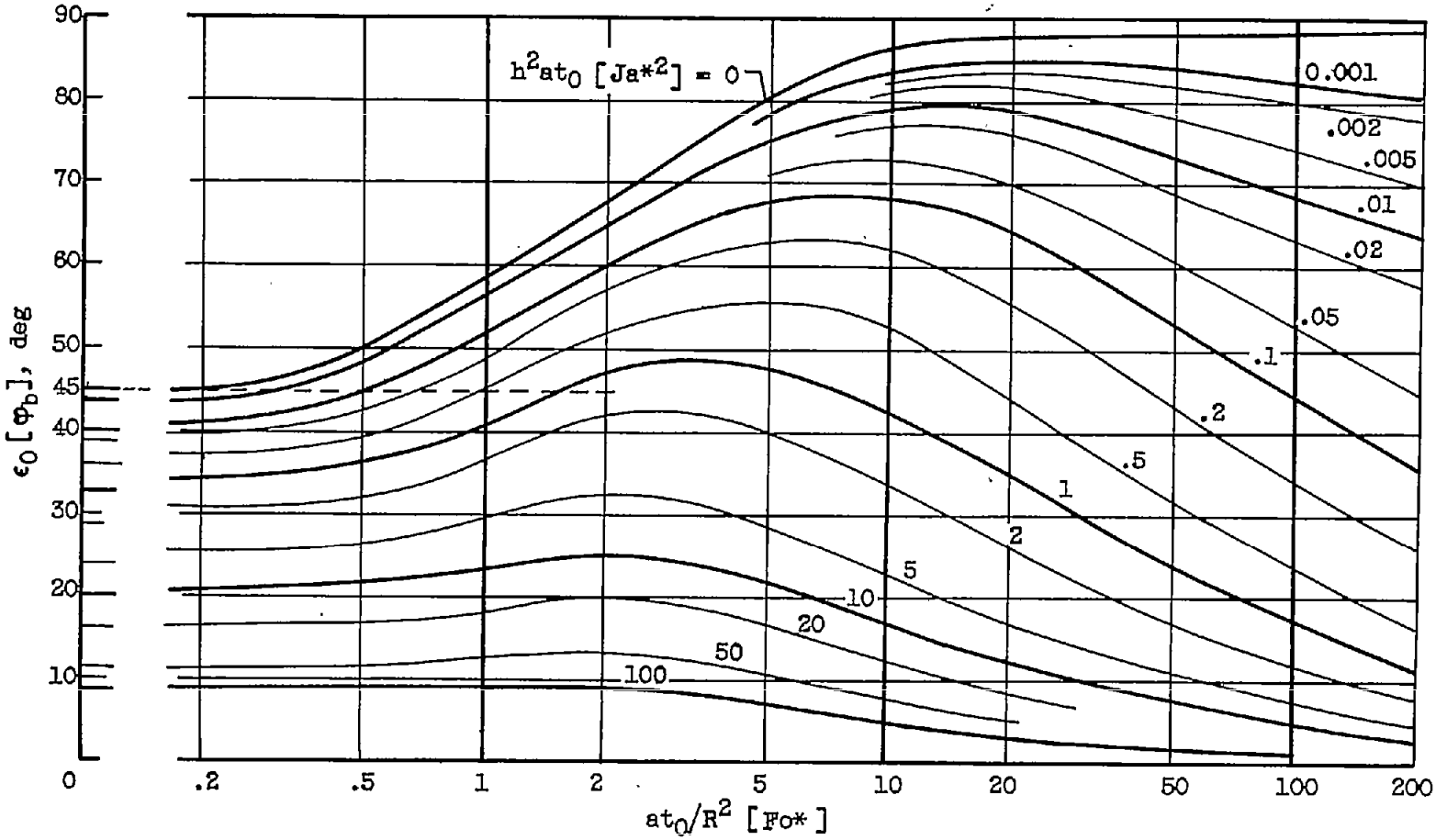

Figure 3. - Phase shift $\epsilon_0[\varphi_b]$.

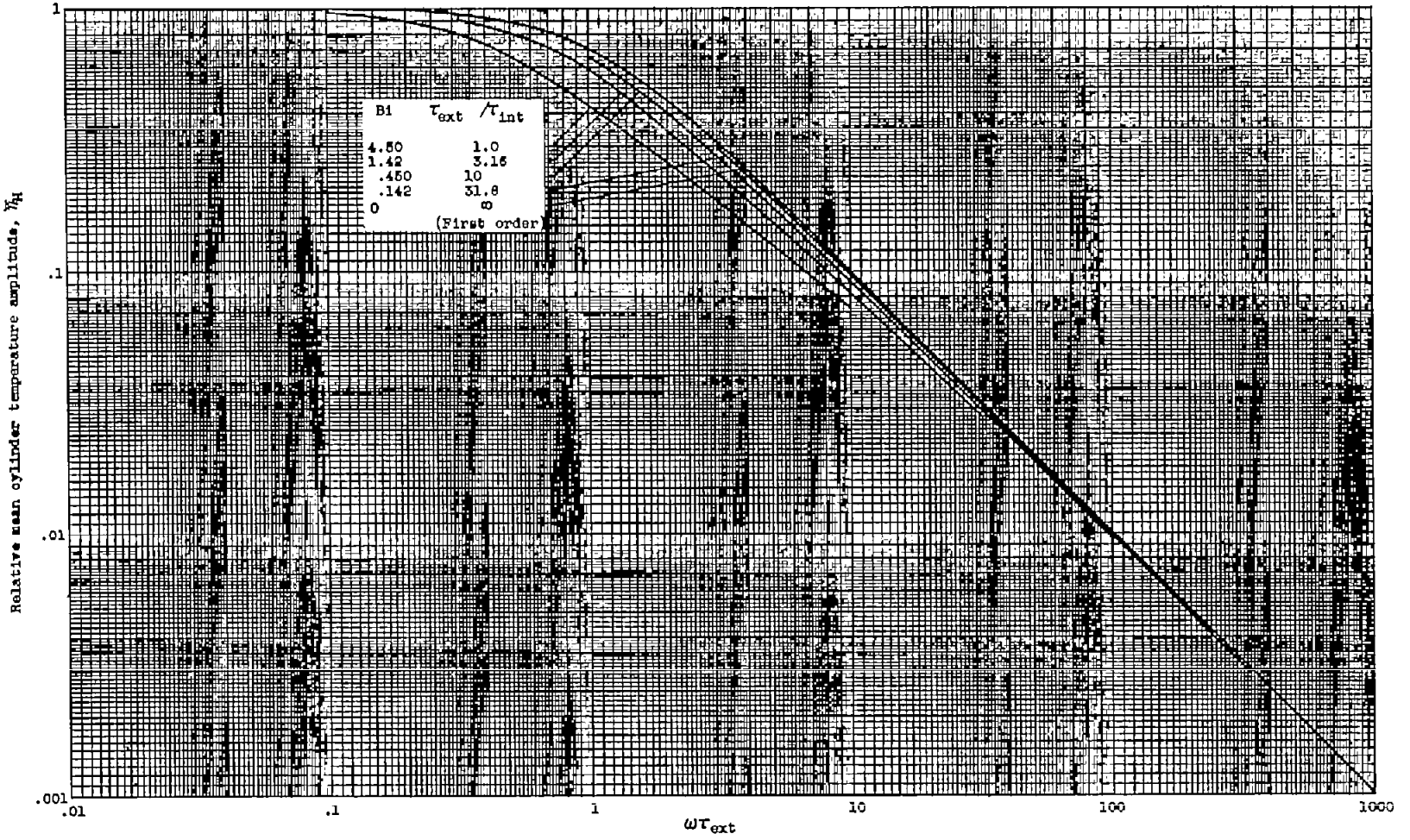

Figure 4. - Mean relative response of homogeneous cylinder.

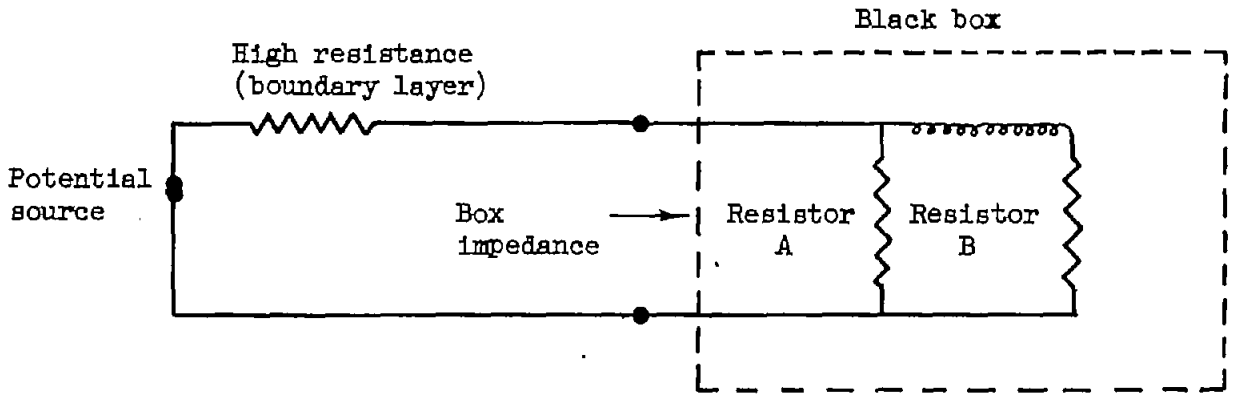

Figure 5. - Approximate electrical equivalent of homogeneous cylinder at high $\omega\tau_{ext}$ values. External (boundary layer) resistance much greater than box impedance.

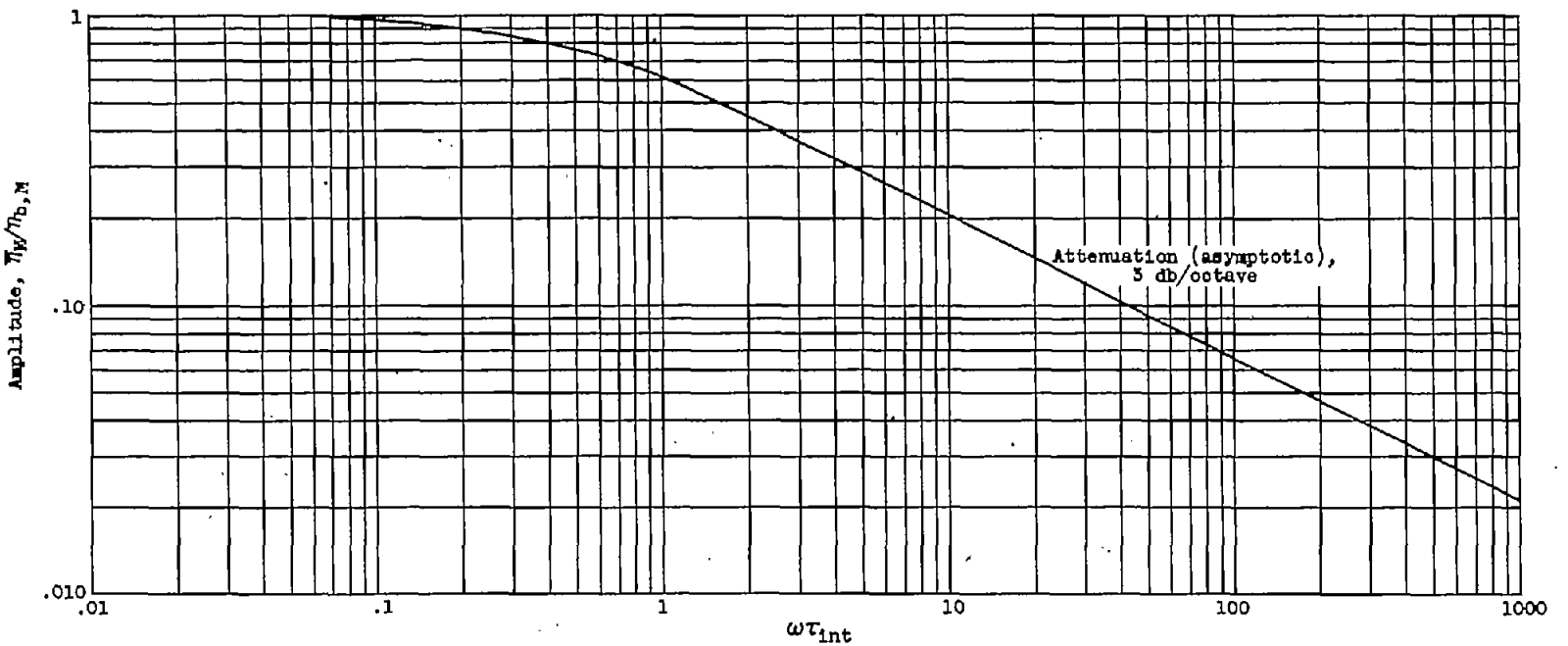

Figure 6. - Mean response of homogeneous cylinder for the case of surface temperature drive.

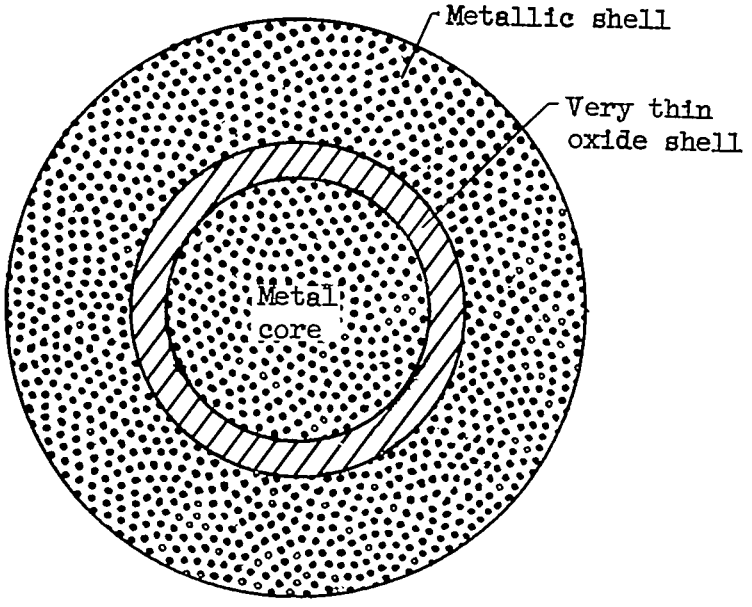

(a) Oxide layer.

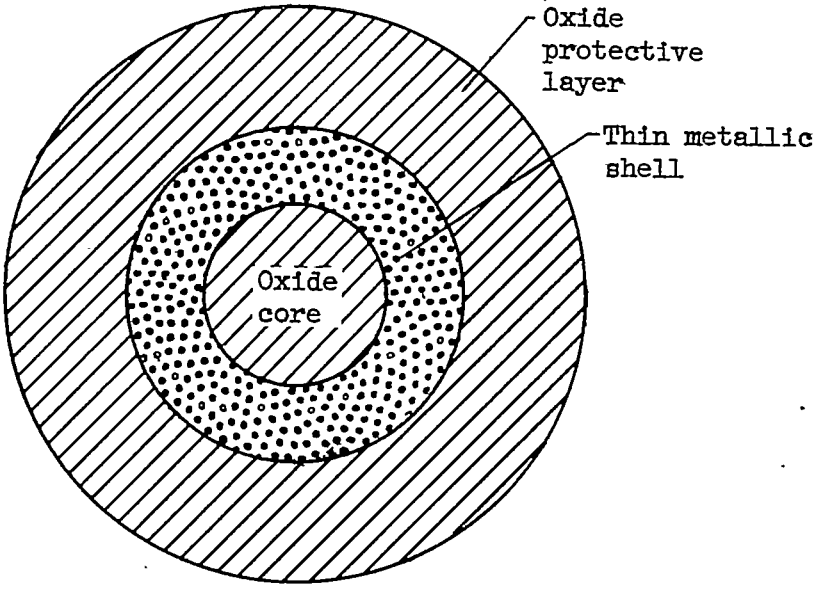

(b) Metallic layer.

Figure 7. - Quasi-homogeneous-cylinder configurations.

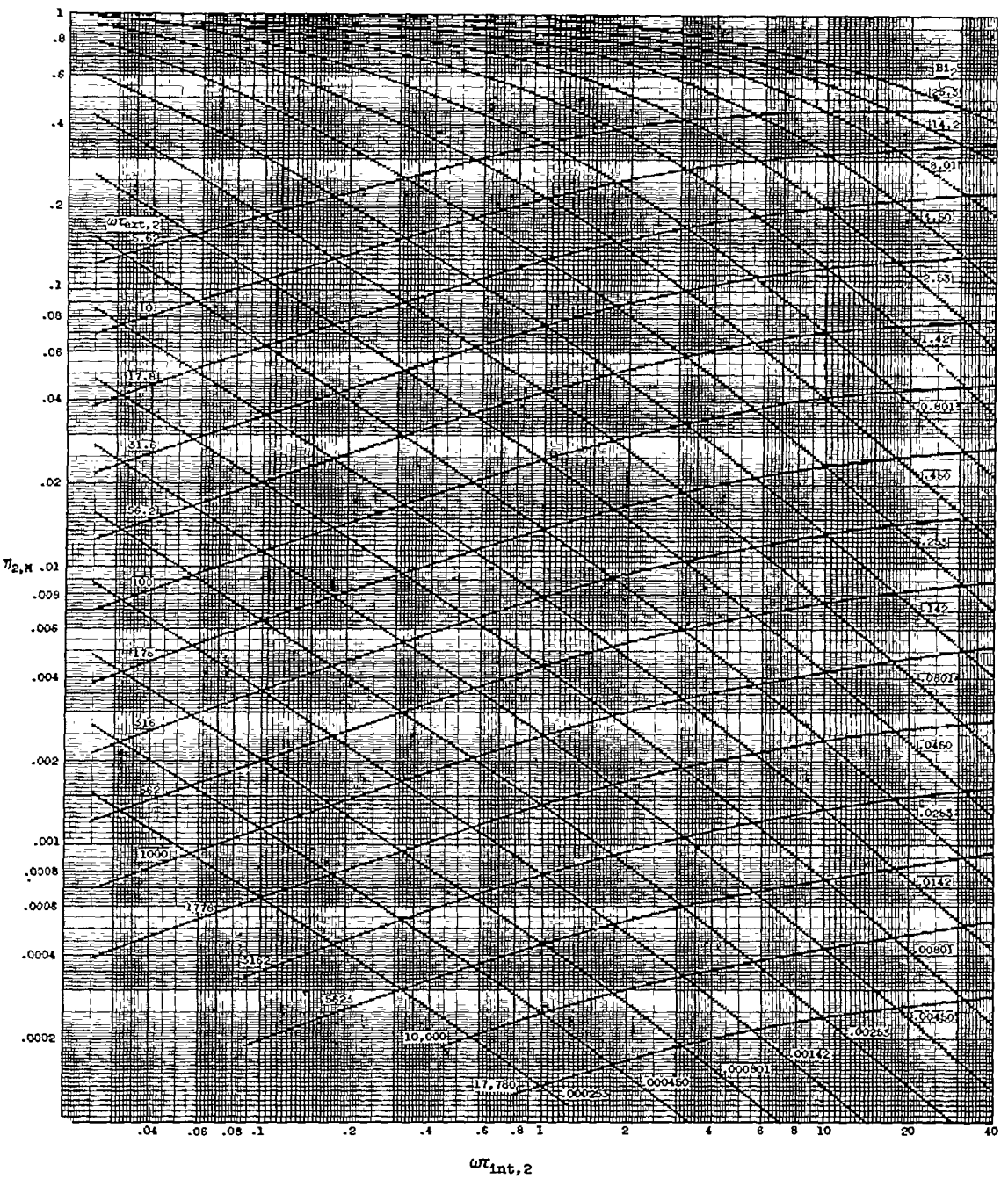

(a) Group A. $\beta = 0.90$; $k_2/k_1 = 5$.

Figure 8. - Relative mean amplitude of cylindrical shell over oxide core.
(Large copies of all parts of this figure may be obtained by using the request card bound in the back of the report.)

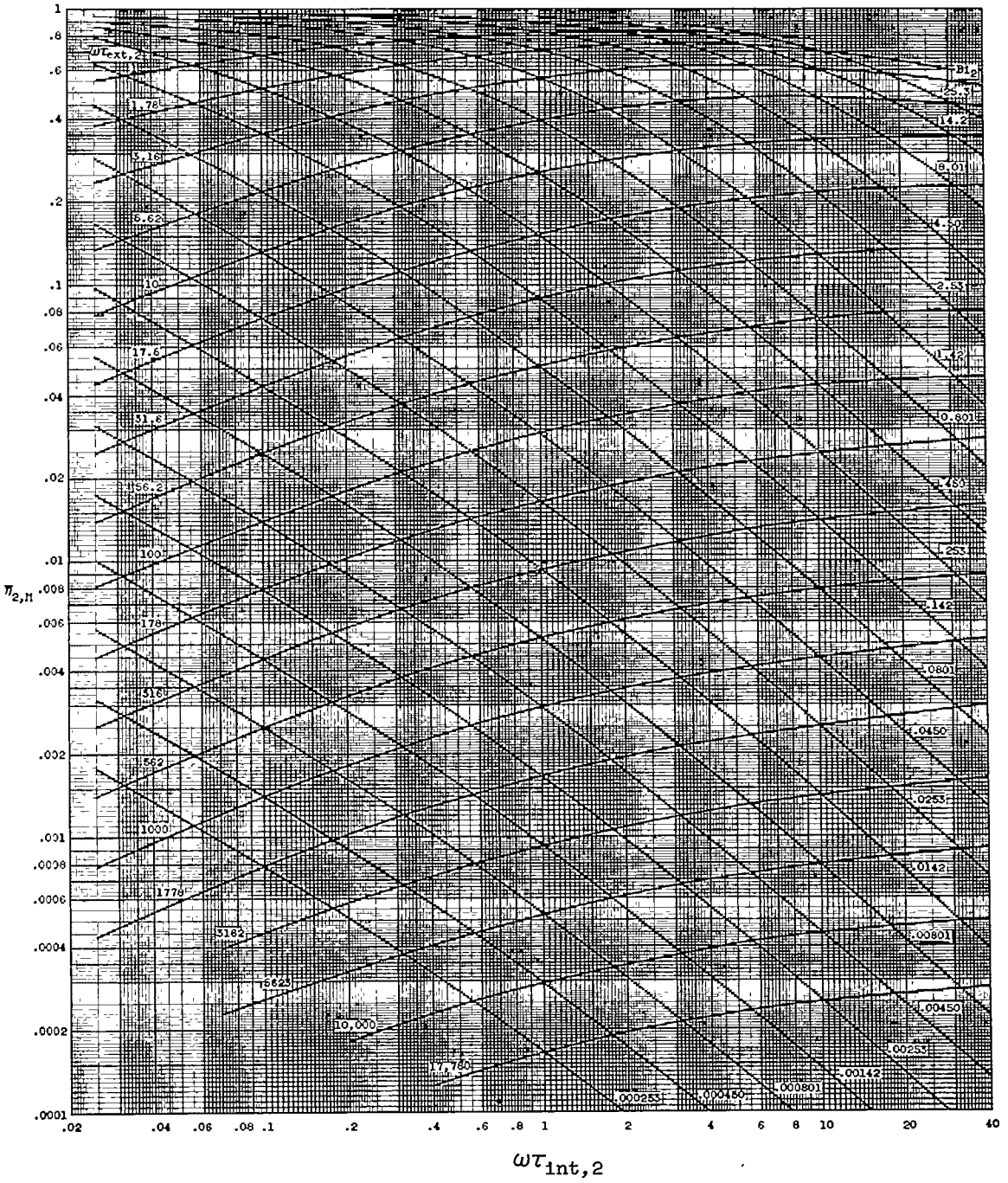

(b) Group B. $\beta = 0.90$; $k_2/k_1 = 10$.

Figure 8. - Continued. Relative mean amplitude of cylindrical shell over oxide core.

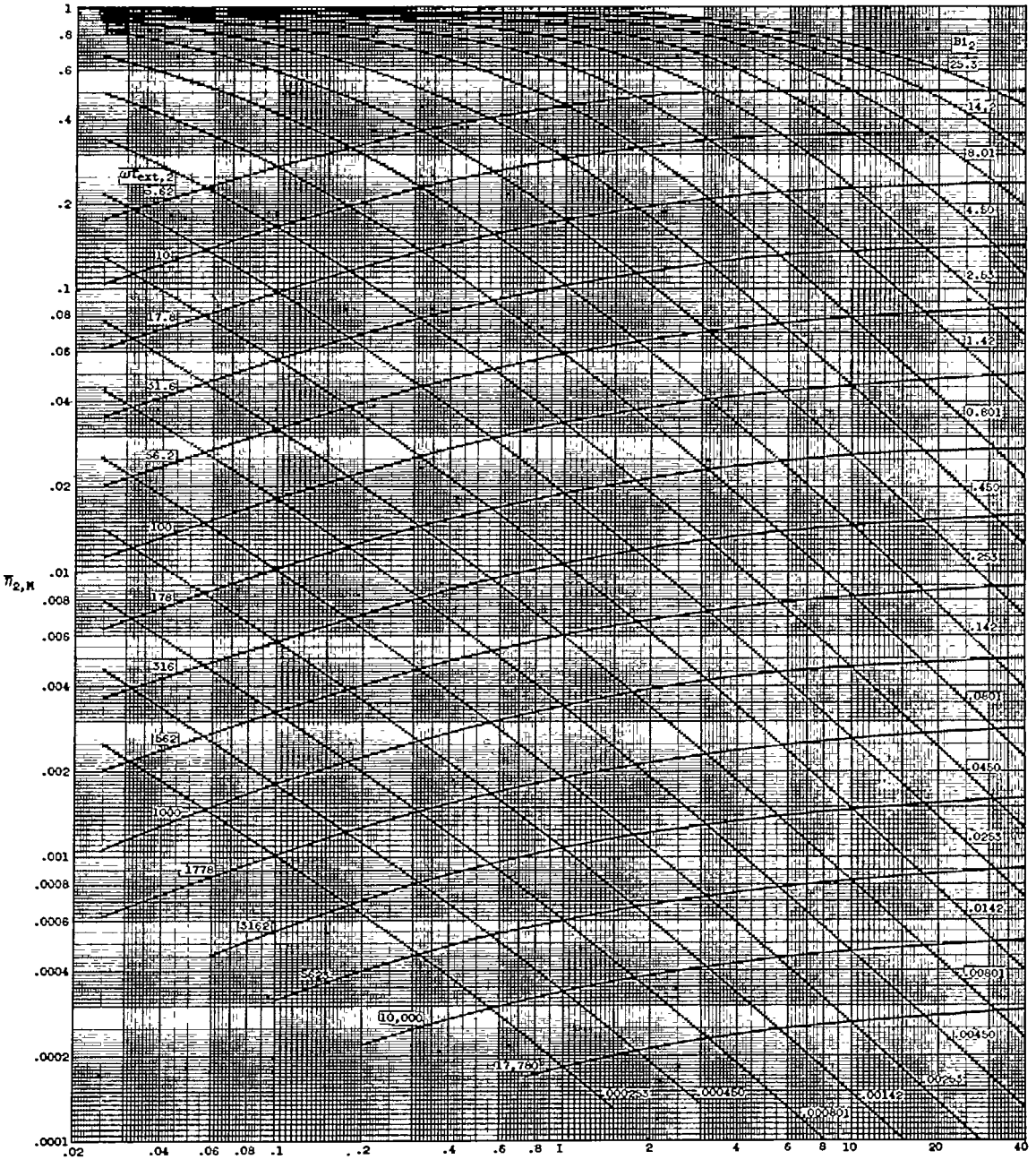

(c) Group C. $\beta = 0.90$; $k_2/k_1 = 20$.

Figure 8. - Continued. Relative mean amplitude of cylindrical shell over oxide core.

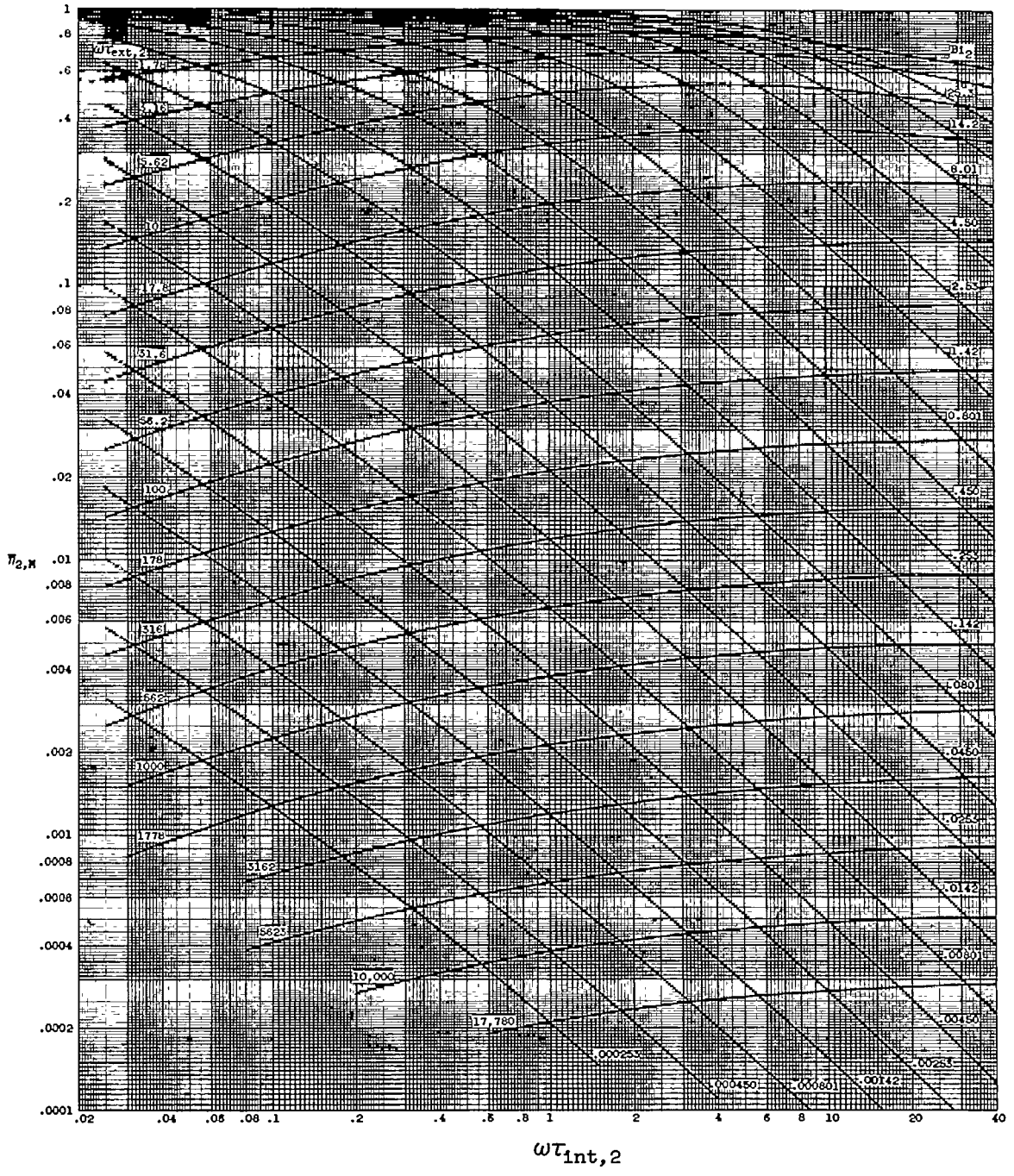

(d) Group D. $\beta = 0.90$; $k_2/k_1 = 40$.

Figure 8. - Continued. Relative mean amplitude of cylindrical shell over oxide core.

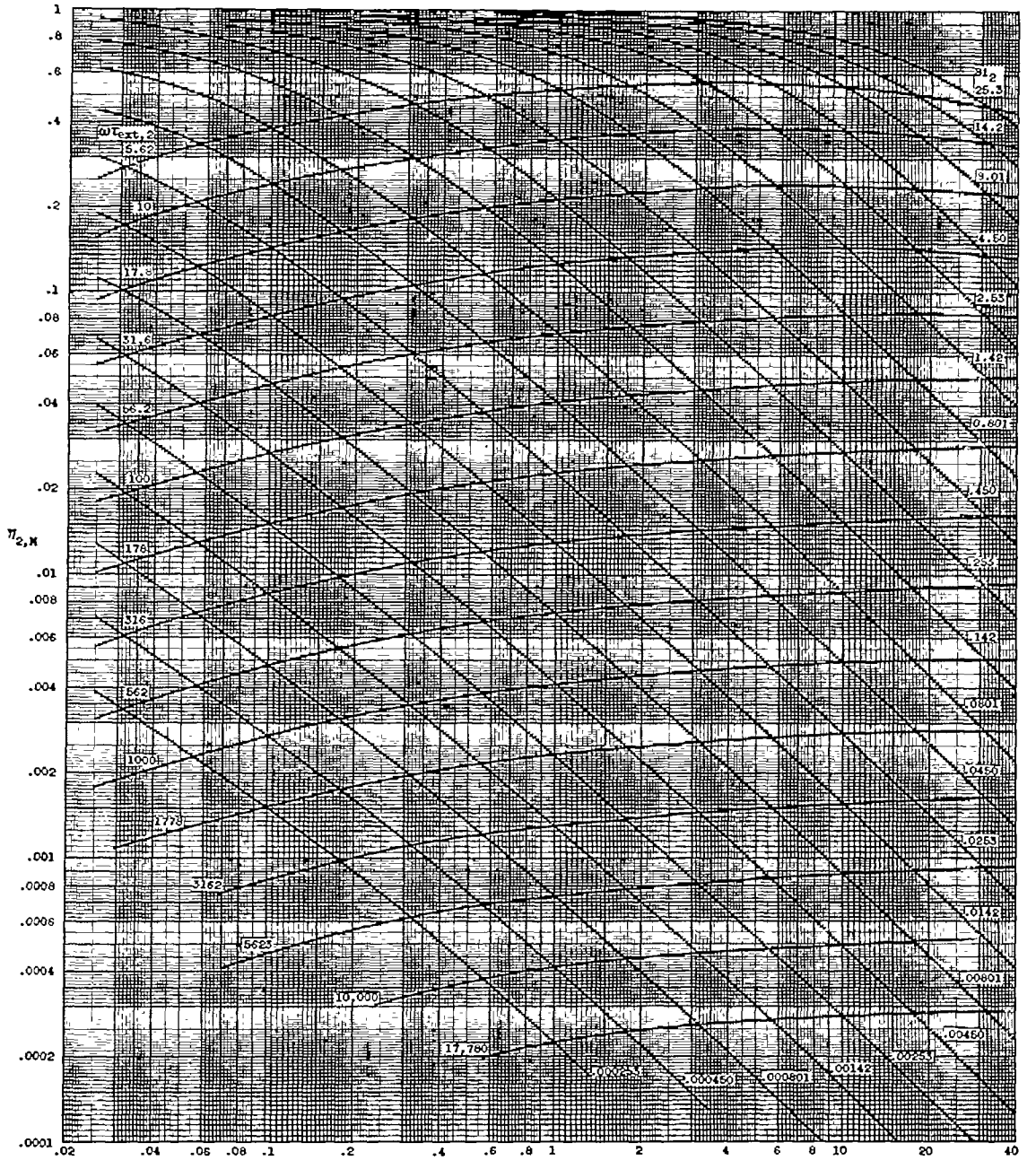

(e) Group E. $\beta = 0.90$; $k_2/k_1 = 80$.

Figure 8. - Continued. Relative mean amplitude of cylindrical shell over oxide core.

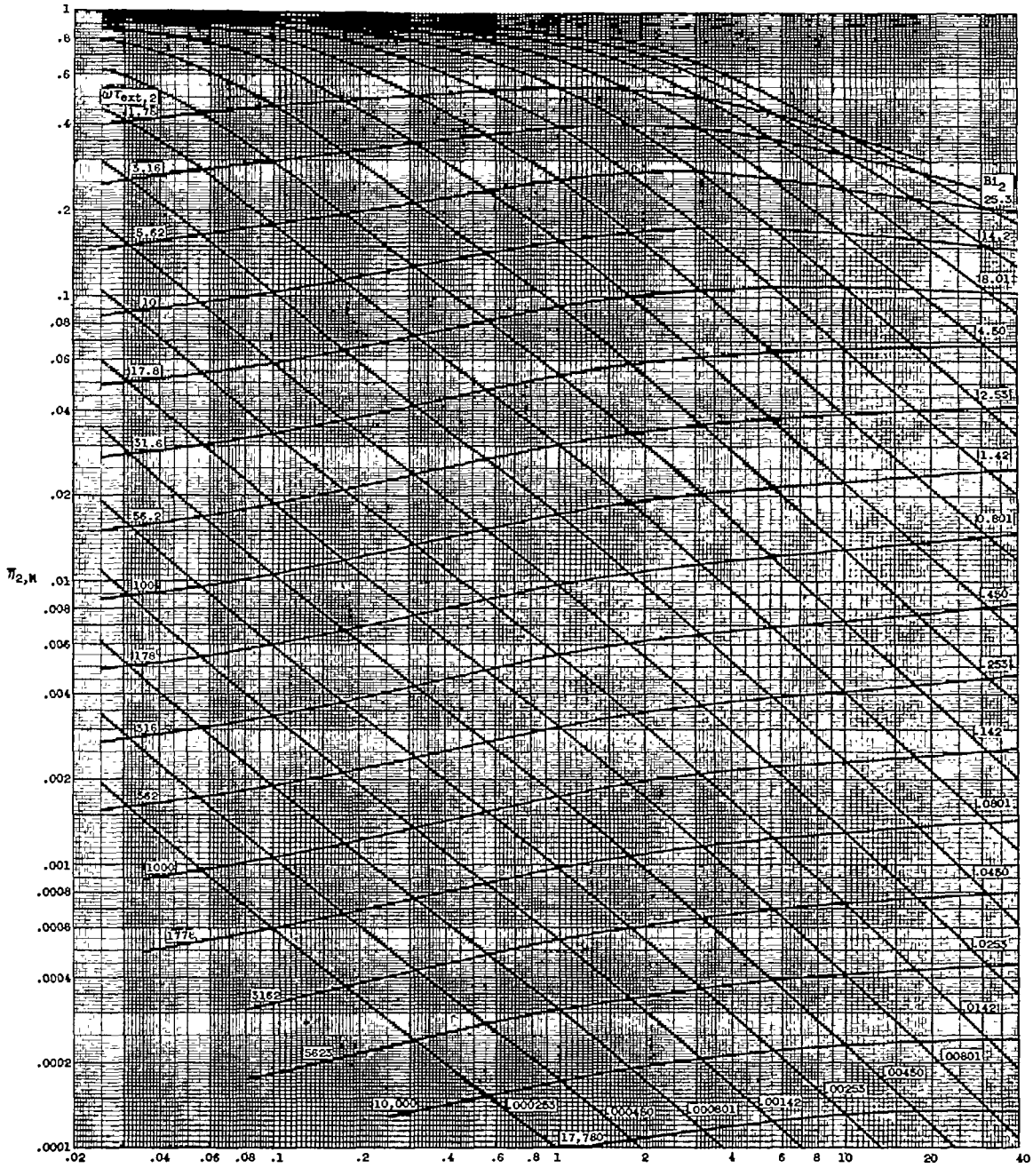

(f) Group F. $\beta = 0.75$; $k_2/k_1 = 5$.

Figure 8. - Continued. Relative mean amplitude of cylindrical shell over oxide core.

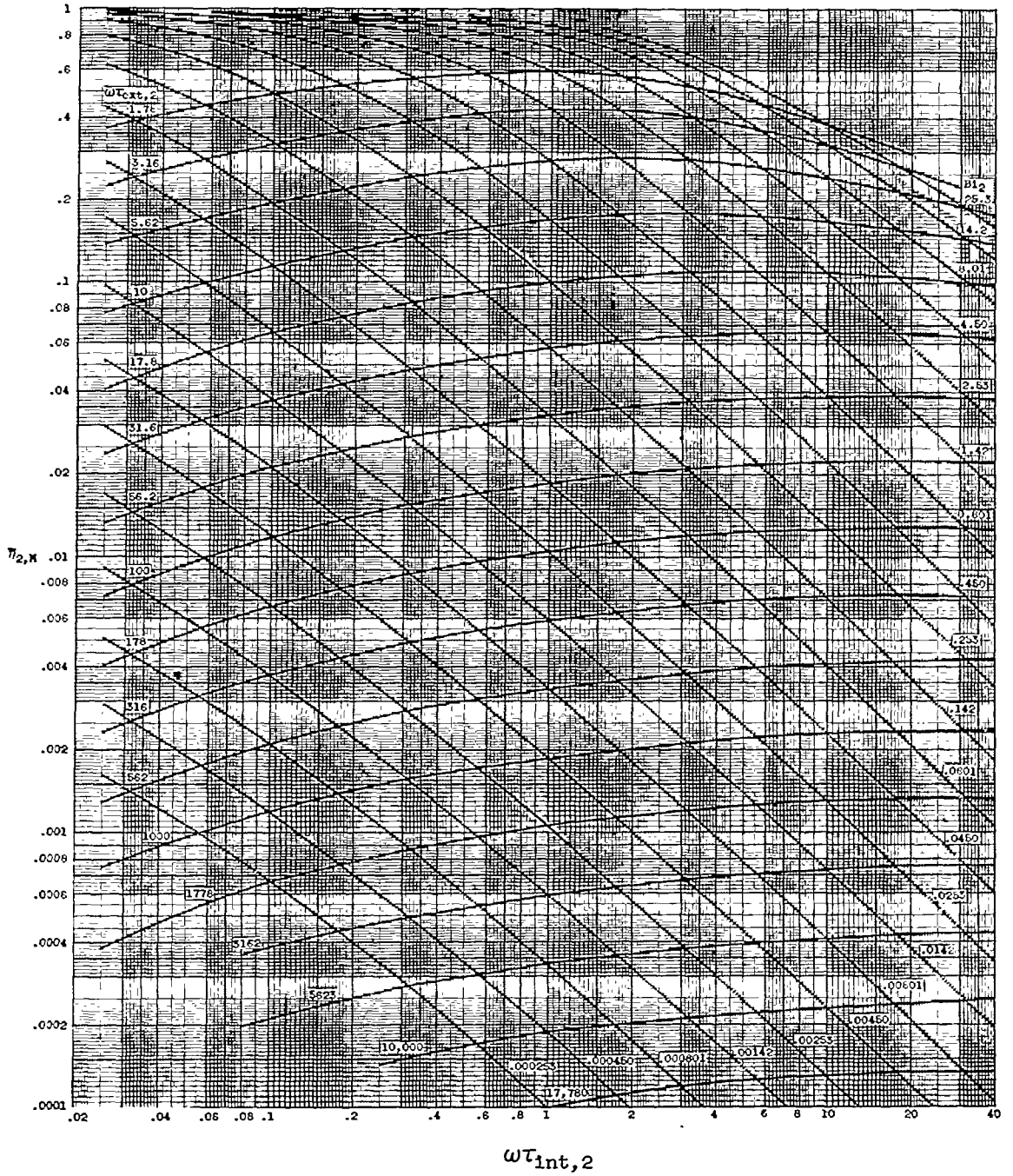

(g) Group G. $\beta = 0.75$; $k_2/k_1 = 10$.

Figure 8. - Continued. Relative mean amplitude of cylindrical shell over oxide core.

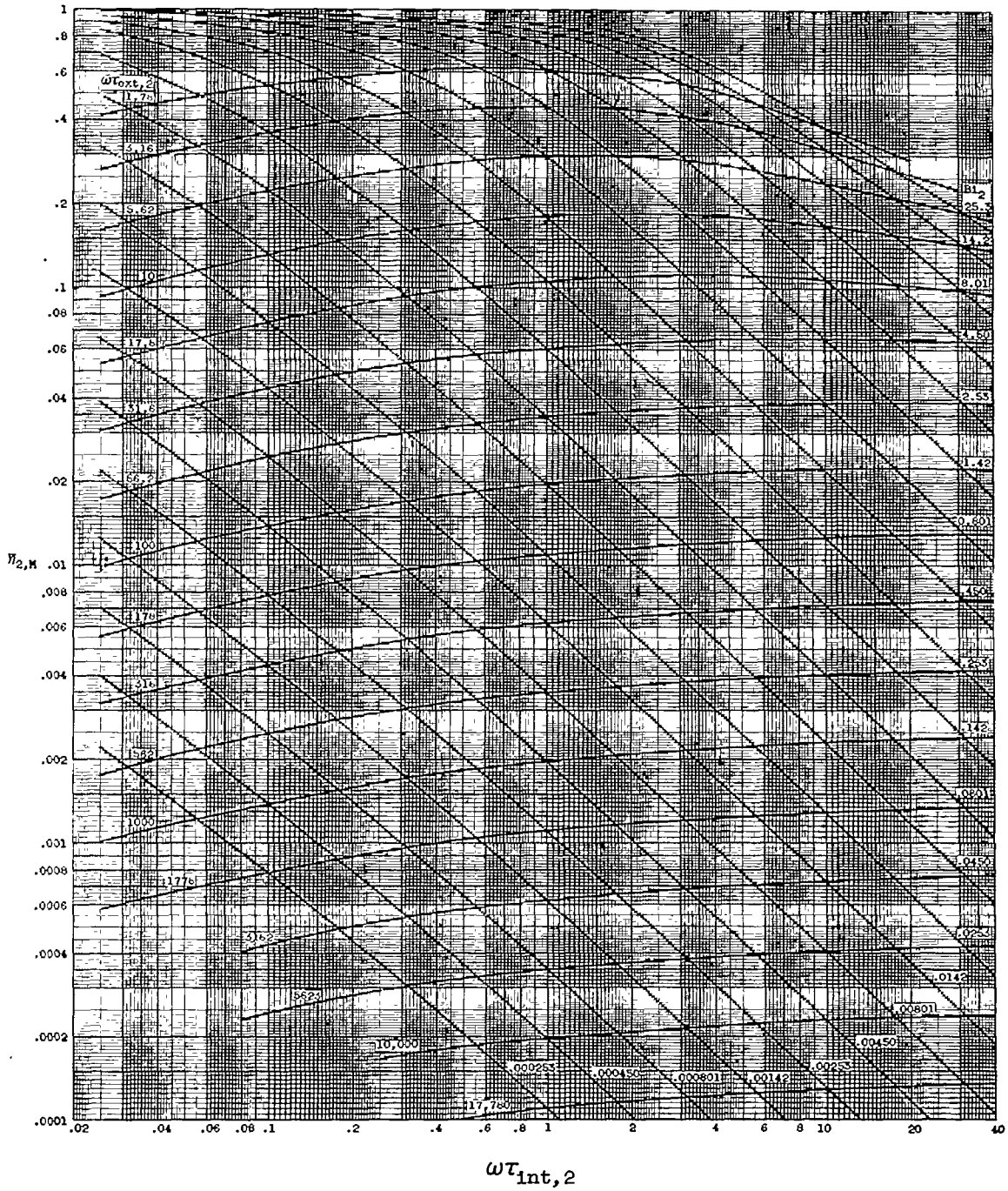

$\omega\tau_{int,2}$

(h) Group H. $\beta = 0.75$; $k_2/k_1 = 20$.

Figure 8. - Continued. Relative mean amplitude of cylindrical shell over oxide core.

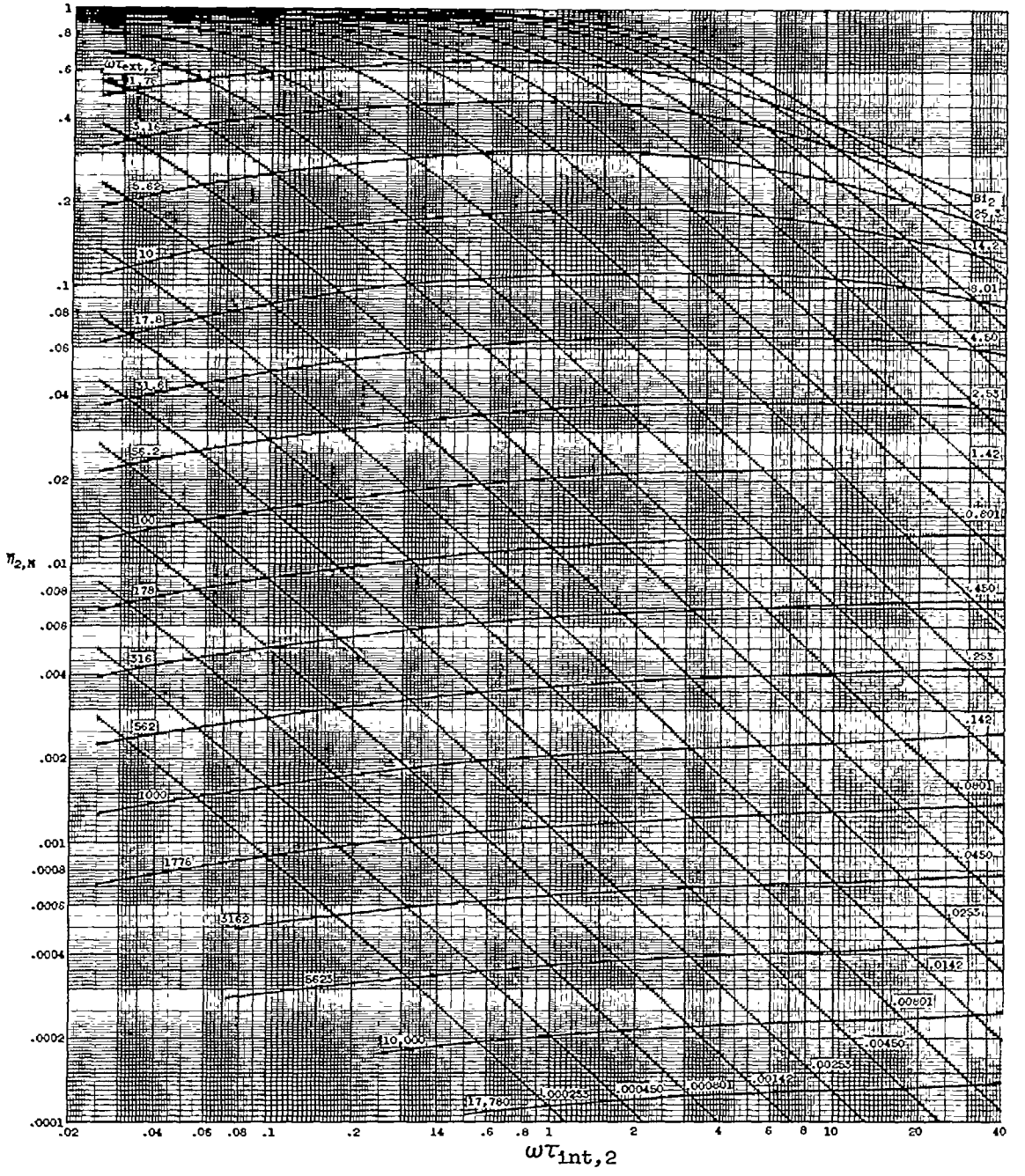

(i) Group I. $\beta = 0.75$; $k_2/k_1 = 40$.

Figure 8. - Continued. Relative mean amplitude of cylindrical shell over oxide core.

2922

CE-17 back

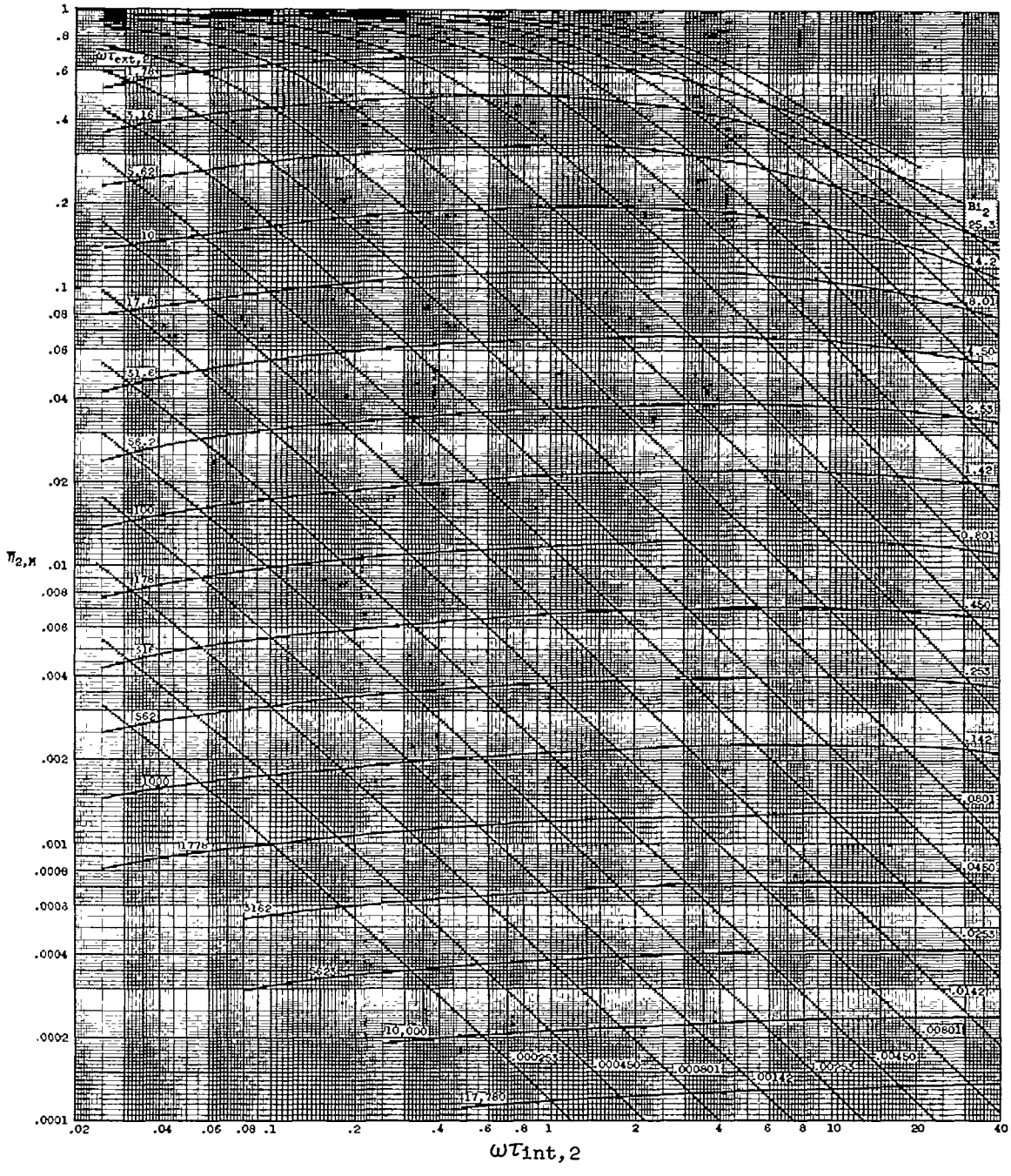

(j) Group J. $\beta = 0.75$; $k_2/k_1 = 80$.

Figure 8. - Concluded. Relative mean amplitude of cylindrical shell over oxide core.

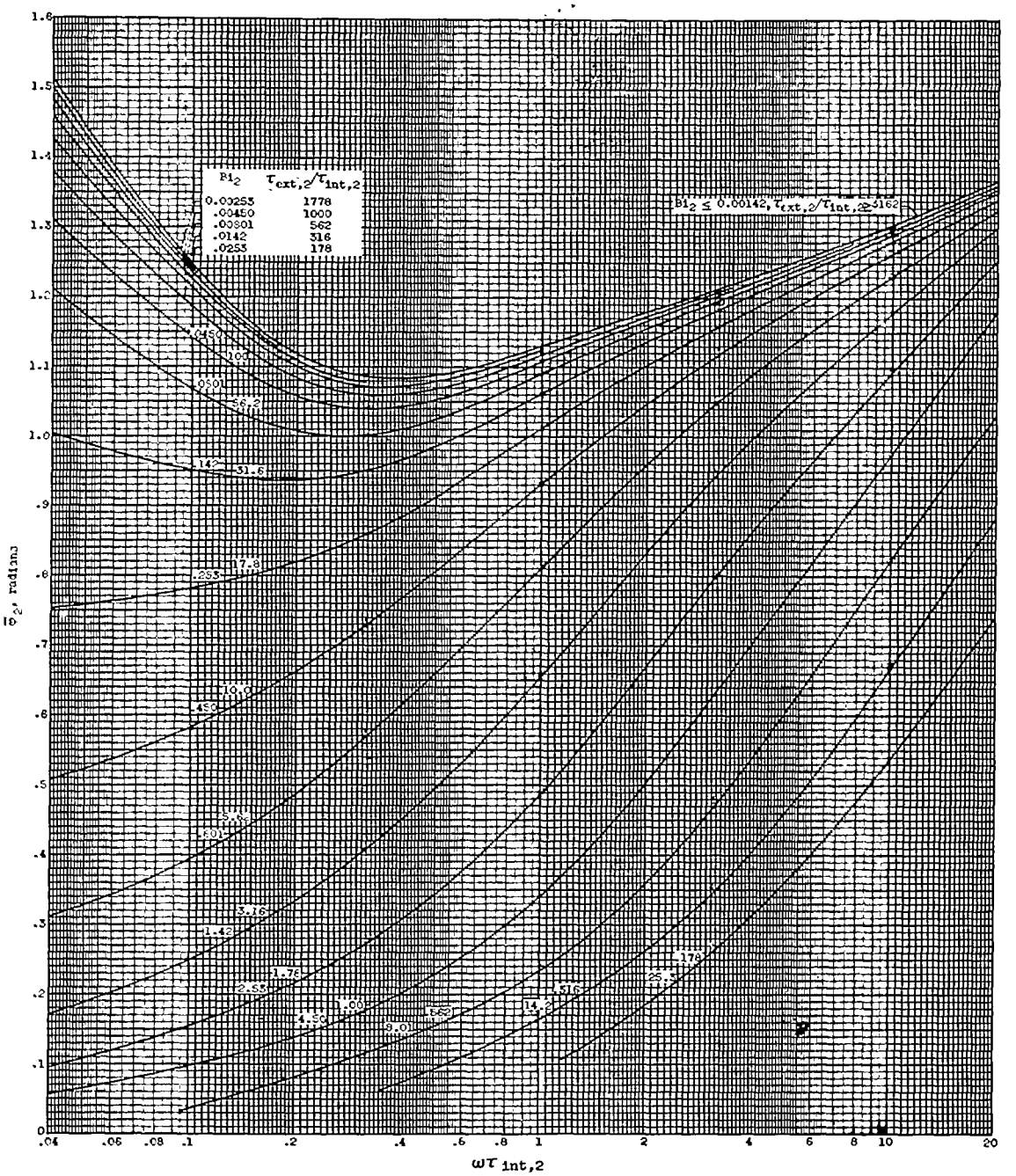

(a) Group A. $\beta = 0.90$; $k_2/k_1 = 5$.

Figure 9. - Relative mean phase shift (lag) of cylindrical shell over oxide core.
(Large copies of all parts of this figure may be obtained by using the request card bound in the back of the report.)

2262

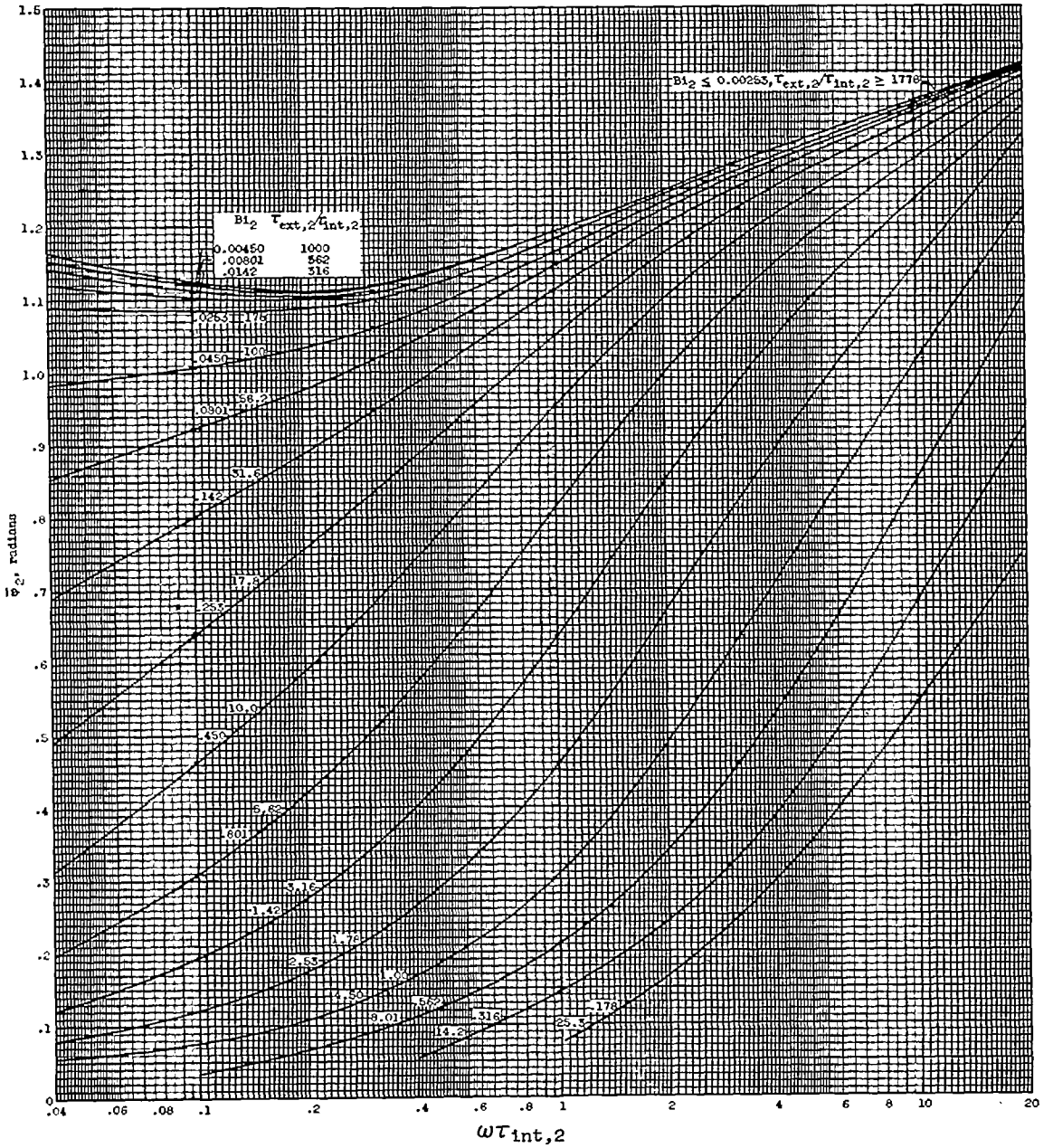

(b) Group B. $\beta = 0.90$; $k_2/k_1 = 10$.

Figure 9. - Continued. Relative mean phase shift (lag) of cylindrical shell over oxide core.

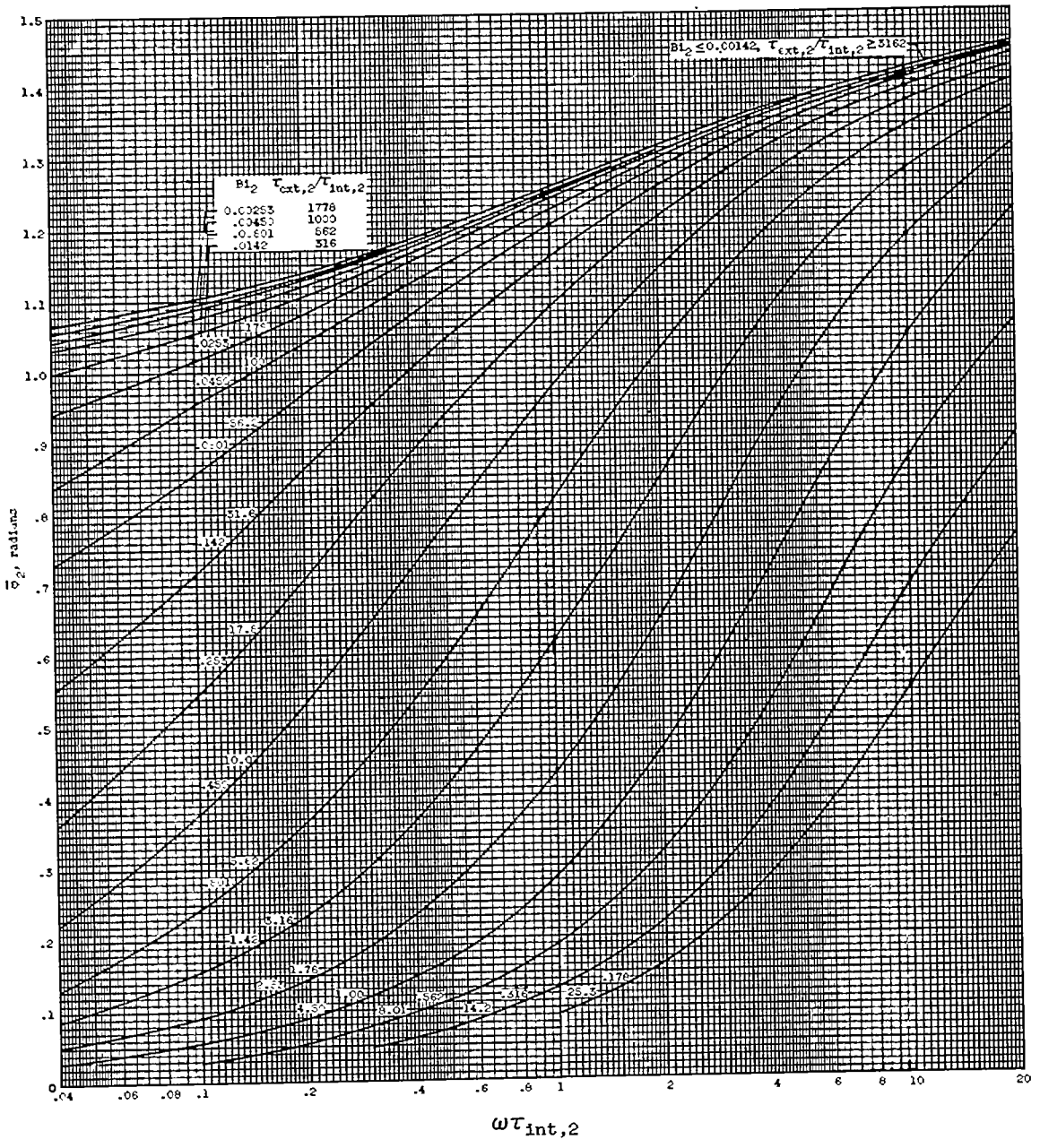

(c) Group C. $\beta = 0.90$; $k_2/k_1 = 20$.

Figure 9. - Continued. Relative mean phase shift (lag) of cylindrical shell over oxide core.

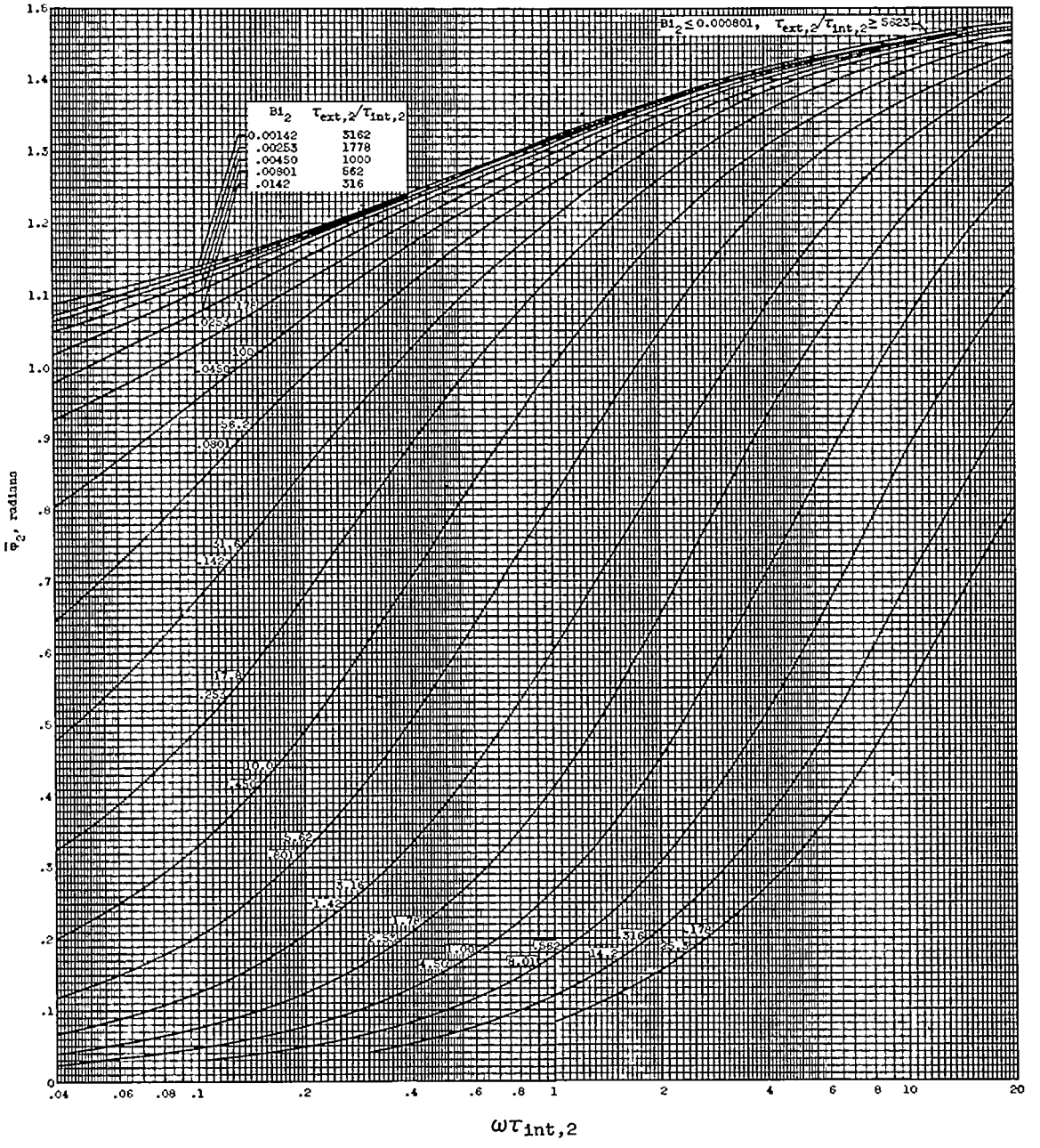

(d) Group D. $\beta = 0.90$; $k_2/k_1 = 40$.

Figure 9. - Continued. Relative mean phase shift (lag) of cylindrical shell over oxide core.

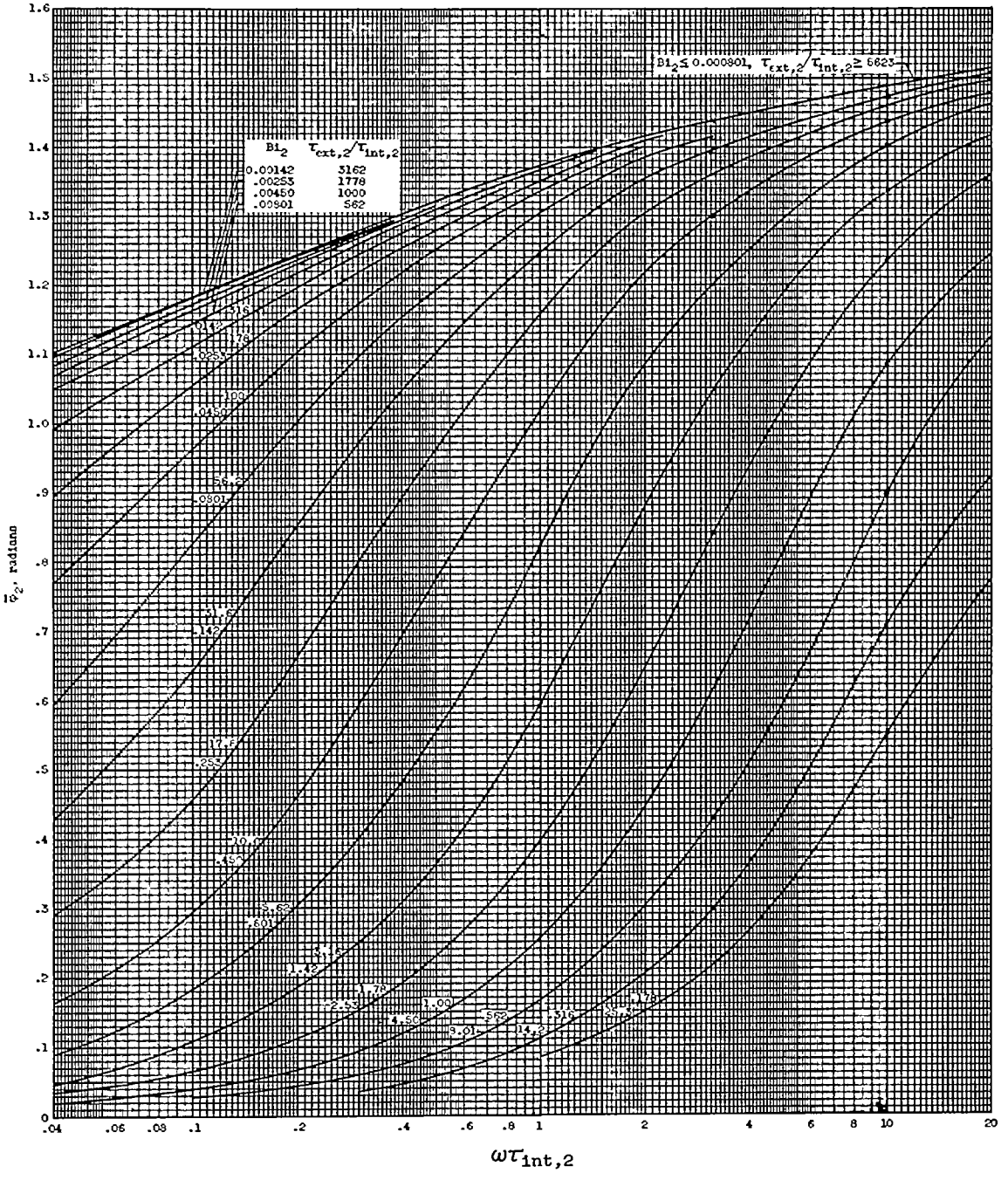

(e) Group E. $\beta = 0.90$; $k_2/k_1 = 80$.

Figure 9. - Continued. Relative mean phase shift (lag) of cylindrical shell over oxide core.

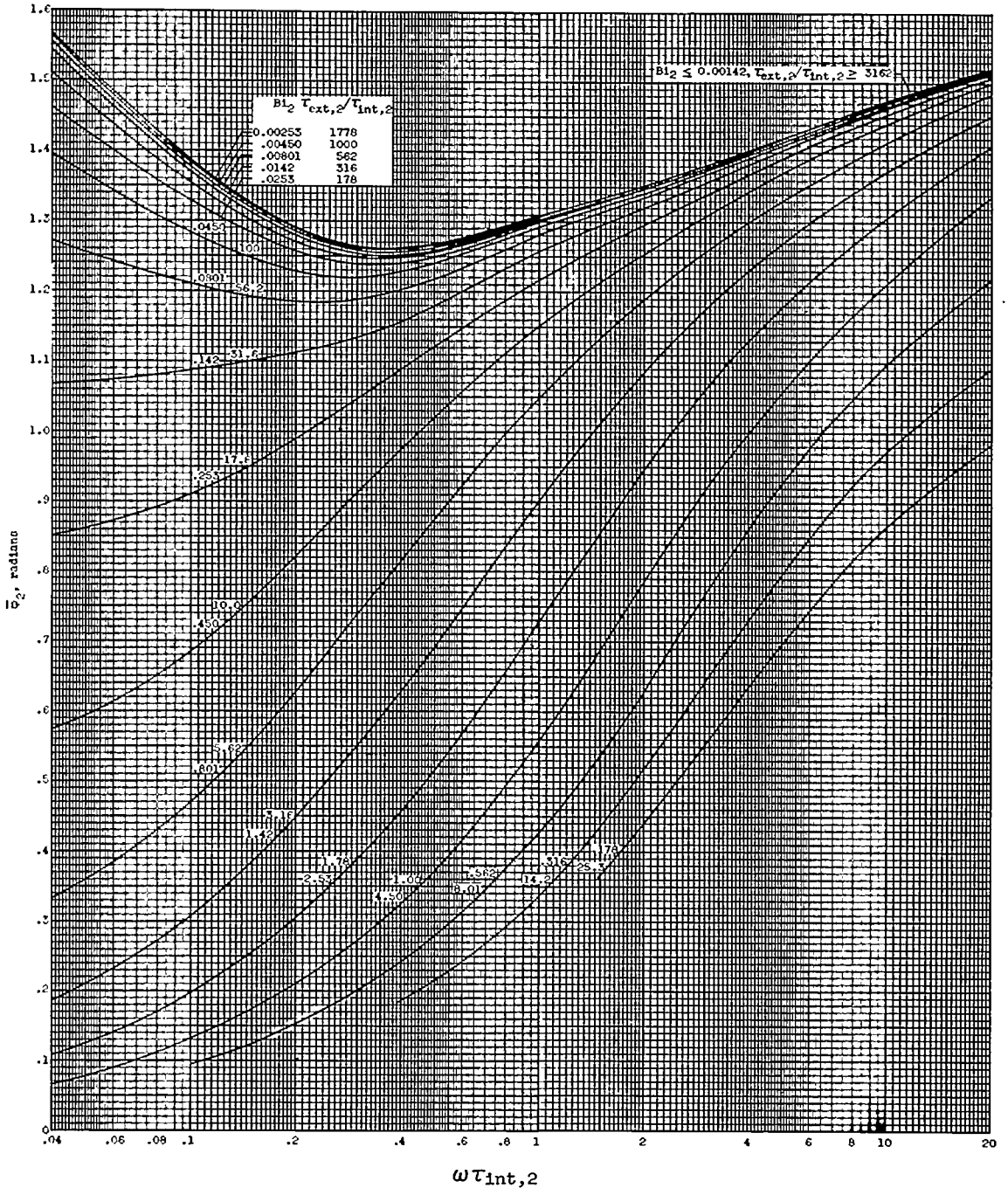

(f) Group F. $\beta = 0.75$; $k_2/k_1 = 5$.

Figure 9. - Continued. Relative mean phase shift (lag) of cylindrical shell over oxide core.

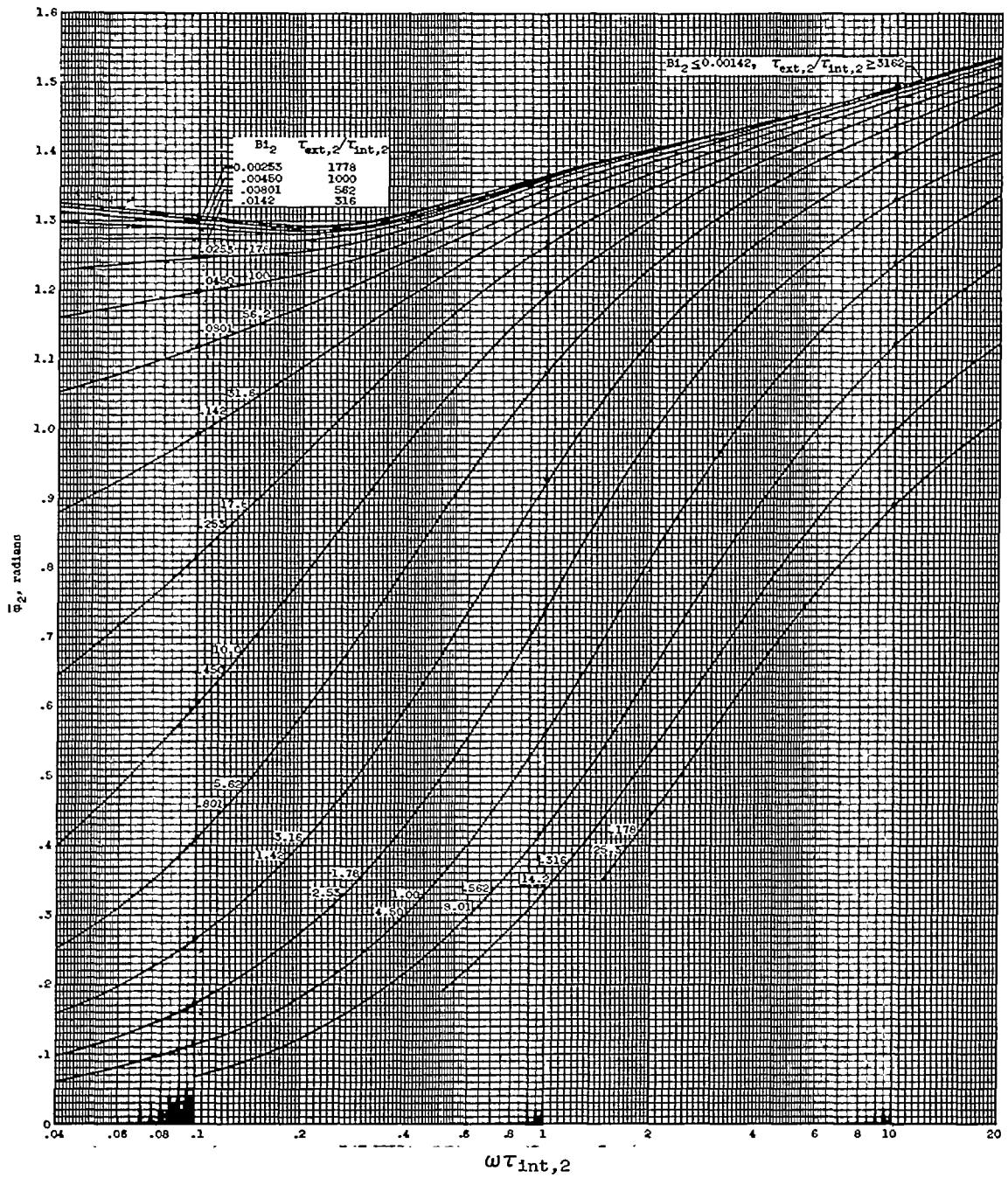

(g) Group G. $\beta \approx 0.75$; $k_2/k_1 = 10$.

Figure 9. - Continued. Relative mean phase shift (lag) of cylindrical shell over oxide core.

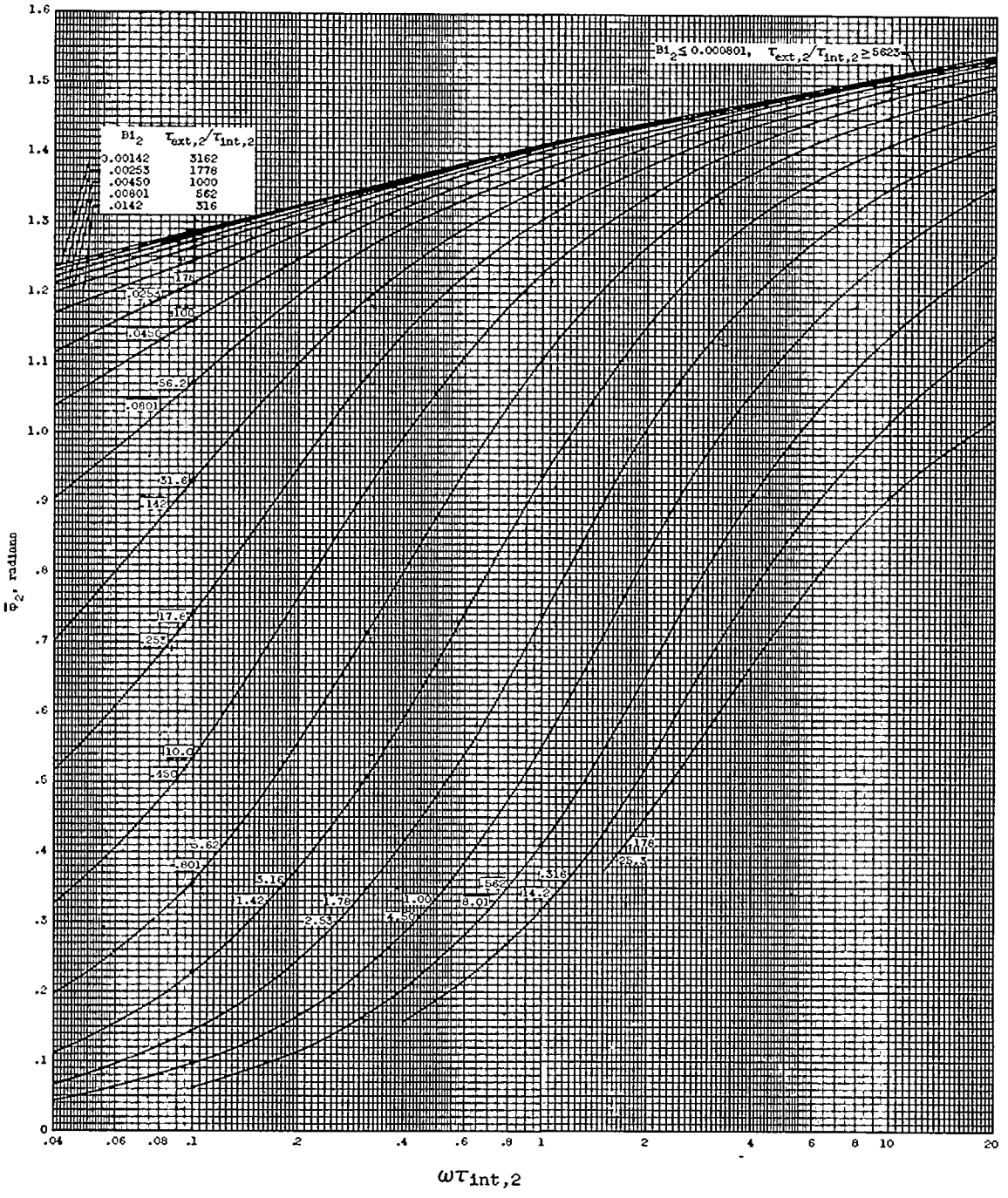

(h) Group H. $\beta = 0.75$; $k_2/k_1 = 20$.

Figure 9. - Continued. Relative mean phase shift (lag) of cylindrical shell over oxide core.

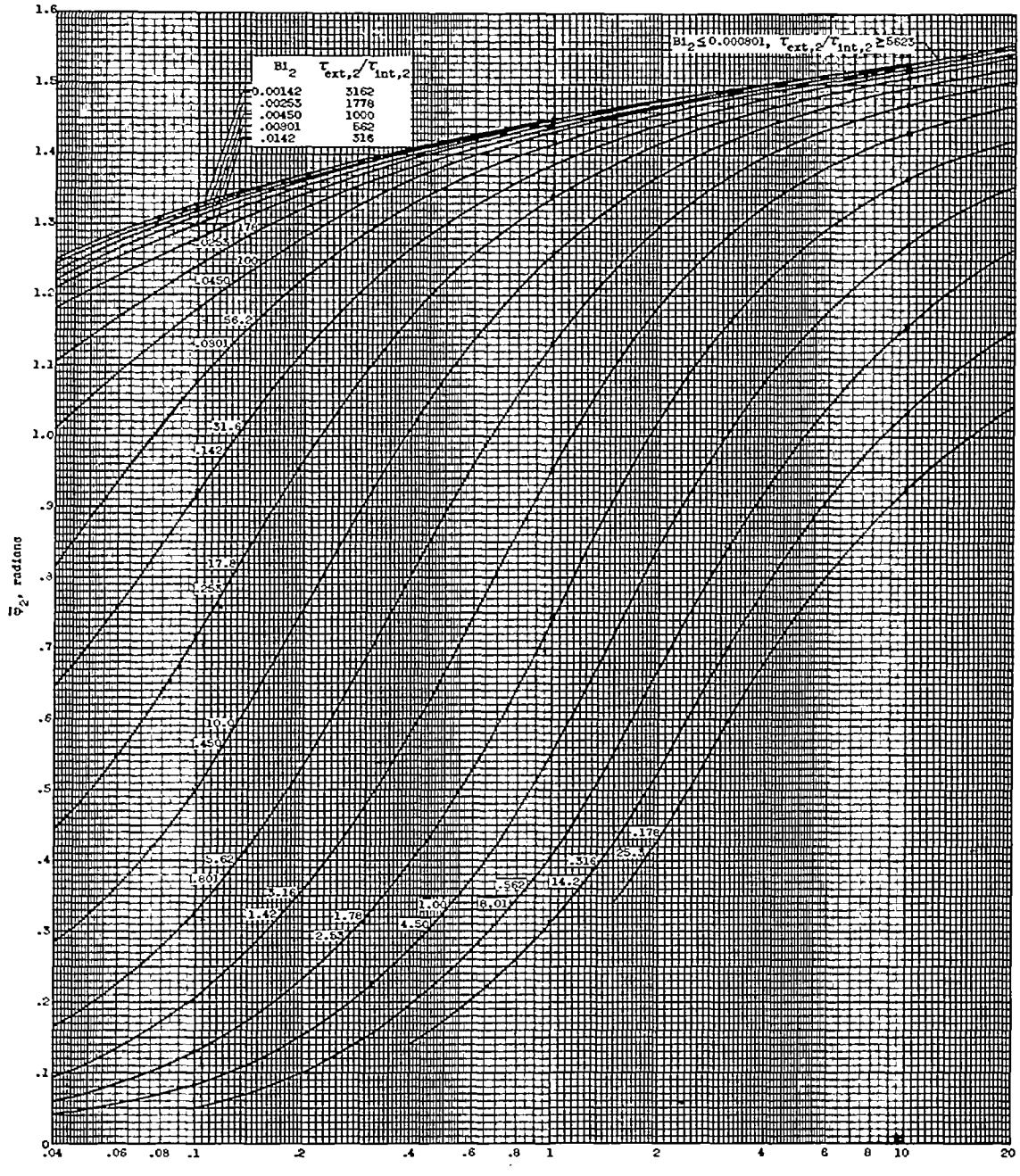

(i) Group I. $\beta = 0.75$; $k_2/k_1 = 40$.

Figure 9. - Continued. Relative mean phase shift (lag) of cylindrical shell over oxide core.

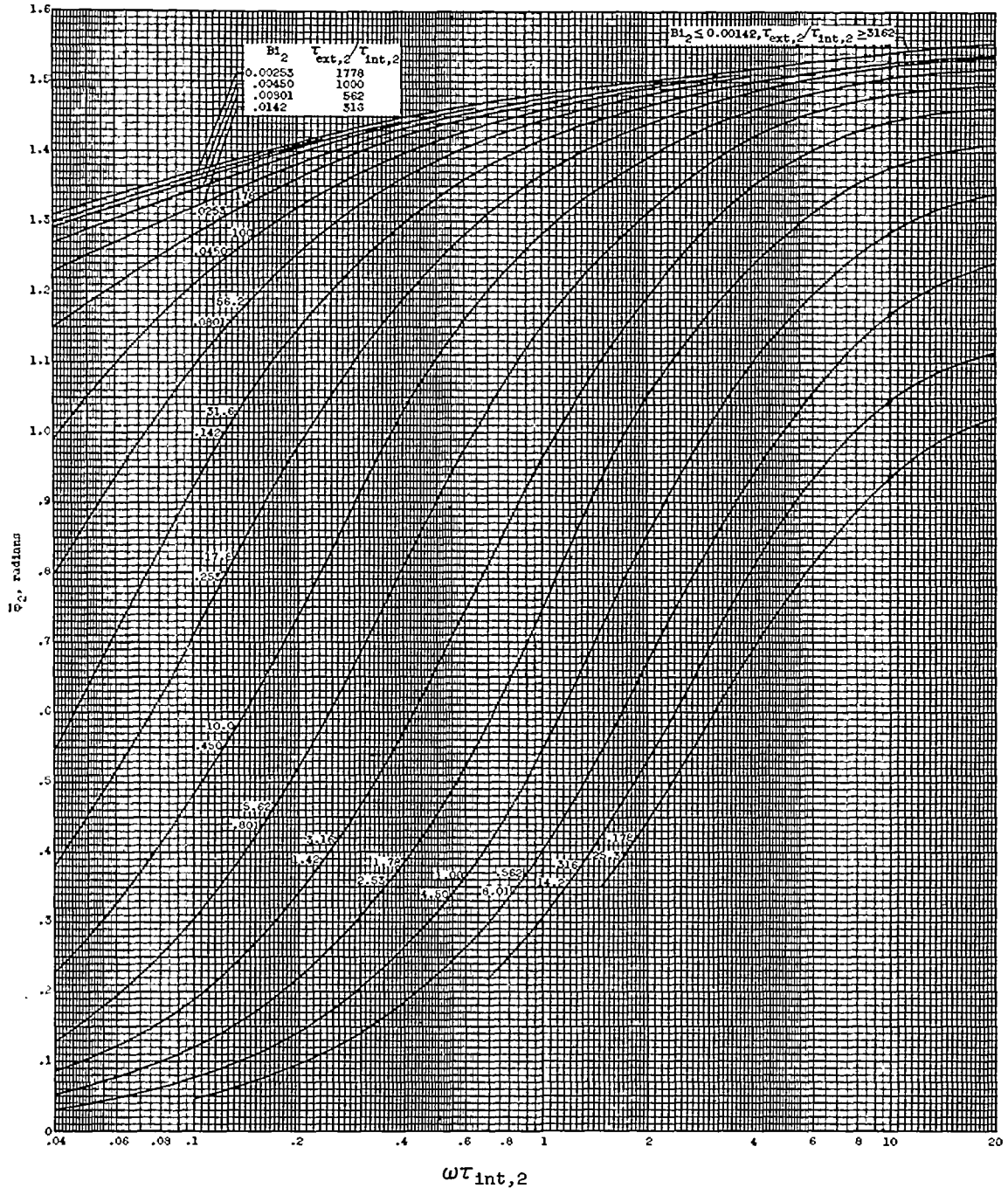

(j) Group J. $\beta = 0.75$; $k_2/k_1 = 80$.

Figure 9. - Concluded. Relative mean phase shift (lag) of cylindrical shell over oxide core.

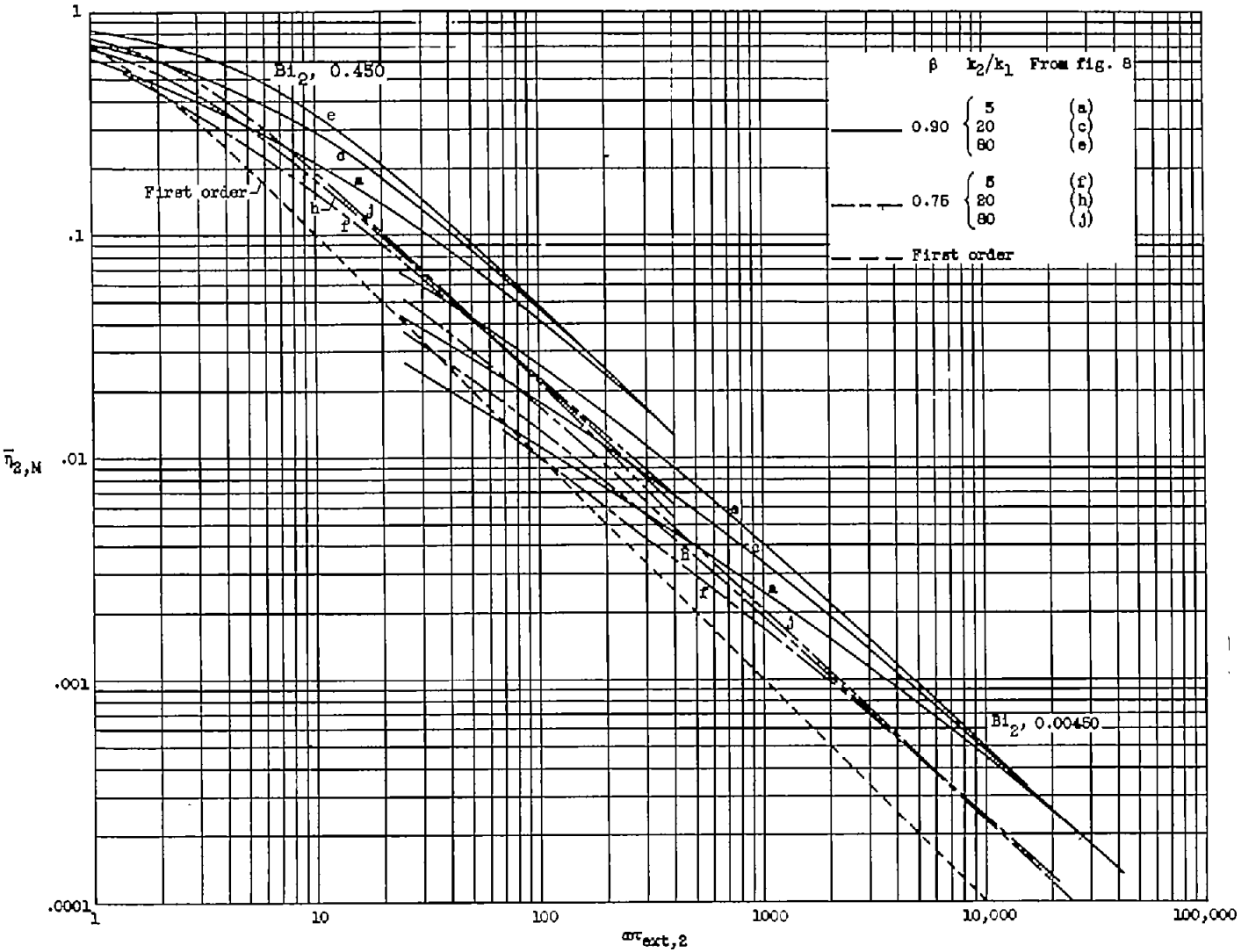

Figure 10. - Relative amplitude as function of $\alpha\tau_{ext,2}$ for selected k_2/k_1, β, and Biot number combinations.

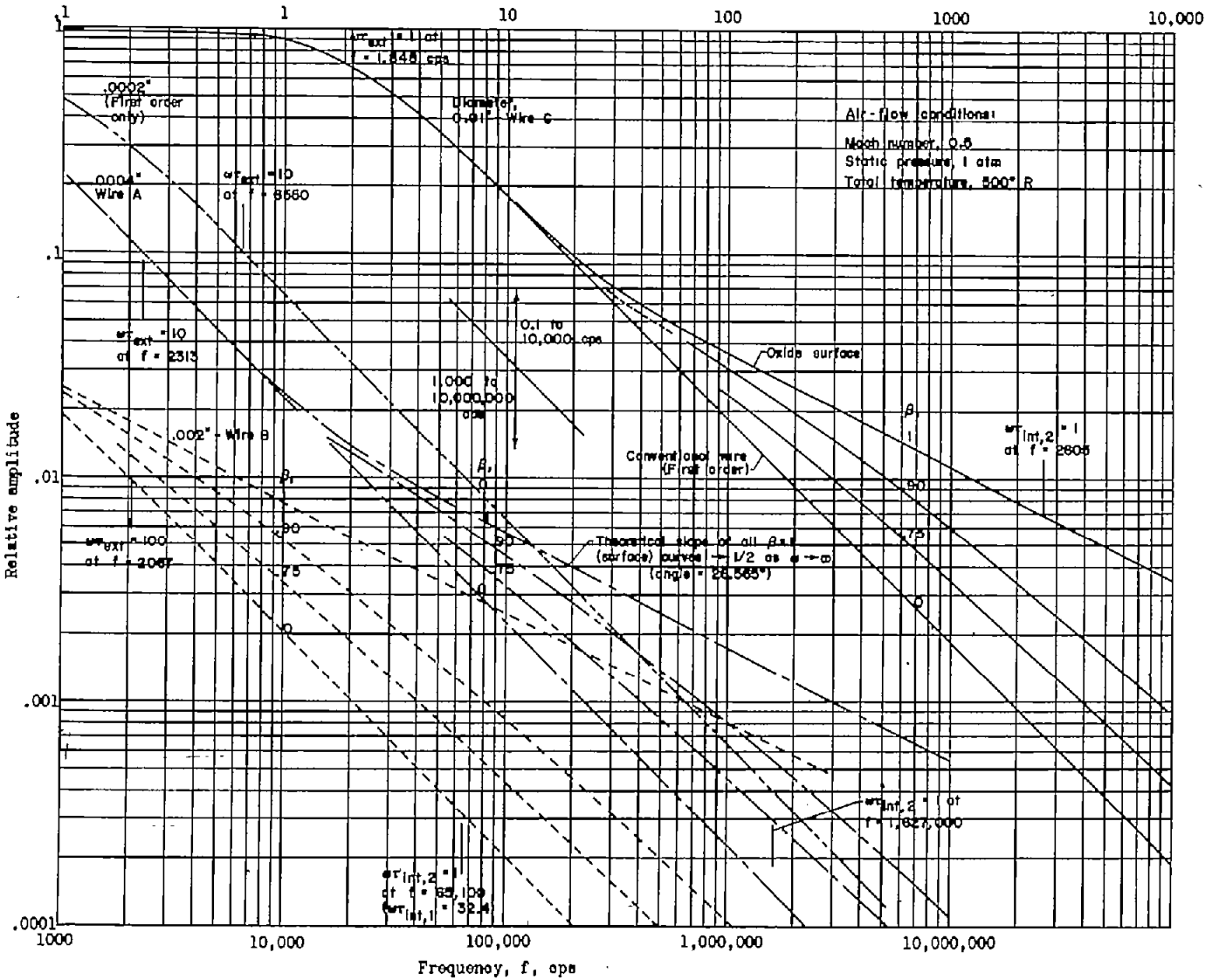

Figure 11. - Response of several typical laminated and homogeneous wires. $k_2/k_1 = 40$; metal, platinum; oxide, fused quartz.